Influence of molecular properties and delivery system design on the transfollicular transport across the skin

Influence of molecular properties and delivery system design on the transfollicular transport across the skin

Proefschrift

ter verkrijging van
de graad van Doctor aan de Universiteit Leiden,
op gezag van de Rector Magnificus Dr.D.D.Breimer,
hoogleraar in de faculteit der Wiskunde en
Natuurwetenschappen en die der Geneeskunde,
volgens besluit van het College voor Promoties
te verdedigen op woensdag 12 januari 2005
klokke 16.15 uur

door

Ylva Yvonne Grams

geboren te Wehrda/Marburg
in 1972

Promotiecommissie

Promotor:	Prof. Dr. J.A. Bouwstra
Referent:	Prof. Dr. rer. nat. J. Lademann (Charité Berlin, Germany)
Overige leden:	Prof. Dr. Th.J.C. van Berkel Prof. Dr. H.E. Junginger Prof. Dr. G.J. Mulder Prof. Dr. H.P. Spaink

The investigations described in this thesis were performed at the Division of Drug Delivery Technology of the **Leiden/Amsterdam Center for Drug Research**, Leiden University, Leiden.

The investigations described in this thesis were financially supported by **Unilever Research**, Port Sunlight, UK.

*A**LTA sobre la tierra*
te pusieron,
dura, hermosa araucaria
de los australes
montes,
torre de Chile, punta
del territorio verde,
pabellón del invierno,
nave
de la fragancia.

(Pablo Neruda, ODA A LA ARAUCARIA ARAUCANA)

Table of contents

I

General introduction

For the treatment of diseases, drugs can be delivered either to the systemic blood circulation or to the local target area. For systemic delivery, various routes are feasible of which the oral route is the most common one. However, the oral route has the disadvantage of the hepatic first-pass effect. Therefore alternative routes of administration are of great interest. One of these routes is the transdermal route. Transdermal delivery has the potential to deliver drugs continuously into the systemic circulation thereby circumventing the first-pass metabolism. However, when focussing on drug delivery to regions in the skin such as the hair follicle, sweat and sebaceous glands, application of the drug on the skin surface also has the potential to increase the drug concentration at the site of action. Additionally the delivery into the systemic circulation might be decreased thereby reducing possible side-effects.

The rational of topical delivery may be of particular interest for skin diseases such as acne, cancer and alopecia, which originate in the pilosebaceous unit (1-4). Furthermore it may also be of interest for cosmetic products to improve e.g. the hair condition. The latter can be achieved by targeting active ingredients to the pilosebaceous unit. Local delivery can be improved by two approaches. The first approach is the selection of an appropriate formulation, which might contain particulate carriers and additives such as ethanol, surfactants and propylene glycol. A second approach is the selection of a possible drug candidate. The physicochemical parameters of the drug, e.g. size, charge and lipophilicity, can affect the degree of delivery and targeting. In those particular cases where adaptation of the formulation is not feasible, delivery and targeting can only be improved by changing the physicochemical parameters of the penetrant itself.

In order to study local drug delivery to the hair follicle, information on changes in drug accumulation in time in the various skin regions is required. Since the hair follicle can reach a depth of more than 2 mm in the subcutaneous fat located below the dermis (5), a technique is required which can detect not only changes in drug accumulation in time in the superficial layers of the skin, but can also provide information in the deep layers of the skin and subcutaneous fat tissue. Drug accumulation in time can only be obtained with unfixed tissue.

SKIN

Function

The skin is the largest organ of the body weighing more than 10 % of the total body mass (6). Forming the outermost layer of the human body, it has two important functions, namely communication and protection (7). The communicative function is based on neuroreceptors, biochemical transmitted

signals and pigmentation. The protective function prevents loss and penetration of a substance from and into the body (8). On the one hand the skin protects the body from the environment such as physical (radiation, abrasion), biological (microorganisms) or chemical factors (toxic substances). On the other hand, water- and ion-loss from the body is prevented as well (9). Additionally the skin including its sweat glands, hair follicles and systemic circulation enables thermo-regulation to ensure correct functioning of the biochemical apparatus.

Despite of this general function, regional variations in skin morphology occur. Not only the thickness (11) and composition of the stratum corneum varies (12,13) but also the presence of appendages and the number of hair follicles is not constant over the whole body surface (14). These variations are of functional origin giving e.g. the soles higher protection against abrasion.

Structure

The basic skin structure is depicted in Figure 1. The skin is basically composed of two layers (epidermis and dermis) with an adjacent subcutaneous fat tissue. The epidermis forms the outer layer of the body comprising non-viable (stratum corneum) and viable cell layers. The epidermis is generated in the undulating basal cell layer at the epidermal dermal junction (15). On their way to the skin surface the keratinocytes start to differentiate and undergo a number of changes in both structure and composition during migration through the stratum spinosum and stratum granulosum. The final differentiation occurs in the stratum corneum (16). The stratum corneum forms the major barrier for substances to permeate across the epidermis. The stratum corneum consists of dead keratinocytes coated with an impermeable proteinous cornified envelope. The corneocytes are surrounded by lipid matrix (16). This lipid matrix is arranged in multiple layers forming lipid lamellae (17). Due to the impermeable cornified envelope the intercellular lipid matrix forms the main rather tortuous pathway for permeation of substances across the stratum corneum.

The dermis is located beneath the epidermis. The thin upper dermis, which is in direct contact with the undulating epidermis, is the papillary dermis while the thicker main part of the dermis is called reticular dermis. It is a fibrous, filamentous and amorphous connective tissue consisting of collagen, elastin, ground substance and fibroblasts (18-21). Its main function is to provide support for the epidermis and embedded structures (blood vessels, nerves, hair follicles, sweat and sebaceous glands) as well as elasticity of the skin (6). In contrast to the epidermis, this tissue is highly vascularised.

The subcutaneous fat tissue is underlying the dermis. It is an assembly of fat cells linked by collagen fibres thereby creating a thermal barrier, energy storage and mechanical cushion for the body (6,7).

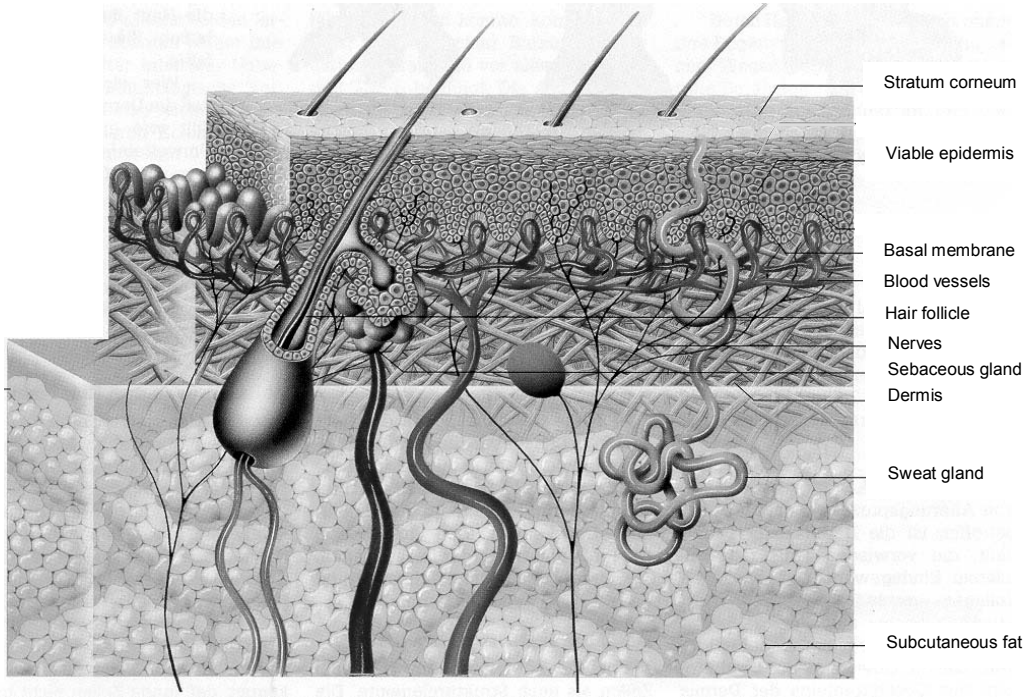

Figure 1. *Skin structure of human skin. The main layers are the stratum corneum, the viable epidermis including the basal membrane, the dermis and the subcutaneous fat. Local skin structures are blood vessels, hair follicles, nerves, sebaceous glands and the sweat glands.*

Appendages

Appendages are skin structures penetrating the skin and originate either from the dermis or the subcutaneous fat. Their presence varies in different skin regions of the body. Since they emerge from the skin, the appendages form discontinuities in the stratum corneum and can therefore act as potential sites of formulation accumulation and routes of penetration.

Sweat gland

Apocrine and eccrine glands are present in large numbers and distributed over the entire body. Apocrine glands emerge into the follicular duct and are located in the axilla and perianal region in adults. Therefore it has been proposed, that the apocrine glands do not contribute to the thermoregulatory function of the sweat glands but are remnants of the secondary sexual organs (7). Eccrine sweat glands are smaller than the apocrine glands and are spread over the whole body surface except from mucosal tissue. They excrete sweat (hypotonic water) via the sweat duct to the skin surface. These sweat ducts perturb the stratum corneum in a spiral form and straighten in deeper skin layers.

The secretory gland itself is coiled and situated in the lower dermis. Their main function is the thermal regulation of the body (6).

Pilosebaceous unit

The pilosebaceous unit consists of the hair follicle and the sebaceous gland. The hair follicle can be divided into two classes. The smaller vellus hair is rather thin and reaches down into the dermis. The larger terminal hair extends down into the subcutaneous fat (22). The terminal hair occurs mainly in the scalp skin which is the region with the highest density of hair follicles.

Sebaceous glands are located at the whole body surface, however, their density and activity depends on age and sex (23-25). A high density of sebaceous glands is present in scalp and forehead skin, while in palm and sole the sebaceous glands are absent (26). Sebum, mainly consisting of trigycerides, free fatty acids, squalene and waxes, is secreted by the sebaceous gland into the hair duct at a depth of about 500 µm (27-30). This sebum protects the body from microbial infection and prevents water loss from the body (30). Additionally it has the potential to interact with topically applied substances on the skin surface and in the upper part of the follicular duct thereby acting as an additional barrier for permeation of substances across the skin.

The hair follicle

The basic structure of the hair follicle is displayed in Figure 2 (31). The hair follicle can be divided into several sections starting from the skin surface. The infundibulum is the upper part of the hair follicle up to the sebaceous duct. In this area, no tight connection between the hair shaft and the skin is present. Therefore, the hair shaft can move freely within the skin. This gap is filled with sebum of the sebaceous gland. The thickness of the stratum corneum decreases deeper in the infundibulum. This thinned stratum corneum provides a weaker barrier for penetration compared to the stratum corneum at the skin surface (32). The isthmus is located just below the sebaceous duct and up to the area where the arector pili muscle is attached to the hair follicle. From the isthmus upward the hair follicle is permanent and does not disintegrate during the growth of the hair follicle. However in this region the inner root sheet is disintegrating and disappears between the outer root sheet and the cuticle further to the surface. The bulge area is located where the arector pili muscle is in contact with the hair follicle. This area is important for regulatory processes during hair growth (33). Below the bulge area starts the lower follicle with the keratogeneous zone. The lowest part of the hair follicle is the hair bulb, where the matrix cells, the basement membrane and the follicular papilla are located. These structures are key features in the regulation of the hair growth (34).

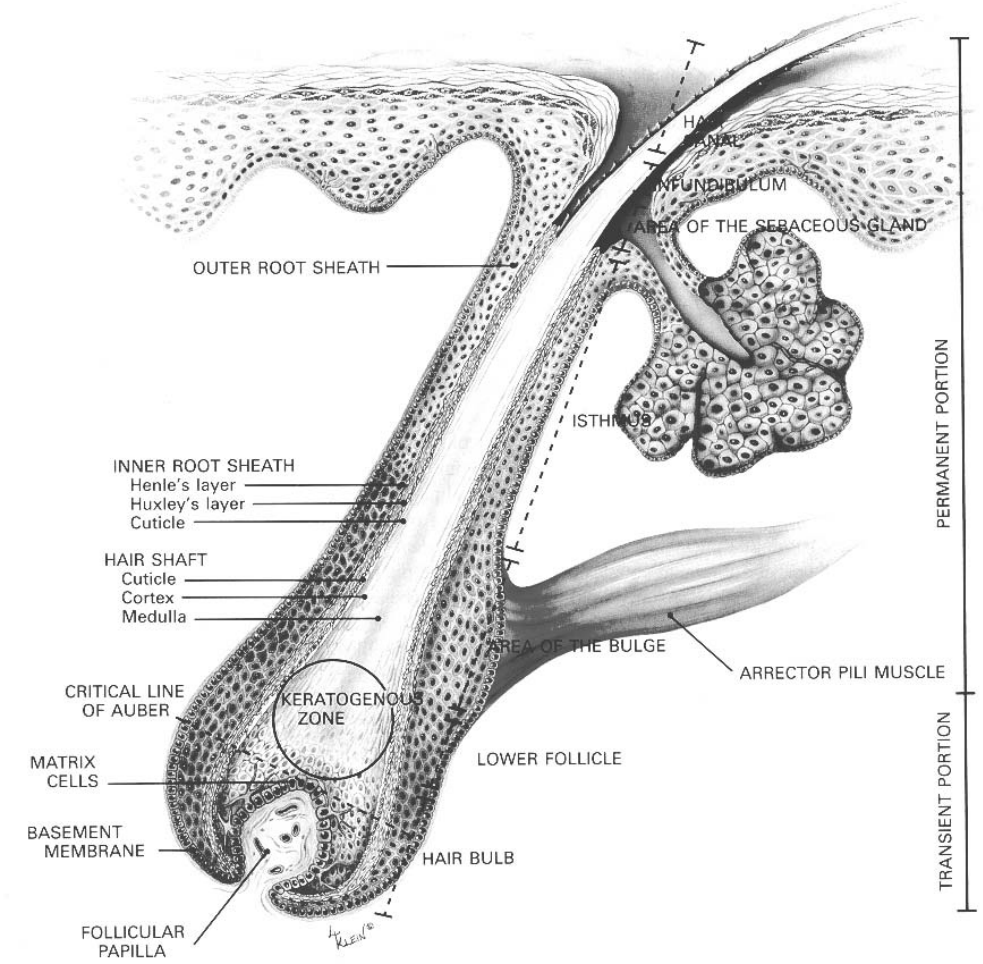

Figure 2. *Hair follicle structure (31). The various layers of the hair follicle, described in this thesis are from the dermis to the centre of the hair: Outer root sheath, inner root sheath (Henle's layer, Huxley's layer), cuticle of the inner root sheath, cuticle of the hair shaft and the remaining hair shaft. Furthermore it is depicted that the epidermis is continuous with the outer root sheath and the stratum corneum decreases in thickness in the opening of the follicular duct. The sebaceous gland secretes the sebum into the opening of the follicular duct. The bulge area is located below the duct of the sebaceous gland.*

In a cross-section of the hair follicle below the bulge area, several almost concentric layers can be identified (Figure 2) (31,34). Basically from the outside of the hair follicle to the centre of the follicle the following layers are encountered: the outer root sheath, the inner root sheath including the Henle's layer, the Huxley's layer and the cuticle. The inner root sheath is in direct contact with the hair shaft. The hair shaft itself is composed of a cuticle (outermost layer), a cortex and a medulla (central part). The cuticle of the inner root sheath and of the hair shaft form the connection, along which the hair shaft is moving outward during hair growth.

Keratinisation is important for hair growth and might have a crucial influence on the transport processes. The outer root sheath is in direct contact with the epidermis. Below the duct of the sebaceous gland, the cells of the outer root sheath are only little keratinised or lack keratinisation completely. This allows the moulding of the hair shaft and at the same time provides sufficient protection for the shaft. From the sebaceous duct upwards, the outer root sheath cells are keratinised and resemble more closely the epidermal cells (34). The inner root sheath keratinises deeper in the hair follicle as compared to the outer root sheath with the Henle's layer being the first, followed by the cuticle and the Huxley's layer (34). The cuticle of the inner root sheath keratinises closer to the hair bulb than the cuticle of the hair shaft. Thereby guidance for the emerging hair is provided combined with a loosening of the tight connection between the two cuticles (34).

Growth cycle of the hair

Hair growth varies between different body regions with about 0.21 mm per 24 hours on the female thigh and approximately 0.38 mm per 24 hours on the male chin (7). The hair growth undergoes a repetitive cycle where the anagen phase is followed by the catagen and telogen phase (35) (Figure 3). In the anagen phase, the hair is actively growing while the catagen is characterised by degeneration and resorption of the lower region of the hair follicle. The resting period, where the hair is inactive, is called the telogen phase. After resting, growth of the hair follicle restarts (36).

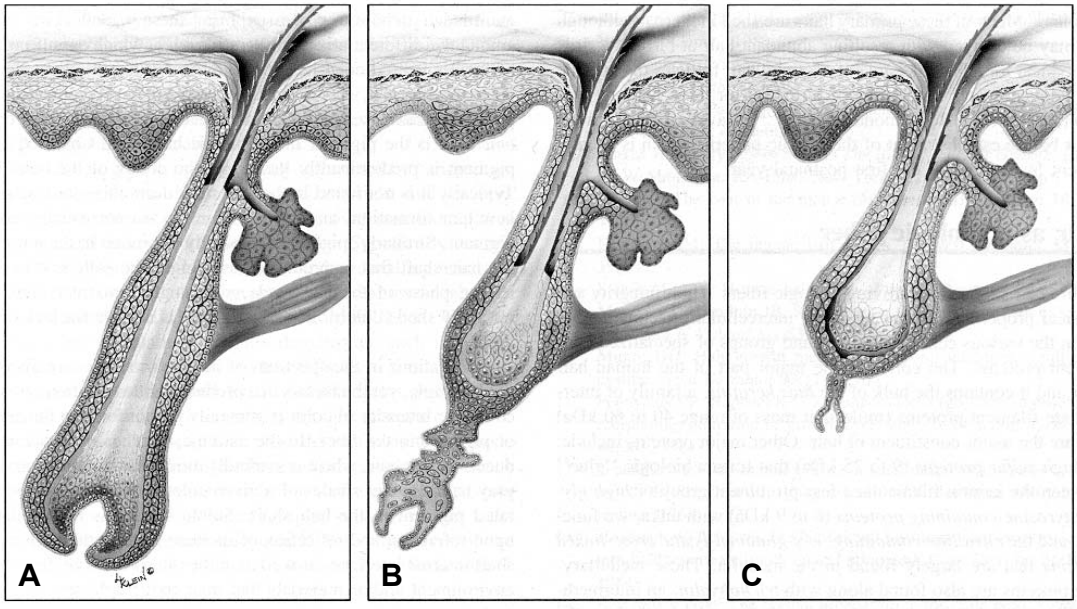

Figure 3. *Growth cycle (31). A – Anagen (growth phase), B – Catagen (transition phase), Telogen (resting phase).*

Currently it is not clear how the hair growth is initiated. This is reflected by the various discussions and hypotheses regarding the activation and differentiation of stem cells (37,38). However the bulge area and the dermal papilla seem to play a crucial role in the growth process.

Local target areas

In the pilosebaceous unit various target areas for topically applied drugs are of interest. One of the potential target areas is the sebaceous gland due to its direct connection with the follicular duct. In case of dysfunction of the sebaceous gland, the topical application has the potential to deliver drugs directly to the target area with limited systemic delivery (39,40). In case of toxic active ingredients, efficient targeting is essential to limit the toxic side effects such as for isotretinoin in the treatment of acne (41). Within the hair follicle, interesting target areas are the bulge area, the bulb and the various concentric layers in the follicle (39). Regulatory receptors for various molecules (e.g. epidermal growth factor) have also been identified (42). Several research groups propose that the bulge area initiate the hair growth, although the exact mechanism is yet unknown. Another reason for targeting to the bulge region is that various forms of skin cancer have been thought to originate from this region (43). In the bulb, melanocytes are present, which are responsible for the hair colour and thus for greying of the hair. Treatment of these melanocytes in albino mice has demonstrated that it is possible to grow pigmented hair (44). Furthermore the bulb contains a proliferating population of cells in the germinal matrix, which are responsible for new cell formation and therefore for hair growth. Sufficient nutrients for the growth process in the bulb area are provided by extensive vascularisation (45). Various attempts for the treatment of hair loss are also of great interest and under discussion (46).

(TRANS)DERMAL DELIVERY

Routes of penetration

When drugs are applied on the skin surface, penetration into and through the skin can occur via various routes. Drugs penetrate either via the stratum corneum (transepidermal) or via the appendages (transappendageal) (Figure 4) (8,47). During penetration through the stratum corneum, two possible routes can be distinguished, i) penetration alternating through the corneocytes and the lipid lamellae (transcellular route) and ii) penetration along the tortuous pathway along the lipid lamellae (intercellular route). Generally it is accepted that the predominant route of penetration through the stratum corneum is the intercellular route. This is mainly caused by the densely cross-linked cornified envelope

coating the keratinocytes. However transcellular transport for small hydrophilic molecules such as water cannot completely be excluded (6).

The appendageal route or shunt route includes either the duct of the eccrine sweat glands or the follicular duct. The content of the eccrine sweat glands is mainly hydrophilic, while the content of the follicular duct is lipophilic. This is mainly due to the sebum excreted into the opening of the follicular duct.

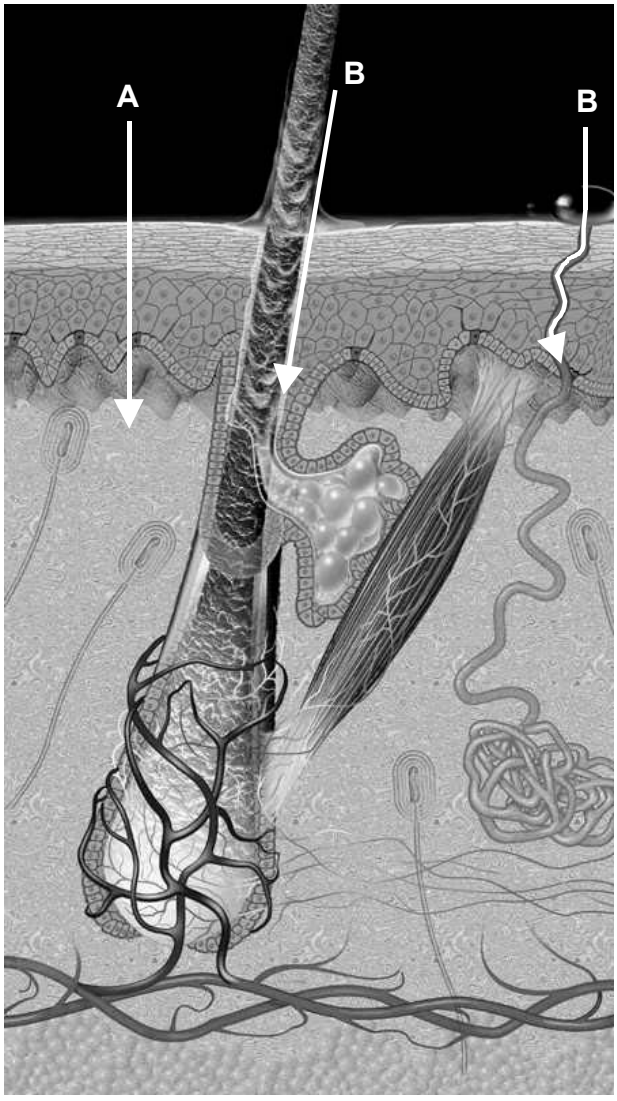

Figure 4. *Transepidermal (A) and transappendageal route of transport into the skin. The transappendageal route (B) includes diffusion via the hair follicle and the sweat gland.*

It is generally accepted that due to its large surface area, passive skin permeation mainly occurs through intact stratum corneum. Since the appendages cover approximately 0.1 % of the total skin surface, it is discussed that the permeation along appendages contributes only slightly to the overall

passive transdermal penetration (48,49). However Scheuplein (49) has calculated that in the initial phase of diffusion, the influence of the shunt route is very important. Investigations of several other groups provided additional data indicating that the contribution of the follicular pathway might be underestimated. They discovered an accumulation of the selected penetrant in the follicular region (50-53). These results are of great interest for drugs used in the treatment of follicle related skin diseases.

Fick's law of diffusion

Diffusion processes in human skin are very complex due to the inhomogeneous and layered structure of the skin and the presence of appendages interrupting the intact stratum corneum. In order to model diffusion processes and compare the diffusion of various drugs, a simplified model of the skin has to be considered. In Fick's first law (equation 1) the skin is considered to be homogeneous and the acceptor phase provides sink conditions for the penetrant. It describes that the transported mass dm [g] per time unit dt [h] through a defined area A [cm^2] is directly proportional to the diffusion coefficient D [cm^2/s], the size of the area and the concentration gradient [g/cm^3]. However it is reverse proportional to the distance dx [cm] of the transported mass.

$$\frac{dm}{dt} = -DA\frac{dc}{dx} \qquad \text{Equation 1}$$

The diffusion coefficient D [cm^2/s] is the proportional factor and depends on physico-chemical characteristics of the medium and the penetrant. If diffusion occurs from a liquid donor phase into the skin, the partition coefficient (K) of the model penetrant is introduced. This partition coefficient links the concentration in the donor phase (c_d) to the concentration in the skin layer exposed to the donor phase. In a steady state situation a constant gradient is present in the membrane. Assuming the concentration in the acceptor phase is negligible, Fick's law can be described as:

$$\frac{dm}{dt} = -DKA\frac{c_d}{dx} \qquad \text{Equation 2}$$

Plotting the cumulative amount of penetrated drug against time, a linear dependency is present in steady state conditions. The steady state flux (J_{ss}) can be determined directly from the slope (equation 3).

$$J_{ss} = \frac{dm}{dt} * \frac{1}{A} \qquad \text{Equation 3}$$

FOLLICULAR DELIVERY

General aspects of follicular delivery

The follicular duct forms an intrusion in the stratum corneum. This interruption of the stratum corneum barrier can serve as a route for drug delivery. Additionally, the orifice of the hair follicle is a site where dermatological formulations may accumulate and deposit, thereby forming a depot for long-term delivery. In the past, the transappendageal route has long been considered of minor importance, since the orifices account for only 0.1 % of the total skin surface. However the density of hair follicles on scalp and face can reach as much as 10 % of the total skin surface, creating a higher local surface area (54) and allow greater absorption by this route (55). The hair follicle openings are continuous with the epidermis but possess a much thinner layer of stratum corneum (39), which terminates at a depth of about 200 µm in the duct. The pilosebaceous unit is also closely surrounded by a high density of blood vessels, having the potential of high absorption of permeating substances into the systemic circulation. Nevertheless, parameters governing the follicular delivery are not clear yet.

Lieb et al. (54) demonstrated that permeation into hair follicles depends on size and charge of the permeant and the formulation in which the permeant is applied. Other chemical properties, like lipophilicity might also play a significant role in follicular penetration. Additionally, a certain degree of lipophilicity for compounds entering the hair follicle might be necessary due to the presence of sebum in the follicular duct from the sebaceous gland (39).

Based on theoretical considerations, it has already been proposed by Scheuplein et al. (49) that the follicular route plays an important role in the initial period of the transport process, but that at a later stage penetration occurs predominantly via the stratum corneum. In fact, only little information is available on the contribution of the hair follicles to the total transport across the skin and even less in known about the effect of formulations and the chemical properties of the penetrant itself on this contribution.

Analysis methods for follicular delivery

Skin models

In skin research, various skin models are used to investigate penetration of drugs in general. Human skin from cosmetic surgery is most favourable (e.g. abdominal and mamma skin). Some researchers use cadaver skin (56) with the danger of skin disintegration once the skin is available. Furthermore pig skin has been reported to have similar barrier properties as human skin and therefore is suggested to be an acceptable model for human skin (57). Due to low availability

of human skin, mouse and rat skin is frequently used in screening experiments. However it has been shown, that permeability of mouse skin is sometimes several orders of magnitude higher than of human skin (58,59) while rat skin is only slightly more permeable (60).

The correlation between the results obtained *in vitro* and *in vivo* is of great importance for the development of new drugs and formulations. Various research groups have studied the *in vitro* - *in vivo* correlation within one skin model however also comparing results between animal models and human skin. Several authors (61-64) have demonstrated a good correlation for *in vitro* and *in vivo* data in rodents (rats and rabbits). Also for the monkey model, a correlation between *in vitro* and *in vivo* data has been reported (65). Even from a comparison of in vitro data obtained from porcine skin compared to in vivo data obtained from humans, literature demonstrates a correlation of the percutaneous absorption (66,67). Other researchers showed a good *in vitro* - *in vivo* correlation in deeper layers of human skin. However, due to clinical practice of disinfecting procedure, poor correlation at the skin surface has been reported (68). While *in vitro* data in human skin have been shown to overestimate the *in vivo* results (69), the low-frequency ultrasound technique had a higher effect *in viv*o than *in vitro* (70). Therefore various parameters such as skin model, used method of penetration enhancement, penetrant and skin treatment during analysis has to be considered when attempting *in vitro* - *in vivo* extrapolation of diffusion data.

In follicular research, the influence of hair follicles on the penetration and accumulation in the follicular area has been studied using several models. The first model is hairless rodent skin. Although hairless rodents lack the actual hair, the hair follicles are still present. These follicles are different and underdeveloped when comparing them to regular follicles (71). Penetration studies using hairless skin might therefore result in an underestimation of the contribution of the follicular pathway to the overall diffusion. Another model used in follicular research is scared skin. The scar formation is obtained after short burning of the skin resulting in absence of hair follicles. In this model hair follicles are absent. However the skin has undergone severe stress and exhibits different histology (52). Therefore also results obtained using this scared skin model might result in over- or underestimation of the contribution of the follicular pathway. A third model used in follicular research is the skin behind the ear of a guinea pig, which is totally follicle free (72). Because the histology of the skin of the hairy part of the animal is comparable to the non-hairy part, a comparison of penetration values within one animal is possible. However depending on the study, different results were obtained for the *in vitro* and *in vivo* set-up. A fourth model, the ear of a Syrian hamster (73) was used to study the sebaceous gland. In the hamster ear, a high density of sebaceous glands is present which resembles the sebaceous glands of the humans. This model has not been used with a focus on the hair itself. Another skin model is pig skin. It is generally accepted to be the best model

for human skin when interested in penetration of drugs. Pig skin deviates from human skin in its appendages. It is void of sweat glands and the hair bulb of the follicle is situated in the dermis. In human skin, the hair follicle reaches into the subcutaneous fat up to a depth of approximately 2-3 mm. Therefore pigskin is not a realistic model for examining transport processes into deeper regions of the hair follicle. Human scalp skin from cosmetic surgery is currently the best skin material to investigate *in vitro* diffusion processes. The only draw back is its limited availability and the difficulties to perform *in vivo* studies using human scalp skin with the currently available techniques.

Quantification

Quantitative access to deposition of substances in the follicular region is a challenging task, since the hair follicle of human skin extends down into the subcutaneous fat. Most studies have been carried out either using fluorophores or radioactive agents as model penetrants. The distribution profiles of these labels were mostly determined by quantification of model penetrants in stratum corneum tape strips in combination with quantification in biopsies (74,75), immunohistochemical analysis (54,76), isolation and dissolution of the various skin regions including hair follicles (76,77), hair plugging and follicle dissection (54). However, when isolating hair follicles, cell structures can be destroyed thereby bearing the danger of delocalisation of the dye resulting in artefacts. Recently, techniques used for relative quantification of penetrant distribution within the skin have been reviewed elsewhere (75). Turner and Guy (78) have published relative quantification data of cryo-fixed hairless mouse skin samples. The authors focused on the fluorophore distribution after iontophoresis *ex vivo*. As far as *in vivo* quantification is involved, particularly non-invasive methods of quantification, such as in depth-resolved near-IR spectroscopy, have still an insufficient resolution (31 µm) for visualisation of the various regions in the hair follicle (79). Furthermore, absolute quantification in unfixed tissue has not yet been reported.

Visualisation

Visualisation in fixed skin

Visualisation methods in skin research have been summarised elsewhere (80). This review provides an excellent overview of advantages and disadvantages of the various available methods (80) to depict penetrated substances. While in conventional light microscopy a penetrant with a strong contrast has to be used, autoradiography requires radioactive labelling of the permeant. Electron microscopy has the advantage of providing images with a very high resolution. However, in most cases the choice of the permeation agent

is limited to substances with high electron density or substances linked to an electron dense marker, such as gold. All of these techniques require fixation, which can be obtained for example by chemical embedding or cryo-fixation of the skin. This fixation procedure in combination with subsequent slicing of the object can introduce artefacts, such as delocalisation of the label. Therefore fixation by chemicals or by cryo-fixation should be avoided.

Visualisation in non-fixed skin

Visualisation techniques which do not require embedding and freezing of the object are magnetic resonance imaging (81-83), video microscopy (84-87), ultrasound backscatter microscopy (88) and confocal laser scanning microscopy (89-95). The combination of the latter technique with confocal raman spectroscopy (96) even enables to obtain a molecular composition of selected spots in the skin with high spatial resolution (97). For these techniques model drugs with adequate characteristics such as raman active substances, dipole structures or fluorescent dyes have to be selected. Confocal raman spectroscopy has already been applied *in vivo* in humans. Magnetic resonance imaging has the advantage that it can be used *in vivo* very deep in the skin and subcutaneous tissue however; the resolution is limited compared to confocal raman or confocal laser scanning microscopy. The resolution of video and ultrasound microscopy is even worse and can therefore not be used for visualisation of substances in hair follicles.

In hair follicle research high resolution of the visualised area is necessary paired with reaching deep layers of the skin for the visualisation of the hair bulb. As pointed out above, the current *in vivo* visualisation techniques are either limited in resolution or depth penetration. Therefore, it was decided to primarily focus on a promising *in vitro* technique fulfilling the requirements of resolution and depth penetration. Therefore confocal laser scanning microscopy is the method of choice, if fixation of the skin is circumvented by alternative methods and if the skin is sliced perpendicular to the skin surface. This immediately limits the confocal method for visualisation in deeper follicular regions to the *ex vivo* situation. Once the confocal method is set up, the *ex vivo* results might be investigated *in vivo* using either confocal raman spectroscopy in combination with confocal laser scanning microscopy or magnetic resonance imaging accepting limited resolution or limited depth visualisation. Although these drawbacks have to be accepted, first *in vitro/in vivo* correlation of penetration into the human hair follicle might be accessible.

THIS THESIS

Objective

Local administration of drugs to the skin with the aim of high accumulation in the follicular area is of great interest. Especially the pharmaceutical industry in case of local drug targeting and the industry in the field of personal care products forms a potentially interested group. However, the influence of factors such as physico-chemical properties of the permeant and the effect of the vehicle is not clearly understood.

Extending the cleansing function of shampoo formulations by providing supplementary nutrients to the hair follicle would be very desirable. However from a formulation point of view, liposomes which have already been reported to improve accumulation of a drug in the follicular duct (98-100) are not applicable in shampoo formulations. The liposomal structure is not expected to be stable in the presence of the surfactants of the shampoo. Therefore the efficiency of alternative approaches has to be studied for their potential to increase accumulation of the active ingredient in the hair follicle.

Furthermore, to study drug accumulation in the human hair follicle, thick skin pieces have to be used since the hair bulb reaches down into the subcutaneous fat. In order to investigate the delivery of drugs to the hair follicle, a powerful method has to be developed. This method has to access the hair bulb in deep skin layers, has to have sufficient resolution to visualise the various layers of the hair follicle, has to limit the danger of artefact formation and has to have the potential to visualise diffusion processes on-line.

From these aspects, the following objectives are formulated:

A. *Develop a method that allows the comparison of degrees of accumulation in the various layers of the hair follicle, the dermis, the viable epidermis and the stratum corneum.*

B. *Examine the influence of permeant lipophilicity on the accumulation in the various follicular layers, the viable epidermis, dermis and stratum corneum.*

C. *Examine the influence of formulation composition on the accumulation in the various follicular layers, the viable epidermis, dermis and stratum corneum.*

D. *Design a method to visualise the diffusion process* ***on-line*** *and examine the diffusion pathways of the permeant in the various regions of the skin, including the gap, along the entire hair follicle to reach the hair bulb. Only in this way information about the permeant penetration pathways can be achieved.*

Organisation

Chapter II: A new method of relative quantification was developed using confocal images of cross-sections perpendicular and parallel to the skin surface. This method enabled the comparison of the dye distribution in the various regions of the skin including the hair follicle after diffusion of the dye over a selected time period. Therefore information was provided about the relative accumulation of dyes in the hair follicle regions.

Chapter III: Diffusion studies with dyes of increasing lipophilicity were performed. Diffusion studies were carried out, after which the fluorophore was visualised in the skin, including the various regions in the hair follicle. Using the method described in chapter II, the relative accumulation of the dyes in the various skin regions was determined and the influence of permeant lipophilicity was accessed.

Chapter IV: Subsequently the influence of the vehicle composition, i.e. the presence of a basic shampoo formulation with and without propylene glycol was accessed. The penetrated amount of the various dyes and the degree of accumulation in the various follicular layers and the non-follicular regions were determined using different formulations.

Chapter V: In the studies described in this chapter a new method was developed in which transport of a lipophilic dye was visualised in real-time (during transport) for a period of 8 hours. In these studies the main focus was to visualise the permeation process in the stratum corneum, epidermis and dermis.

Chapter VI: In a subsequent series of studies, on-line diffusion was examined with a lipophilic fluorescent dye. The diffusion process was visualised close to the opening of the hair follicle (the gap) to a depth of approximately 400 μm. The diffusion process was followed over a time period of 16 hours.

Chapter VII: In order to study the diffusion process along the entire hair follicle, the diffusion process of the lipophilic dye was visualised in several sections at selected depths. This included the diffusion of the dye to the hair bulb.

Chapter VIII summarises the studies described in this thesis. In addition the future perspectives of the on-line method and the use of basic shampoo formulations for local targeting to the hair follicle are discussed.

REFERENCES

1. G. Cotsarelis, T. Sun and R. M. Lavker. Label-retaining cells reside in the bulge area of pilosebaceous unit: implications for follicular stem cells, hair cycle, and skin carcinogenesis. *Cell* ***61*****:**1329-1337 (1990).
2. F. J. G. Ebling, P. A. Hale and V. A. Randall. Hormones and hair growth. In: L. A. Goldsmith (ed.), *Physiology, Biochemistry and Molecular Biology of the skin*. Oxford Press, Oxford, 1991, pp. 660-696.

3. G. Plewig. Models to study follicular diseases. In: G. Plewig (ed.), *Skin models to Study Function of and Disease of Skin*. Springer, Berlin, 1986, pp. 13-23.
4. V. H. Price. Alopecia areata: clinical aspects. *J. Invest. Dermatol.* ***101*****:**68S (1991).
5. M. L. Price and W. A. D. Griffiths. Normal body hair-a review. *Clin. Experimental Dermatol.* ***10*****:**87-97 (1985).
6. H. Schaefer and T. E. Redelmeier. *Skin Barrier: Principles of Percutaneous Absorption,* Karger, Basel, 1996.
7. B. W. Barry. *Dermatological formulations: Percutaneous absorption,* Marcel Dekker, 1983.
8. J. Hadgraft. Skin, the final frontier. *Int. J. Pharm.* ***224*****:**1-18 (2001).
9. T. Winsor and G. E. Burch. Differential roles of layers of human epigastric skin on diffusion of water. *Arch. Intern. Med.* ***74*****:**428-444 (1944).
10. G. F. Odland. Structure of the skin. In: L. A. Goldsmith (ed.), *Physiology, Biochemistry and Molecular Biology of the skin*, New York, 1991, pp. 3-62.
11. R. Marks and S. P. Barton. The significance of size and shape of corneocytes. In: R. Marks and G. Plewig (eds.), *Stratum corneum*, Springer, Berlin, 1983, pp. 175-180.
12. R. S. Greene, D. T. Downing and P. E. S. J. S. Pochi. Anatomical variation in the amount and composition of human skin surface. *J. Invest. Dermatol.* ***54*****:**240-247 (1970).
13. M. A. Lampe, A. L. Burlingame, J. Whitney, M. L. Williams, B. E. Brown, E. Roitman and P. M. Elias. Human stratum corneum lipids: Characterization and regional differences. *J. Lipid Res.* ***24*****:**120-130 (1983).
14. G. Szabo. The regional frequency and distribution of hair follicles in human skin. In: W. Montagna (ed.), *Biology of hair growth*, 1958, pp. 33-38.
15. R. A. Briggaman and C. E. Wheeler. The epidermal-dermal junction. *J. Invest. Dermatol.* ***65*****:**71-84 (1975).
16. P. W. Wertz and D. T. Downing. Stratum Corneum: Biological and Biochemical Considerations. In: J. Hadgraft and R. H. Guy (eds.), *Transdermal drug delivery*. Marcel Dekker, New York, 1989, pp. 1-22.
17. A. S. Breathnach, T. Goodman, C. Stolinski and M. Gross. Freeze fracture replication of cells of stratum corneum of human epidermis. *J. Anat.* ***114*****:**65-81 (1973).
18. H. P. Bachinger, N. P. Morris, G. P. Lunstrum, D. R. Keene, L. M. Rosenbaum, L. A. Compton and R. E. Burgeson. The relationship of the biophysical and biochemical characteristics of type VII collagen to the function of anchoring fibrils. *J. Biol. Chem.* ***265*****:**10095-101(1990).
19. K. A. Holbrook and K. Wolff. The structure and development of skin. In: T. B. Fitzpatrick, A. Z. Eisen, K. Wolff, I. M. Freedberg and K. F. Austen (eds.), *Dermatology in General Medicine*. McGraw-Hill, New York, 1993, pp. 97-154.
20. L. B. Sandberg, N. T. Soskel and T. B. Wolt. Structure of elastic fibre: An overview. *J. Invest. Dermatol.* ***79*****:**128S-132S (1982).
21. J. Uitto. Biology of dermatological cells and extracellular matrix. In: T. B. Fitzpatrick, A. Z. Eisen, K. Wolff, I. M. Freedberg and K. F. Austen (eds.), *Dermatology in General Medicine*. McGraw-Hill, New York, 1993, pp. 221-240.
22. L. C. Sperling. Hair anatomy for the clinician. *J. Am. Acad. Dermatol.* ***25*****:**1-17 (1991).
23. U. Blume, J. Ferracin, M. Vershoore, J. M. Czernielewski and H. Schaefer. Physiology of the vellus hair follicle: Hair growth and sebum excretion. *Br. J. Dermatol.* ***124*****:**21-28 (1991).
24. D. Saint-Leger. Physiology of the pilosebaceous follicle. *Rev. Prat.* ***43*****:**2315-2319 (1994).
25. R. C. Wester and H. I. Maibach. Animal Models for Percutaneous Absorption. In: V. P. Shaw, and H. I. Maibach (eds.), *Topical Drug Bioavailability, Bioequivalence and Penetration*. Plenum Press, New York, 1993, pp. 333-350.
26. P. M. Elias. Epidermal lipids, barrier function and desquamation. *J. Invest. Dermatol.* ***80*****:**44S-49S (1983).
27. M. E. Stewart and D. T. Downing. Chemistry and function of mammalian sebaceous lipids. *Adv. Lipid Res.* ***24*****:**263-301 (1991).
28. G. F. Odland. A submicroscopic granular component in human epidermis. *J. Invest. Dermatol.* ***34*****:**11-15 (1960).
29. K. Hashimoto and T. Kanzaki. Surface ultrastructure of human skin. *Acta Derm. Venerol.* ***55*****:**413-430 (1975).
30. C. Cullander and R. H. Guy. Routes of delivery: Case studies; Transdermal delivery of peptides and proteins. *Adv. Drug Deliv. Rev.* ***8*****:**291-329 (1992).
31. A. P. Bertolino, L. M. Klein and I. M. Freedberg. Biology of hair follicles. In: T. B. Fitzpatrick, A. Z. Eisen, K. Wolff, I. M. Freedberg and K. F. Austen (eds.), *Dermatology in General Medicine*. McGraw-Hill, New York, 1993, pp. 289-293.
32. H. Schaefer and J. Lademann. The role of follicular penetration - A differential view. *Skin Pharmacol. Appl. Skin Physiol.* ***14 Suppl. 1*****:**23-27 (2001).

33. P. A. Viragh and M. Meuli. Human scalp hair follicle development from birth to adulthood: statistical study with special regard to putative stem cells in the bulge and proliferating cells in the matrix. *Arch. Dermatol. Res.* ***287*****:**279-284 (1995).
34. K. Hashimoto and S. Shibazaki. Ultrastructural Study on Differentiation and Function of Hair. In: T. Kobori, W. Montagna, K. Toda, Y. Ishibashi, Y. Hori, and F. Morikawa (eds.), *Biology and Disease of the Hair*, University of Tokyo Press, Tokyo, 1976, pp. 23-57.
35. H. B. Chase. Growth of the hair. *Phys. Rev.* ***34*****:**113-126 (1954).
36. K. S. Stenn and R. Paus. Controls of hair follicle cycling. *Physiol. Rev.* ***81*****:**449-494 (2001).
37. E. Fuchs, B. J. Merrill, C. Jamora and R. DasGupta. At the roots of a never-ending cycle. *Dev. Cell* ***1*****:**13-25 (2001).
38. A. A. Panteleyev, C. A. B. Jahoda and A. M. Christiano. Hair follicle predetermination. *J. Cell Sci.* ***114*****:**3419-3431 (2001).
39. N. Kitson and E. W. van-Lennep. Intercellular junctions and the permeability barrier in human sebaceous glands. *Br. J. Dermatol.* ***110*****:**601-606 (1984).
40. R. Agarwal, O. P. Katare and S. P. Vyas. The pilosebaceous unit: A pivotal route for topical drug delivery. Methods Find. Exp. Clin. Pharmacol. ***22*****:**129-133 (2000).
41. E. J. Lowenstein. Isotretinoin made S.M.A.R.T. and simple. *Cutis* ***70*****:**115-120 (2002).
42. M. H. Hardy. The secret life of hair follicle. *Trends Genet.* ***8*****:**55-61 (1992).
43. T. J. Ryan. Cutaneous circulation. In: L. A. Goldsmith (ed.), *Physiology, Biochemistry and Molecular Biology of the skin.* Oxford Press, Oxford, 1991, pp. 10190-1084.
44. V. Alexeev, O. Igoucheva, A. Domashenko, G. Cotsarelis and K. Yoon. Localized *in vivo* genotypic and phenotypic correction of the albino mutation in skin by RNA-DNA oligonucleotide. *Nature Biotechnol.* ***18*****:**43-47 (2000).
45. K. Hashimoto, M. Ito and Y. Suzuki. In: C. E. Orfanos and R. Happle (eds.), *Hair and Hair Diseases.* Springer, 1990, pp. 117-147.
46. G. Cotsarelis and S. E. Millar. Towards a molecular understanding of hair loss and its treatment. *Trends Mol. Med.* ***7*****:**293-301 (2001).
47. K. Moser, K. Kriwet, A. Naik, Y. N. Kalia and R. H. Guy. Passive skin penetration enhancement and its quantification in vitro. *Eur. J. Pharm. Biopharm.* ***52*****:**103-112 (2001).
48. J. C. Keister and G. B. Kasting. The use of transient diffusion to investigate transport pathways through skin. *J. Control. Release* ***4*****:**111-117 (1986).
49. R. J. Scheuplein. Mechanism of percutaneous absorption. II. Transient diffusion and the relative importance of various routes of skin penetration. .*J Invest. Dermatol.* ***48*****:**79-88 (1967).
50. R. J. Feldman and H. Maibach. Regional variations in percutaneous penetration of ^{14}C-cortisol in man. *J Invest Dermatol.* ***48*****:**181-183 (1967).
51. J. Kao, J. Hall and Helman G.. In vitro percutaneous absorption in mouse skin: Influence of skin appendages. *Toxicology and Applied Pharmacology* ***94*****:**93-103 (1988).
52. H. Schaefer, F. Watts, J. Brod and B. Illel. Follicular penetration. In: Scott, R. C., Guy, R. H., and Hadgraft, J. (eds.), *Prediction of Percutaneous Penetration; Methods, Measurements, Modelling*. IBC Technical Services, 1990, pp. 163-173.
53. J. Wepierre, O. Doucet and J. P. Marty. Percutaneous absorption of drugs in vitro: Role of transepidermal and transfollicular routes. In: R.C. Scott, R. H. Guy and J. Hadgraft (eds.), *Prediction of percutaneous penetration; methods measurements modelling*, IBC Technical Services, 1990, pp. 129-134.
54. L. M. Lieb, A. P. Liimatta, R. N. Bryan, B. D. Brown and G. G. Krueger. Description of the intrafollicular delivery of large molecular weight molecules to follicles of human scalp skin in vitro. *J. Pharm. Sci.* ***86*****:**1022-1029 (1997).
55. A. C. Lauer, L. M. Lieb, C. Ramachandran, G. L. Flynn and N. D. Weiner. Transfollicular drug delivery. *Pharm. Res.* ***12*****:**179-186 (1995).
56. R. C. Wester, J. Christoffel, T. Hartway, N. Poblete, H. I. Maibach and J. Forsell. Human cadaver skin viability for in vitro percutaneous absorption: Storage and detrimental effects of heat-separation and freezing. *Pharm. Res.* ***15*****:**82-84 (1998).
57. M. Bartek and J. A. LaBudde. Skin permeability *in vivo*: Comparison in rat, rabbit, pig and man. *J. Invest. Dermatol.* ***58*****:**114-123 (1972).
58. J. R. Bond and B. W. Barry. Limitations of hairless mouse skin as a model for *in vitro* permeation studies through human skin: Hydration damage. *J. Invest. Dermatol.* ***90*****:**486-489 (1988).
59. J. R. Bond and B. W. Barry. Hairless mouse skin is limited as a model for assessing the effects of peneration enhancers in human skin. *J. Invest. Dermatol.* ***90*****:**810-813 (1988).
60. A. Rougier, C. Lotte and H. I. Maibach. The hairless rat: a relevant animal model to predict *in vivo* percutaneous absorption in humans? *J. Invest. Dermatol.* ***88*****:**577-581 (1987).

61. S. A. Hotchkiss, M. A. Chidgey, S. Rose and J. Caldwell. Percutaneous absorption of benzyl acetate through rat skin in vitro. 1. Validation of an in vitro model against in vivo data. *Food Chem. Toxicol.* ***28*****:**443-447 (1990).
62. S. A. Hotchkiss, P. Hewitt, J. Caldwell, W. L. Chen and R. R. Rowe. Percutaneous absorption of nicotinic acid, phenol, benzoic acid, and triclopyr butoxyethyl ester through rat and human skin in vitro: further validation of an in vitro model by comparison with in vivo data. *Food Chem. Toxicol.* ***30:***891-899 (1992).
63. Y. B. Huang, L. R. Hsu, P. C. Wu, H. M. Ko and Y. H. Tsai. Crude drug (zingiberaceae) enhancement of percutaneous absorption of indomehtacin: in vitro and in vivo permeation. *Gaoxiong Yi Xue Ke Xue Za Zhi* ***9:***392-400 (1993).
64. T. Ogiso, Y. Ito, M. Iwaki and H. Atago. Absorption of indomethacin and its calcium salt through rat skin: effect of penetration enhancers and relationship between in vivo and in vitro penetration. *J. Pharmacobiodyn.* ***9:***517-525 (1986).
65. R. L. Bronaugh and H. I. Maibach. Percutaneous absorption of nitroaromatic compounds: in vivo and in vitro studies in the human and monkey. *J. Invest. Dermatol.* ***84*****:**180-183 (1985).
66. M. P. Carver, P. L. Williams and J. E. Riviere. The isolated perfused porcine skin flap. III. Percutaneous absoption pharmacokinetics of organophosphates, steroids, benzoic acid, and caffeine. *Toxicol. Appl. Pharmacol.* ***97*****:**324-337 (2002).
67. R. C. Wester, J. Melendres, L. Sedik, H. Maibach and J. E. Riviere. Percutaneous absorption of salicylic acid, theophylline, 2, 4-dimethylamine, diethyl hexyl phthalic acid, and p-aminobenzoic acid in the isolated perfused porcine skin flap compared to man in vivo. *Toxicol. Appl. Pharmacol.* ***151*****:**159-165 (1998).
68. H. Wagner, K. H. Kostka, C. M. Lehr and U. F. Schaefer. Human skin penetration of flufenamic acid: in vivo/in vitro correlation (deeper skin layers) for skin samples from the same subject. *J. Invest. Dermatol.* ***118*****:**540-544 (2002).
69. F. Benech-Kieffer, W. J. Meuling, C. Leclerc, L. Roza, J. Leclaire and G. Nohynek. Percutaneous absorption of Mexoryl SX in human volunteers: comparison with in vitro data. *Skin Pharmacol. Appl. Skin Physiol.* ***16*****:**343-355 (2003).
70. H. Tang, D. Blankschtein and R. Langer. Effects of low-frequency ultrasound on the transdermal permeation of mannitol: comparative studies with in vivo and in vitro skin. *J. Pharm. Sci.* ***91*****:**1776-1794 (2002).
71. D. W. Osborne and D. A. Hatzenbuhler. The influence of skin surface lipids on topical formulations. In: D. W. Osborne and A. H. Amann (eds.), *Topical Drug Delivery Formulations*. Marcel Dekker, New York, 1990, pp. 69-85.
72. J. E. Wahlberg. Transepidermal or transfollicular absorption? *Acta derm.-venereol.* ***48*****:**336-344 (1968).
73. L. M. Lieb, C. Ramachandran, K. Egbaria and N. D. Weiner. Topical delivery enhancement with multilamellar liposomes into pilosebaceous units: I. In vitro evaluation using fluorescent techniques with the hamster ear model. *J. Invest. Dermatol* ***99*****:**108-113 (1992).
74. B. Kammerau, A. Zesch and H. Schaefer. Absolute concentrations of dithranol and triacetyl-dithranol in the skin layers after local treatment: *in vivo* investigations with four different types of pharmaceutical vehicles. *J. Invest. Dermatol.* ***64*****:**145-149 (1975).
75. E. Touitou, V. M. Meidan and E. Horwitz. Methods for quantitative determination of drug localized in the skin. *J. Control. Release* ***56*****:**7-21 (1998).
76. W. G. Reifenrath, G. S. Hawkins and M. S. Kurtz. Percutaneous penetration and skin retention of topically applied compounds: an *in vitro-in vivo* study. *Pharm. Sci.* ***80*****:**526-532 (1991).
77. J. C. Tsai, G. L. Flynn, N. Weiner and J. J. Ferry. Influence of application time and formulation reapplication on the delivery of minoxidil through hairless mouse skin as measured in Franz diffusion cells. *Skin Pharmacol.* ***7*****:**270-277 (1994).
78. N. G. Turner and R. H. Guy. Visualization and quantitation of iontophoretic pathways using confocal microscopy. *J. Invest. Dermatol. Symp. Proc.* ***3*****:**136-142 (1998).
79. N. G. Nerella and J. K. Drennen. Depth-resolved near-infrared spectroscopy. *Appl. Spectrosc.* ***50*****:**285-291 (1996).
80. P. Corcuff and G. E. Pierard. Skin imaging: State of the art at the dawn of the year 2000. *Skin Bioeng.* ***26*****:**1-11 (1998).
81. S. Richard, B. Querleux, J. Bittoun, I. Idy-Peretti, O. Jolivet, E. Cermakova and J. L. Leveque. In vivo proton relaxation times analysis of the skin layers by magnetic resonance imaging. *J. Invest. Dermatol.* ***97*****:**120-125 (1991).
82. H. K. Song, F. W. Wehrli and J. F. Ma. In vivo MR microscopy of the human skin. *Magn. Reson. Med.* ***37*****:**185-191 (1997).

83. M. Szayna and W. Kuhn. In vivo and in vitro investigations of hydration effects of beauty care products by high-field MRI and NMR microscopy. *J. Eur. Acad. Dermatol. Venerol.* ***11*****:**122-128 (1998).
84. R. H. Bull, D. O. Bates and P. S. Mortimer. Intravital video-capillaroscopy for the study of the microcirculation in psoriasis. *Br. J. Dermatol.* ***126*****:**436-445 (1992).
85. J. L. Morris. Cotransmission from sympathetic vasoconstrictor neurons to small cutaneous arteries in vivo. *Am. J. Physiol. Heart Circ. Physiol.* ***46*****:**H58-H64(1999).
86. T. Salmon, R. A. Walker and N. K. Pryer. Advances in Microscopy-Part III; Video-Enhanced Differential Interference Contrast Light Microscopy. *Biotechniques* ***7*****:**624-633 (1989).
87. A. W. B. Stanton, H. S. Patel, J. R. Levick and P. S. Mortimer. Increased dermal lymphatic density in the human leg compared with the forearm. *Microvasc. Res.* ***57*****:**320-328 (1999).
88. D. H. Turnbull, B. G. Starkoski, K. A. Harasiewicz, J. L. Semple, L. From, A. K. Gupta, D. N. Sauder and F. S. Foster. 40-100 MHz B-SCAN ultrasound backscatter microscope for skin imaging. *Ultrasound Med. Biol.* ***21*****:**79-88 (1995).
89. D. Aghassi, R. R. Anderson and S. Gonzalez. Time-sequence histologic imaging of laser-treated cherry angiomas with in vivo confocal microscopy. *J. Am. Acad. Dermatol.* ***43*****:**37-41 (2000).
90. C. Bertrand and P. Corcuff. In vivo spatio-temporal visualization of the human skin by real-time confocal microscopy. *Scanning.* ***16*****:**150-154 (1994).
91. P. Corcuff, C. Bertrand and J. L. Leveque. Morphometry of human epidermis in vivo by real-time confocal microscopy. *Arch. Dermatol. Res.* ***285*****:**475-481 (1993).
92. C. Cullander. Light microscopy of living tissue: the state and future of the art. *J. Invest. Dermatol. Symp. Proc.* ***3*****:**166-171 (1998).
93. B. S. Grewal, A. Naik, W. J. Irwin, G. Gooris, G. J. de-Grauw, H. G. Gerritsen and J. A. Bouwstra. Transdermal macromolecular delivery: Real-time visualization of iontophoretic and chemically enhanced transport using two-photon excitation microscopy. *Pharm. Res.* ***17*****:**788-795 (2000).
94. A. J. Hoogstraate, C. Cullander, J. F. Nagelkerke, F. Spies, J. Verhoef, A. H. G. J. Schrijvers, H. E. Junginger and H. E. Bodde. A novel in-situ model for continuous observation of transient drug concentration gradients across buccal epithelium at the microscopical level. *J. Control. Release* ***39*****:**71-78 (1996).
95. M. Rajadhyaksha, S. Gonzalez, J. M. Zavislan, R. R. Anderson and R. H. Webb. In vivo confocal scanning laser microscopy of human skin II: Advances in instrumentation and comparison with histology. *J. Invest. Dermatol.* ***113*****:**293-303 (1999).
96. P. J. Caspers, G. W. Lucassen, R. Wolthuis, H. A. Bruining and G. J. Puppels. In vitro and in vivo Raman spectroscopy of human skin. *Biospectroscopy* ***4*****:**S31-S39(1998).
97. P. J. Caspers, G. W. Lucassen, E. A. Carter, H. A. Bruining and G. J. Puppels. In vivo confocal Raman microspectroscopy of the skin: Noninvasive determination of molecular concentration profiles. *J. Invest. Dermatol.* ***116*****:**434-442 (2001).
98. A. C. Lauer, C. Ramachandran, L. M. Lieb, S. Niemiec and N. D. Weiner. Targeted delivery to the pilosebaceous unit via liposomes. *Adv. Drug Del. Rev.* ***18*****:**311-324 (1996).
99. L. Li, R. M. Hoffman and V. Lishko. Liposomes can specifially target entrapped melanin to hair follicles in histocultured skin. *In Vitro Cell Dev. Biol.* ***29A*****:**192-194 (1993).
100. N. Weiner. Targeted follicular delivery of macromolecules via liposomes. *Int. J. Pharm.* ***162*****:**29-38 (1998).

II

A new method to determine the distribution of a fluorophore in scalp skin with focus on hair follicles

*YY Grams and JA Bouwstra. Pharmaceutical Research **19** (3): 350 – 354 (2002)*

INTRODUCTION

The contribution of the follicular pathway for passive transdermal drug penetration is still unclear. In literature it has been discussed that the characteristic of the formulation and/or of the drug itself is crucial for the delivery and absorption process (1-8). In developing new dermal delivery systems especially focused on local targeting in the skin, quantification of substances in the various compartments of the skin is important. Recently skin imaging techniques (9) and quantification procedures used in skin research (10) have been summarised.

Quantitative access to deposition of substances in the follicular region is a challenging task, since the hair follicle extends down into the subcutaneous fat. The distribution profiles of compounds were mostly determined by tape stripping in combination with biopsies (11), immunohistochemical analysis (5,12) or isolation and dissolution of skin parts (12). However, these techniques limit the analysis of label distribution to the skin surface and bear the danger of delocalisation of the label due to fixation procedures. Non-invasive methods of quantification such as depth-resolved near-IR spectroscopy have unfortunately still an insufficient resolution (31 µm) for the detailed visualisation of the hair follicle (13). Turner and Guy (14) have published relative quantification data in the follicular region of cryo-fixed hairless mouse skin using Confocal Laser Scanning Microscopy (CLSM). However, details of the fluorophore distribution in the various parts of the hair follicle were not reported which is essential for the understanding of the transport route of a substance into the skin and the hair follicle.

The advantage of CLSM is its high resolution and the possibility to circumvent tissue fixation, thereby avoiding label delocalisation during the preparation method. Furthermore the label distribution can be visualised in deeper layers of the skin using optical cross-sections. The objective of this paper is to introduce a new method of relative quantification with CLSM. This method enables the determination of the degree of accumulation in the stratum corneum, epidermis, dermis, outer root sheath, inner root sheath, cuticular area and hair shaft as a first quantitative step in non-fixed fresh human scalp skin.

MATERIALS AND METHODS

Materials

Bodipy® 564/570 C_5 (B564) was purchased from Molecular Probes, Netherlands. Fresh human scalp skin from patients aged 45 to 66 years was

obtained within three hours after cosmetic surgery. The pieces were temporarily stored on a filter paper soaked with phosphate buffered saline (PBS) at pH 7.4 (139 mM NaCl, 2.5 mM KCl, 8 mM Na_2HPO_4, 1.5 mM KH_2PO_4, 25 mg/L Streptomycin and 25000 U/l Penicillin). Flow-through diffusion cells prepared from Kel-F (Chlorotrifluoroethylene) were used made by the Fine Mechanical Department at the Gorlaeus Laboratories in Leiden.

Methods

In vitro delivery experiments

Upon arrival in our laboratory the skin was directly dermatomed to a thickness of 1100 μm +/- 150 μm, equivalent to the total thickness of epidermis and dermis. The skin surface was cleaned and the skin mounted in the diffusion cell with a supporting membrane (dialysis membrane, MW cut off 50000, SpectraPor). The donor phase consisted of a saturated B564 solution (5.5 μg/ml) in 50 mM citric acid buffer pH 5.0 (CAB) containing 30% (v/v) ethanol. The spectrum of our selected model penetrant is insensitive to pH and solvent polarity according to the manufacturer. The acceptor phase consisted of PBS at pH 7.4. It was pumped at a flow rate of 2.0 +/- 0.2 ml/h. After 18 hours of diffusion, the label was removed from the donor compartment and the skin was washed with and excess of purified water. In order to determine autofluorescence a skin piece without label was analysed from each donor. In a pilot experiment CAB containing 30% (v/v) ethanol without dye served as control for permeation and visualisation.

Visualisation by Confocal Laser Scanning Microscopy (CLSM)

The confocal microscope consisted of a Bio-Rad MRC 600 unit, equipped with a HeNe laser (543 nm). The microscopic unit was an inverted Zeiss IM-35. Fixed microscopic settings of the CLSM were used, whereas the laser intensity varied between 3 and 30% of its total intensity. At the fixed settings autofluorescence did not interfere with our measurements.

After completion of the diffusion experiments the skin was directly transferred to the confocal microscope. The skin was visualised in the x/y-direction parallel to the skin surface and at the bottom edge (dermis side of the skin). In order to obtain a cross-sectional view, the unfixed skin was manually cut perpendicular to the surface of the skin using a device modified from Meuwissen *et al.* (15). This cross sectional view allows the visualisation of the compound with increasing depth and parallel to the hair shaft circumventing the scattering and absorption drawback. Follicular images were obtained either from the bottom or the cross sectional perspective at a depth of 800 – 1100 μm. Investigated skin

areas are the stratum corneum, epidermis, dermis, outer and inner root sheath, cuticle and the hair shaft.

Relative quantification: Calculation of the relative accumulation factor (f_{acc})

For the final calculations at least 3 different donors have been analysed. The general calculation procedure follows the scheme depicted in Figure 1. Capital letters (A-F) in the figure correspond to the equivalent calculation step described below in this section.

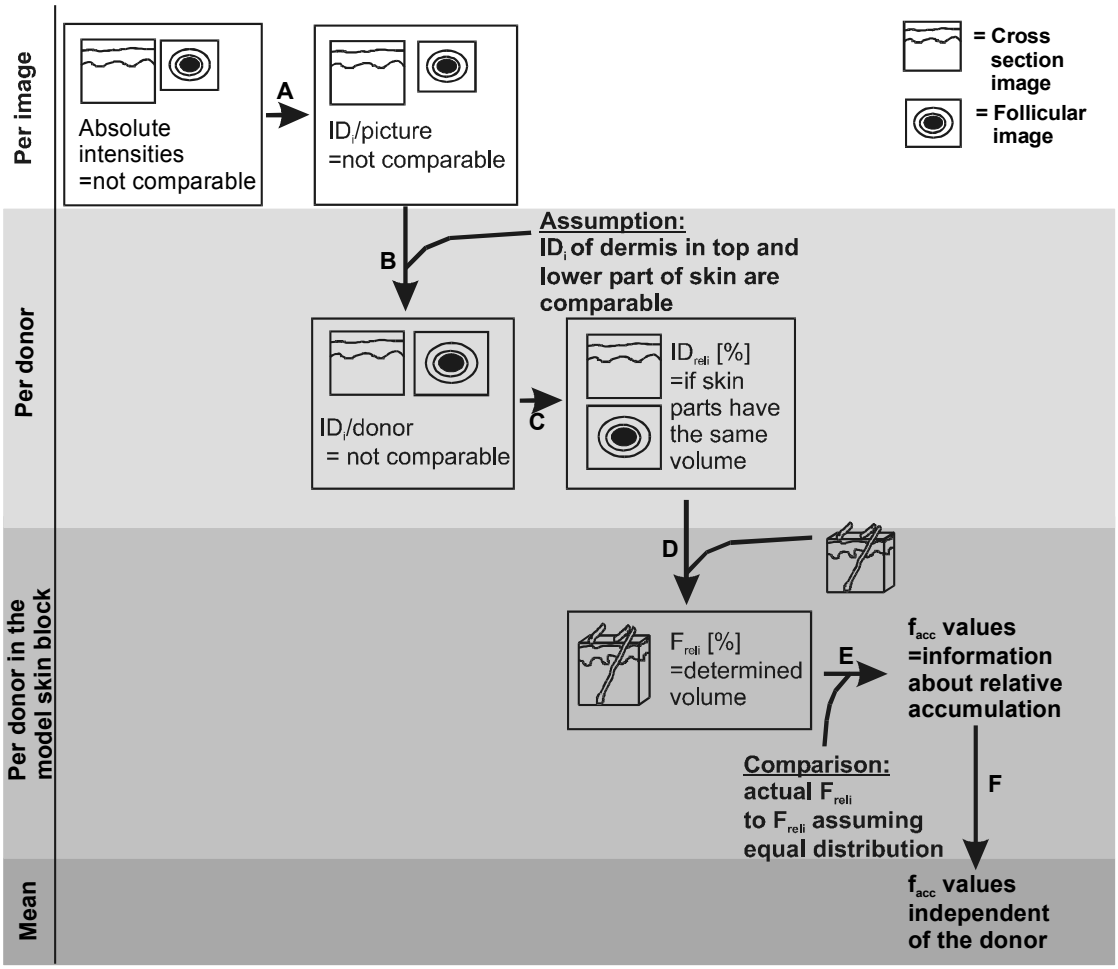

Figure 1. *Scheme of the relative quantification of the label distribution in human scalp skin. Average fluorescence intensities are obtained from CLSM images (cross section and follicular image). (A) The ID_i is calculated for every skin part and (B) scaled for every donor (C) followed by the determination of the relative ID in %. (D) For every donor the F_{rel} is determined by incorporating specific volumes of an assumed skin block (1.1*1.1*1.1 mm^3). (E) The f_{acc} value is obtained for every donor by comparing the actual F_{rel} with the F_{rel} at equal distribution (= V_{rel}). (F) The f_{acc} values are averaged over different donors. ID_i = intensity density in part i of the skin, ID_{rel} = relative ID, F_{rel} = relative fluorescence, V_{rel} = relative volume.*

A. Calculation of the Intensity Density (ID_i) of every area in each picture

The CoMOS software (Bio-Rad) of the CLSM is based on grey-scaling and provides the average intensity per pixel (I_{av}), the area (A) in μm^2, the number of pixels (n_{pix}) and the total pixel value of a selected area. The total pixel value provided by the CoMOS software is the integrated pixel intensity (IPI) of the selected area, which is calculated according to equation 1.

$$IPI = I_{av} * n_{pix} \quad (1)$$

The intensity density (ID) of the selected area normalises the Intensity to μm^2 and can directly be calculated from the provided information (equation 2).

$$ID = IPI / A \quad (2)$$

Since the intensity per pixel is in fact the integral intensity over a certain depth in the z-direction perpendicular to the optical cross section, which is the resolution in z-direction (1-2 μm), the intensity density is not per unit area but per unit volume. In our calculation we assume that this “band width” of the confocal image in z-direction is the same for the different parts in the tissue when pinhole and objective are kept constant.

B. Combination of the surface pictures with the follicle pictures of one donor

From the two types of images (follicle, surface) the relative intensity densities ($ID_{rel\ i}$) have to be calculated. Since the dermis is present in both pictures, the ID_i of the dermis has been used as scaling instrument. In doing so, we assume that the distribution within the dermis is independent of depths and that the ID`s are independent from the image direction accepting minimal underestimation of accumulation in the top layers.

C. Calculation of the relative intensity density ($ID_{rel\ i}$) for part i of the skin in %

After averaging the ID_i's for each area, the sum of all ID_i's can be calculated ($ID_{i\ tot}$). The relative intensity density ($ID_{rel\ i}$) per area of interest is then calculated as follows (equation 3):

$$ID_{rel\ i} = ID_i / ID_{tot\ i} * 100\% \quad (3)$$

In fact these values provide the relative intensity distribution in the various parts of the skin assuming that all areas occupy the same volume.

D. Calculation of the relative fluorescence ($F_{rel\ i}$) for part i of the skin

For calculating the relative fluorescence for part i of the skin, the relative volumes occupied by each area of interest have to be estimated. For this purpose we assumed a skin block of a standard size (1.1 mm * 1.1 mm * 1.1 mm) with n follicles. In order to decompose this volume in the various regions the size of each area was determined from confocal pictures (Table I), whereas the number of follicles was counted (160/cm^2). The volumes of the various follicular areas have been approached by assuming a cylindrical shape perpendicular to the skin surface. Microscopically the cuticle of the follicle and of the hair could not be distinguished. Therefore both cuticles will be referred to as cuticle.

In order to be able to determine the integral relative fluorescence $F_{rel\ i}$ of each skin part, the total volume and the volume of each part of the skin were calculated (Table I). The calculated relative intensity density per μm^3 of each part of the skin has to be multiplied by its calculated volume to obtain the total relative intensity in that area. Since we are interested in the contribution of each part to the total relative intensity in the skin, we divide the total relative intensity of each part ($ID_{rel\ i}*V_i$) by the total relative intensity of the tissue ($\Sigma\ (ID_{rel\ i}*V_i)$) (equation 4). The sum of the relative fluorescence of all the skin parts is 1 (equation 5) and can be expressed as percentage (equation 6). V_i is the volume of part i of the skin whereas $F_{rel\ i}$ is the relative fluorescence of part i of the skin.

$$F_{rel\,i} = \frac{ID_{rel\,i} * V_i}{\Sigma(ID_{rel\,i} * V_i)} \tag{4}$$

$$\Sigma F_{rel\,i} = 1 \tag{5}$$

$$\Sigma F_{rel\,i} * 100 = 100\% \tag{6}$$

The percentage $F_{rel\ i}$ value gives only information about the integral relative amount of intensity in the volume of a certain area compared to the total relative amount of the intensity in the assumed skin block. That means, it includes the relation between the volume of a certain region to the total volume.

E. Calculation of the accumulation factor ($f_{acc\ i}$) for part i of the skin

In order to obtain information about the degree of accumulation in each skin part, we have to go one step further. The actual relative distribution values

($F_{rel\ i}$) have to be compared to the relative distribution assuming no accumulation in any part of the skin. In the latter situation, the distribution value ($F_{rel\ i}$) should be the same as the percentage of the respective volume compared to the total volume ($V_{rel\ i}$). Dividing the relative fluorescence ($F_{rel\ i}$) by the relative volume ($V_{rel\ i}$) in % leads to an accumulation factor (f_{acc}) for each examined part of the skin:

$$f_{acc\ i} = \frac{F_{rel\ \ i} \quad (in\ \%)}{V_{rel\ \ i} \quad (in\ \%)} \tag{7}$$

If the compound is equally distributed in all skin parts, the accumulation factor ($f_{acc\ i}$) for all parts would be 1. If the relative distribution value ($F_{rel\ i}$) is higher than the equal distribution value (expressed in $V_{rel\ i}$ [%]), i.e. a value above 1, label accumulation in the selected part is present.

F. Averaging the f_{acc}'s from all donors

At this point, the accumulation factors of the different donors can be averaged and the standard deviation can be calculated. This enables as well the statistical analysis. It is important to realise that from the accumulation factor no conclusions can be drawn about the absolute amounts of the penetrant in the skin.

RESULTS

The lipophilic B564 exhibited very bright staining of the epidermis, whereas the stratum corneum and the dermis showed a lower content of dye (Figure 2A). The hair follicle, which reaches down into the dermis reveals a characteristic staining. Whereas the outer root sheath and the cuticular area exhibits staining, only a low amount of label was detected in the inner root sheath and hardly any label was seen in the hair shaft itself (Figure 2B).

When calculating the relative fluorescence intensity ($F_{rel\ i}$) according to equation 4, 77% of the label is located in the dermis (Table I) although in the image only low fluorescence intensity was observed in this region. 10% of the total relative fluorescence was estimated in the epidermis and less than 1% in the stratum corneum of the model skin block. The hair follicle including the hair shaft contains 12% of the total relative fluorescence. Therefore the relative fluorescence intensity values give access to the relative content of a target area. However, they do not represent a sensitive means to investigate the changes in

accumulation of the label in certain skin areas, since due to the limited follicular volume, the total amount of fluorescence in the follicular area is limited.

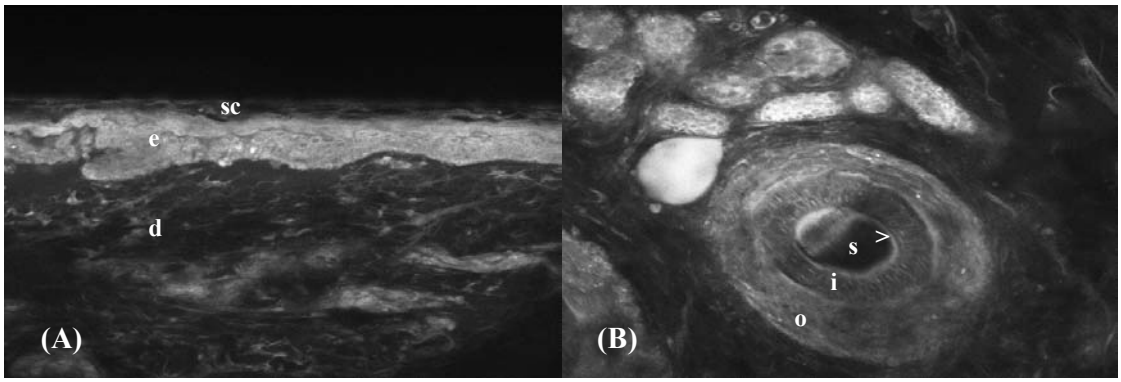

***Figure 2**. Distribution of B564 in fresh human scalp skin. In the cross sectional view (A) the stratum corneum (sc), the epidermis (e) and the dermis (d) are visualised. In the parallel view from the dermis side of the skin (B) a hair follicle with its characteristic areas, outer root sheath (o), inner root sheath (i), cuticular area (>) and the hair shaft (s) as well as a sweat gland (g) and the dermis (d) is depicted.*

***Table I.** Measured thickness or radius and calculated volumes of the different parts of the skin from 20 CLSM images for the determination of the relative fluorescence intensity values ($F_{rel\ i}$). $V_{rel\ i}$ is the relative volume of part i of the skin. Determined $F_{rel\ i}$ values of B564 in various skin parts after 18 hours penetration of 0.025% dye from CAB containing 30% (v/v) ethanol are shown as well.*

	Stratum corneum	Epidermis	Dermis	Outer root sheath	Inner root sheath	Cuticle	Shaft
Thickness [µm]	8.4	50.9	1040.7	50.4	28.0	4.0	
Radius [µm]							31.9
Volume [10^6 µm^3]	9.5	57.6	1178.4	59.0	18.3	1.8	6.7
$V_{rel\ i}$ [%]	0.7	4.3	88.5	4.4	1.4	0.1	0.5
$F_{rel\ i}$ [%]	0.8	10.1	76.7	9.6	2.1	0.2	0.5

Focussing on the relative accumulation, f_{acc} values of 2.3 for the epidermis, 2.2 for the outer root sheath, 1.5 for the inner root sheath and 1.8 for the cuticular area were determined (Figure 3). These values which are above 1.0 indicate accumulation of the dye in these areas. The stratum corneum and the

hair shaft exhibited values, which were not different from 1.0, while a relative accumulation value below 1.0 has been detected for the dermis indicating no accumulation.

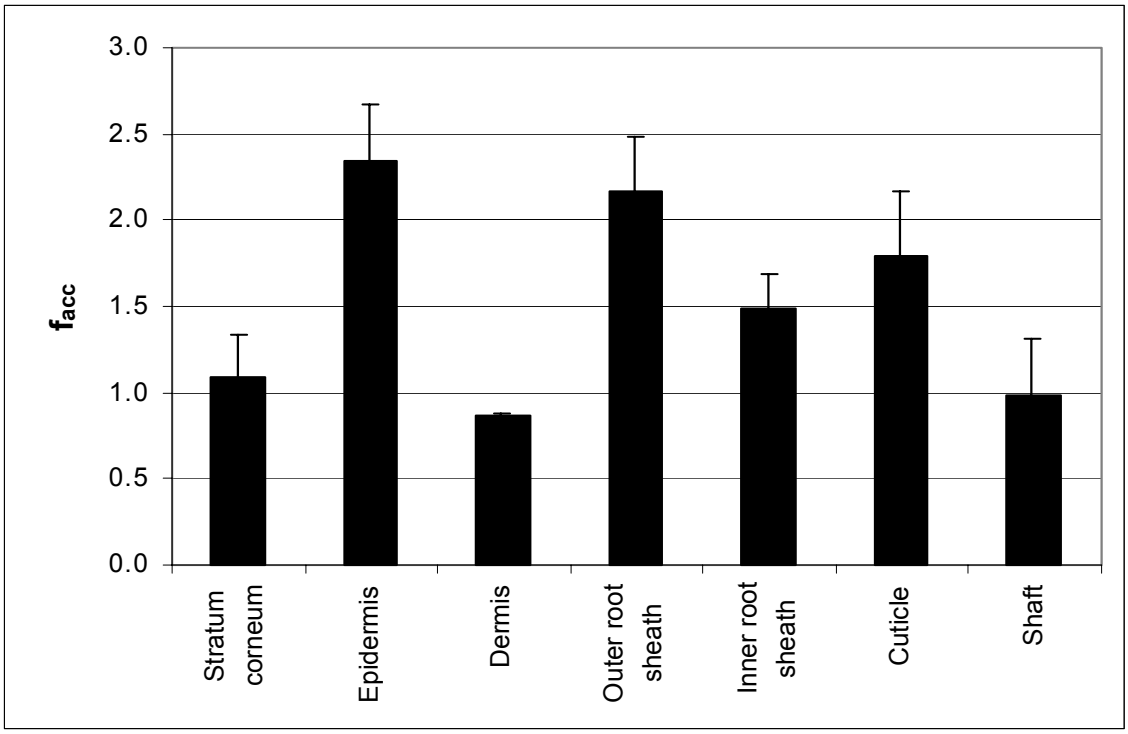

Figure 3. *Relative accumulation values (f_{acc}) of B564 from citric acid buffer pH 5.0 containing 30% (v/v) ethanol (EtOH) are depicted after application of 0.025% (w/v) label on 4 different donors.*

DISCUSSION

In stratum corneum B564 (log $P_{oct/wat}$ value of 4 at pH 5.0) penetrates mainly paracellular in the lipid regions. Since no label was detected inside the corneocytes only a small relative accumulation value in this skin barrier was determined. The adjacent viable epidermis is much brighter stained than the stratum corneum. In the viable epidermis, the cornified envelope has not been developed yet, which allows the label to permeate into the (Figure 2A). The deeper layer of the skin (dermis) shows only slight labelling (Figure 2A and B) and no accumulation of the dye (Figure 3). However parts of the hair follicle which are situated in this part of the dermis exhibit increased accumulation values, namely the outer root sheath and the cuticular area. These results lead to the discussion whether the dermis has a low affinity for the fluorophore or whether the hair follicle represents a favoured penetration route for the lipophilic B564. Since it is known from literature, that various small substances (14,16,17), charged lower molecular weight dextrans (5) and adapalene-loaded

microspheres with a diameter of 5 μm (6) showed increased penetration via the follicular route, it might also be the case for B564.

In order to obtain a tool for the elucidation of the follicular distribution, the qualitative visualisation via Confocal Laser Scanning Microscopy was extended by quantifying the relative dye distribution in the hair follicle. In CLSM an absolute quantification of label concentration within a certain skin area is impossible (18).

During relative quantification the bleaching of the fluorophores has to be minimised in CLSM. Bleaching of our dye is minimal, since even after 150 scans the reduction in fluorescence intensity was difficult to detect. In our studies 5 scans (Kalman) were used. Additionally short one-time exposures were chosen and z-scans were avoided. The thickness of the optical slice is also a crucial parameter in relative quantification. It depends on the objective used (magnification and numerical aperture) and the confocal aperture (pinhole). Therefore the same objective and pinhole are used during the visualisation studies.

In the course of the calculation procedure the CoMOS software determines the intensity of the marked pixels and the size of the marked area. Since the intensity density is expressed per μm^2, this value is independent of the pixel density and thus independent of the zoom used for the image. The assumed total volume of the skin block and the relative volumes of each skin part do not have any influence on the intensity density values. When evaluating the relative fluorescence (F_{rel}) data the more voluminous parts of the skin i.e. dermis and epidermis exhibit the highest relative fluorescence values. When focusing on targeting the hair follicle one aims at an increased accumulation of the investigated drug in the target area. Therefore the relative accumulation value (f_{acc}) gives more information about a certain skin and follicle region. However, it has to be noted that the F_{rel} and the f_{acc} are dependent on the relative volume of each skin region but independent of the assumed total volume of the skin block.

However, the relative quantification has certain limits. First, in case of small areas, the selection of this region on the computer screen might introduce some inaccuracy. This can result in an underestimation of the amount of label deposited in that specific area, e.g. cuticular region, stratum corneum. Secondly, relative accumulation values give no information regarding the absolute concentration in certain areas of interest. This means, that although the accumulation value for a certain region increases, the total amount of label in the skin might be decreased at the same time. Therefore, the relative accumulation values determined in this publication do not correlate with the total amount of label in the skin.

Turner and Guy (14) were the first to semi-quantitatively determine the amount of calcein in the follicular area after iontophoresis using CLSM. Only values obtained from one image were used for the determination of the different transport fractions. Images taken from the top were analysed semi-quantitatively

whereas the cross section images (manual or optical) were used for qualitative evaluation of the diffusion pathway. The resolution was limited to a non-follicular area, a follicular area and the hair shaft itself. With the analysis presented in this paper, follicular layers deep in the skin can be analysed thereby giving detailed information about the distribution and accumulation within the hair follicle.

The main advantage of this relative quantification method is that it enables numerical access to accumulation changes in various skin parts in deeper skin layers. Unfixed skin can be used minimising delocalisation of the dye and artefact formation in skin. Indirect comparison of two images from one donor is also possible. However this method requires fluorophores and one post-experimental cut of unfixed tissue which limits this method to *in vitro* and *ex vivo* studies. At this moment studies are in progress in our laboratory in order to examine the accumulation of various compounds and vehicles in the hair follicle. Different compounds and/or delivery vehicles will be compared to optimise a formulation. Hence, this analysis procedure can be of great advantage not only in the research of follicular targeting but also in local skin targeting.

ACKNOWLEDGMENTS

The authors thank Unilever Research, Port Sunlight, UK for financing this project.

REFERENCES

1. R. Agarwal, O.P. Katare, and S P. Vyas. The pilosebaceous unit: A pivotal route for topical drug delivery, Methods Find. Exp. Clin. Pharmacol. 22:129-133 (2000).
2. B. Illel. Formulation for transfollicular drug administration: Some recent advances, Crit. Rev. Ther. Drug Carrier Syst. 14:207-219 (1997).
3. A.C. Lauer, L.M. Lieb, C. Ramachandran, G.L. Flynn, and N.D. Weiner. Transfollicular drug delivery, Pharm. Res. 10:179-186 (1995).
4. A.C. Lauer, C. Ramachandran, L.M. Lieb, S. Niemiec, and N.D. Weiner. Targeted delivery to the pilosebaceous unit via liposomes, Adv. Drug Deliv. Rev. 18:311-324 (1996).
5. L.M. Lieb, A.P. Liimatta, R.N. Bryan, B.D. Brown, and G.G. Krueger. Description of the intrafollicular delivery of large molecular weight molecules to follicles of human scalp skin in vitro, J. Pharm. Sci. 86:1022-1029 (1997).
6. A. Rolland, N. Wagner, A. Chatelus, B. Shroot, and H. Schaefer. Site-specific drug delivery to pilosebaceous structures using polymeric microspheres, Pharm. Res. 10:1738-1744 (1993).
7. C.C. Sumian, F.B. Pitre, B.E. Gauthier, M. Bouclier and S.R. Mordon. A new method to improve penetration depth of dyes into the follicular duct: Potential application for laser hair removal, J. Am. Acad. Dermatol. 41:172-175 (1999).
8. N. Weiner. Targeted follicular delivery of macromolecules via liposomes, Int. J. Pharm. 162:29-38 (1998).
9. P. Corcuff, and G.E. Pierard. Skin imaging: State of the art at the dawn of the year 2000, Skin Bioeng. 26:1-11 (1998).
10. E. Touitou, V.M. Meidan, and E. Horwitz. Methods for quantitative determination of drug localized in the skin, J. Control. Release 56:7-21 (1998).
11. B. Kammerau, A. Zesch, and H. Schaefer. Absolute concentrations of dithranol and triacetyl-dithranol in the skin layers after local treatment: in vivo investigations with four different types of pharmaceutical vehicles, J. Invest. Dermatol. 64:145-149 (1975).

12. W.G. Reifenrath, G.S. Hawkins, and M.S. Kurtz. Percutaneous penetration and skin retention of topically applied compounds: an in vitro-in vivo study, J. Pharm. Sci. 80:526-532 (1991).
13. N.G. Nerella, and J.K. Drennen. Depth-resolved near-infrared spectroscopy. Appl. Spectrosc. 50:285-291 (1996).
14. N.G. Turner, and R.H. Guy. Visualization and Quantitation of Iontophoretic Pathways Using Confocal Microscopy, J. Invest. Dermatol. Symp. Proc. 3:136-142 (1998).
15. M. E. M. J. Meuwissen, J. Janssen, C. Cullander, H. E. Junginger and J. A. Bouwstra. A cross-section device to improve visualization of fluorescent probe penetration into the skin by Confocal Laser Scanning Microscopy, Pharm.l Res. 15:352-356 (1998).
16. F. Hueber, H. Schaefer, and J. Wepierre. Role of transepidermal and transfollicular routes in percutaneous absorption of steroids: in vitro studies on human skin, Skin Pharmacol. 7:237-244 (1994).
17. B. Illel, H. Schaefer, J. Wepierre, and O. Doucet. Follicles play an important role in percutaneous absorption, J. Pharm. Sci. 80:424-427 (1991).
18. M. Laurent, G. Johannin, N. Gilbert, L. Lucas, D. Cassio, P.X. Petit, and A. Fleury. Power and limits of laser scanning confocal microscopy, Biol. Cell 80:229-240 (1994).

III

Penetration and distribution of three lipophilic probes in vitro in human skin focussing on the hair follicle

YY Grams and JA Bouwstra. J Control Release. ***83*** *(2): 253-62 (2002)*

ABSTRACT

Fluorescent model substances of increasing lipophilicity (Oregon Green® 488, Bodipy® FL C5 and Bodipy® 564/570 C5) were selected to enable the visualisation in the skin using Confocal Laser Scanning Microscopy. After measuring the penetration for 18 hours, the non-fixed human scalp skin was imaged from the bottom parallel to the stratum corneum and in a cross section view perpendicular to the skin surface. The images were evaluated by calculating relative accumulation values for different penetrants. The studies indicate that the penetrated amount is highest for BFL (medium lipophilicity) and lowest for B564 (high lipophilicity) whereas B564 (high lipophilicity) reveals the highest relative accumulation in parts of the hair follicle compared to OG (low lipophilicity). The addition of 30 % (v/v) ethanol to the donor phase of substance with a low lipophilicity increases the follicular delivery. From our results we conclude that delivery to the hair follicle can be improved by increasing the drugs lipophilicity and optimising the composition of the donor phase. However, no conclusion can be drawn about the actual route of transport to the hair follicle.

INTRODUCTION

Local skin targeting is of interest for the pharmaceutical and the cosmetic industry. In case of skin diseases and in case of cosmetic products, delivery to sweat glands or to the pilosebaceous unit is essential for the effect of the drug. Local delivery can be improved by two approaches. First, the choice of formulation such as particulate carriers and variation in medium additives such as ethanol can optimise local targeting. Secondly, the physicochemical parameters of the drug itself, e.g. size, charge and lipophilicity, can affect the degree of delivery as well. In cases where formulation variation is not feasible, more attention has to be paid to the optimisation of the penetrant itself.

In the early years Scheuplein *et al*. [1,2] and Keister *et al.* [3] described the importance of the follicular pathway in the initial penetration process and its dependency on the membrane diffusion constant. Numerous studies followed presenting experimental data mainly based on permeation studies, which have been reviewed by Lauer *et al.* [4]. Up to now, various authors reported delivery to the hair follicle by variation of the formulation. Weiner *et al*. [5] summarised delivery studies of liposomal formulations, which showed enhanced delivery to the pilosebaceous unit for peptides, antibodies and DNA. In addition iontophoresis is also known to occur mainly via the follicular route where the stratum corneum barrier is non-continuous [6]. Next to liposomal or current related targeting, particles of 7 µm [7] or of 5 µm [8,9] were reported to be localised in the pilosebaceous unit after topical application. However titaniumoxide particles (size not stated) remain in the follicle orifice [10]. Lieb *et al.* [11] observed that large molecular weight dextrans and oligonucleotides were encountered in the hair follicle after topical application. Additionally they proposed that transport occurs between the inner and the outer root sheath namely the companion layer. The influence of ethanol on the delivery to the hair follicle has not been studied intensively. Tata *et al.* [12] and Touitou *et al.* [13] reported that the effect of minoxidil application is increased when using ethanol or ethanol in combination with vesicular systems with no information presented on the detailed localisation within the hair follicle. It has also been stated that the appendageal route contributes to the penetration when the vehicle contains propylene glycol, dimethylsulfoxide or ethanol [14].

In contrast to the influence of formulation, limited groups have studied the influence of drug lipophilicity on the effect of follicular deposition mainly focussing on permeation studies. Hueber *et al.* [15,16] reported a significant contribution of the pilosebaceous unit to the penetration of lipophilic drugs into the skin. The delivery to the pilosebaceous unit of hydrophilic low molecular weight model substances from various vehicles was studied by Lieb *et al.* [11]. They observed that liposomes were more effective than solutions containing

ethanol, propylene glycol or no additive. Reviews on the effect of vehicle, drug and available skin models on follicular delivery are given by Lauer *et al.* [4,17], Illel [18] and Agarwal *et al.* [19].

In the studies reported in literature, it is striking that frequently animal skin with post-experimental fixation has been used. During fixation either cryo-freezing or embedding have been used. Both methods bear the danger of delocalisation of the substance during fixation and modification of cell structures. In previous studies a method was introduced in which confocal laser scanning microscopy (CLSM) was used to visualise label localisation in 200 □m thick skin without embedding [20]. Very recently this method was extended to full thickness skin and combined with a new relative quantification model [21]. Advantages of this method are high resolution, no fixation or embedding thereby avoiding delocalisation of the dye, specific and sensitive detection due to use of fluorophores, visualisation of deeper skin layers due to optical sectioning and calculating changes of accumulation in skin layers. The disadvantages such as the necessity of dyes and the limitation to *in vitro* use do not interfere with this study. Additionally, it has to be pointed out that this method does not give any information about the absolute amount of permeant in the skin however information is obtained about changes in distribution and thus on delivery to various skin compartments. Therefore in the present study the influence of permeant lipophilicity on the penetration and distribution in non-fixed human scalp skin is examined using the new relative quantification method. Especially the influence of permeant lipophilicity on the delivery of model substances to the hair follicle is investigated.

MATERIALS AND METHODS

Model penetrants

Fluorescent labels used as model compounds (Oregon Green® 488 (OG), Bodipy® FL C5 (BFL) and Bodipy® 564/570 C5 (B564)) were purchased from Molecular Probes, The Netherlands.

Determination of the octanol/buffer partition coefficient

The water phase consisted of either a 50 mM citric acid buffer (CAB) pH 5.0 or phosphate buffered saline (PBS) pH 7.4 (139 mM NaCl, 2.5 mM KCl, 8 mM Na_2HPO_4, 1.5 mM KH_2PO_4, 25 mg/L Streptomycin and 25000 U/L Penicillin). The solutions are filtered through a Nylon 66 membrane (0.2 μm *47 mm) from Supelco (Bellefonte, PA, USA) before use. These two buffers were chosen, since they represented the donor (CAB) and the acceptor phase (PBS) of the diffusion

experiments. 1-octanol p.a. (Fluka) and the equivalent buffer were mixed 4:1 after previous mutual saturation.

During the experiment, the fluorophore was dissolved in the octanol phase followed by the addition of the aqueous phase and vigorous mixing (2 minutes). The two-phase-system was additionally shaken for one hour at 600 rpm, 25 °C. Ensuring a complete equilibrium of the dye between the two phases, the samples were left for 48 h at room temperature while protected from light. Subsequently, the samples were centrifuged at 3000 rpm for 30 min to obtain complete separation of the octanol and the buffer. The concentration of the fluorophore in each phase was determined using a Perkin-Elmer MPF-4 fluorescence spectrophotometer. In order to calculate a partition coefficient independent of the concentration, it was necessary to measure three different label concentrations and extrapolate to infinite low concentrations. The $logP_{oct/buf}$ values for the different concentrations of each fluorophore were determined 10 times.

Diffusion experiment

Fresh human scalp skin was obtained 4 to 5 hours after face-lift surgery and stored on a filter paper soaked with PBS until used the same day. Hairs were cut with scissors prior to dermatoming to a thickness of 1100 +/- 15 µm followed by cleaning of the skin surface with a PBS- and 70 % (v/v) ethanol-wipe. At least 5 skin pieces of at least 3 different donors were used. The tested donor vehicles consisted of 0.25 mg/ml OG (80% saturated), BFL (50% saturated) or B564 (100% saturated with crystals present) in CAB containing 30 % (v/v) ethanol. Diffusion experiments were performed using flow-through diffusion cells (PermeGear). Exposing a 38.5 mm^2 area of the fresh skin occlusively to 250 µl of the donor phase, hourly fractions of the PBS containing acceptor phase were collected over a period of 18 hours. This 18-hour diffusion experiment was followed by label visualisation using CLSM. Additionally, 0.1 mg/ml OG in CAB (100 % saturation) and 0.25 mg/ml OG or BFL in CAB containing 30 % (v/v) ethanol were exposed to the skin over 72 hours with fractions collected every hour up to 18 hours followed by 3-hour interval. The concentration of the different labels in each fraction was determined using an HPLC system comprised of an Isochrom LC pump, a Chromguard precolumn SS 10*3 mm, a LiChrosorb RP18 column (3*100 mm) with a particle size of 7 µm, a Gilson 234 autoinjector and a Jasco Version 6.01 821 FP fluorescence detector. The mobile phase consisted of 50 % acetonitril in purified water (flow rate = 1.0 ml/min). Oregon Green® 488 and Bodipy® FL C_5 were detected at 488/514 nm (excitation/emission), whereas the wavelengths for Bodipy® 564/570 C_5 were set at 564/574 nm, respectively. The limit of quantification was 93 ng/ml (OG), 130 ng/ml (BFL) and 466 ng/ml (B564) respectively.

Confocal Laser Scanning Microscopy

The visualisation of the fluorophores in the *non-fixed* scalp skin was carried out using a Bio-Rad MRC 600 unit followed by an evaluation of their distribution by relative quantification as previously described [21]. Images are taken from the bottom (parallel to the skin surface) and the cross section (perpendicular to the skin surface). The parallel images reveal information about label distribution in the hair follicles and the dermis, while the cross sectional view provides information about label distribution in dermis, epidermis and stratum corneum. The cross sectional view of the skin is obtained by using a modified cutting device according to Meuwissen *et al.* [20], which is used as a sample holder at the same time. From the confocal images the relative accumulation factor (f_{acc}) is calculated. A detailed explanation of the method is described elsewhere [21]. Briefly, the intensity is measured in the various skin parts after which the intensities between the follicular and the cross sectional image are normalised. Subsequently, relative intensities of various compartments in an assumed skin block are calculated. After normalising steps the relative fluorescence (F_{rel}) in percent for the non-follicular (stratum corneum, epidermis, dermis) and the follicular (outer root sheath, inner root sheath, cuticle, hair shaft) volume is obtained within this assumed skin block. By comparing this F_{rel} in one skin region with the relative intensity assuming a homogeneous distribution in the model skin block, a relative accumulation value (f_{acc}) for each skin compartment is obtained. These regional values serve to estimate the change in accumulation when label lipophilicity or donor solutions are modified.

RESULTS

Partition Coefficient

The partition coefficients of the labels increased in the order OG, BFL and B564 (Table 1) indicating that B564 is the most lipophilic and OG the most hydrophilic label for both, pH 5 and pH 7.4. However, at pH 7.4 the degree of lipophilicity for all labels was reduced compared to pH 5. A change in pH from 5 to 7.4 increased the ionisation of the carboxylic groups of the substances. At pH 7.4, OG has a negative $\log P_{oct/buf}$ value, which indicates a higher affinity for the aqueous phase than for octanol.

Table 1. *Partition coefficient of three model penetrants expressed as logPoct/buf in a citric acid buffer solution at pH 5.0 (donor phase) and in a phosphate buffered saline solution at pH 7.4 (acceptor phase) is depicted in this table.*

	$logP_{oct/buf}$	
	Citric acid buffer pH 5.0	Phosphate buffered saline pH 7.4
Oregon Green® 488	1.6	-2.5
Bodipy® FL C_5	2.5	1.2
Bodipy® 564/574 C_5	4.3	3.0

Diffusion

The diffusion profiles of the three model substances during 18 hours have been plotted in Figure 1A. No steady state flux was reached. B564 revealed a 250 times lower cumulative flux after 18 hours than BFL, which was significant ($p<0.01$). All other cumulative amounts did not differ significantly from each other. Since only a very small difference in flux between the OG and BFL was observed we decided to examine the diffusion profile of these labels also for a period of 72 hours. The cumulative amount is plotted in Figure 1B. A significant difference in cumulative amount of the two labels was detected after 24 hours of diffusion. This difference increases with an increasing diffusion period. The steady state flux and lag-time are provided in Table 2. For BFL a decreasing flux rate is observed after 57 hours (Figure 1B). This is most likely due to depletion in the donor phase since after 54 hours 47 % of the applied BFL has been detected in the acceptor fluid. A decrease in flux is not observed for OG.

Table 2. *Diffusion parameters of 0.25 mg/ml label applied on human scalp skin in a citric acid buffer vehicle containing 30 % (v/v) of ethanol.*

	Oregon Green® 488	Bodipy® FL C_5
Steady State flux [µmol/cm²*h]	1.26	6.79
Lag time [h]	27	22

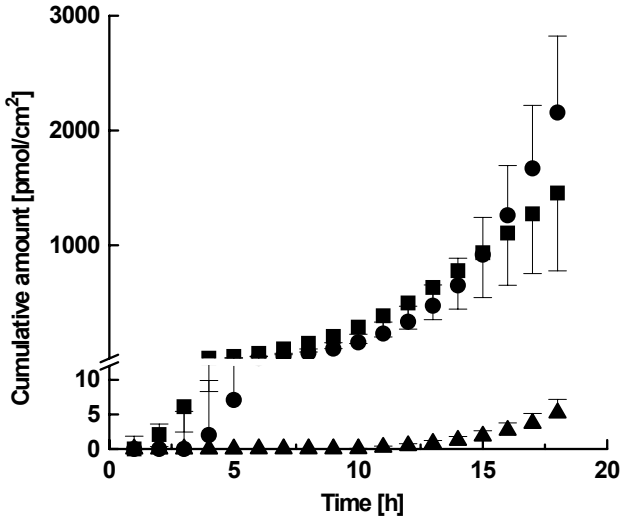

***Figure 1A**. Diffusion (18 hours) of 0.25 mg/ml of three model permeants (OG-Oregon Green® 488, BFL-Bodipy® FL C5 and B564-Bodipy® 564/570 C5) through fresh full thickness human scalp skin applied occlusively in citric acid buffer pH 5.0 containing 30 % (v/v) ethanol. The applied dose was 440 nmol/cm² (OG), 507 nmol/cm² (BFL) and 9 nmol/cm² (B564). Depicted is the mean including standard error with n=6 for BFL and n=8 for OG and B564.*

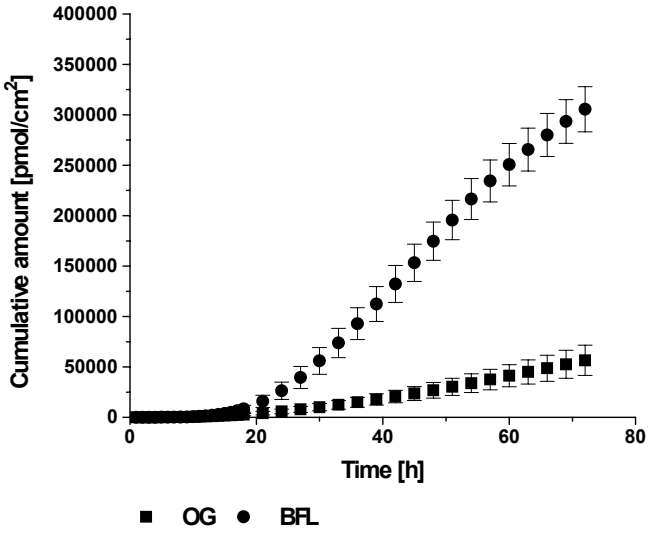

***Figure 1B**. 72 hour diffusion of Oregon Green® 488 (OG, 0.25 mg/ml) and Bodipy® FL C_5 (BFL, 0.25 mg/ml) from a 30 % (v/v) ethanol containing citric acid buffer vehicle pH 5.0. The applied dose was 440 nmol/cm² (OG) and 507 nmol/cm²(BFL). Depicted is the mean including standard error with n=6 for BFL and OG.*

In order to study the effect of ethanol on the skin barrier we decided to examine the permeation also in the absence of ethanol. The least lipophilic label OG was chosen since the effect of ethanol on the barrier function was expected to increase the flux of a hydrophilic dye more efficient than that of the more lipophilic dye BFL. The diffusion profile was measured during 72 hours. After 18 hours of diffusion (time point of CLSM images), no significant difference between the cumulative amount of OG in the absence and presence of ethanol is observed. The difference in flux was significant after 24 hours. 72 hours of diffusion resulted in a cumulative amount of OG in the presence of ethanol which is 25.7-fold higher (56.5 μmol/cm^2) than in the absence of ethanol (2.2 μmol/h*cm^2) (Figure 1C).

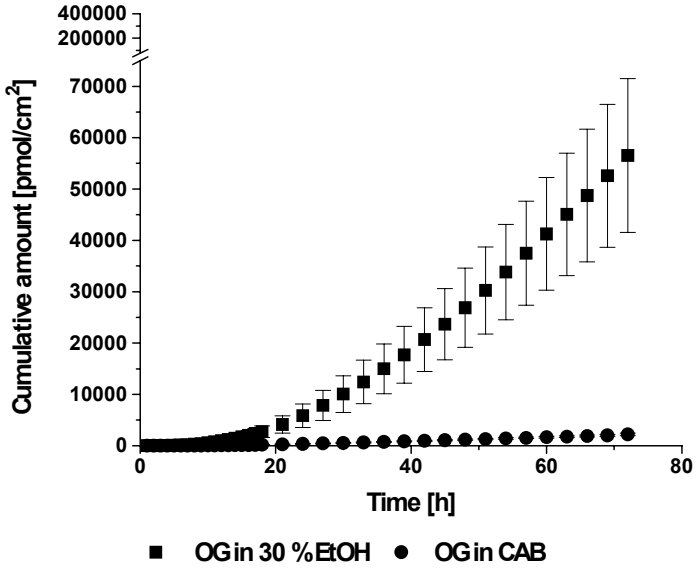

Figure 1C. *72 hour diffusion experiment of nearly saturated Oregon Green® 488 (OG) solution (0.25 mg/ml, 440 nmol/cm^2) from a citric acid buffer vehicle containing 30 % (v/v) ethanol and a saturated OG solution (0.25 mg/ml, 176 nmol/cm^2) without additives (CAB) are shown. Depicted is the mean including standard error with n=6 for OG in 30 % (v/v) ethanol and n=3 for OG in CAB only.*

Distribution

Autofluorescence could only be detected in a follicle at 100 % laser intensity. Since images of the experiments were taken at laser intensities <30 %, no interference from autofluorescence occurred. In general, the permeation pathway across the stratum corneum resides in the intercellular lipid domains (not shown). This is in contrast to the viable epidermis, in which the fluorophore is not

restricted to the cell membranes only, but also accumulates in the cytosol of the various cells. A dependency on the lipophilicity of the applied substance was observed in the accumulation of the label in stratum corneum and viable epidermis. While the lipophilic Bodipy® labels exhibit bright staining of the epidermis and a much lower staining of the stratum corneum (Figure 2C, E), the

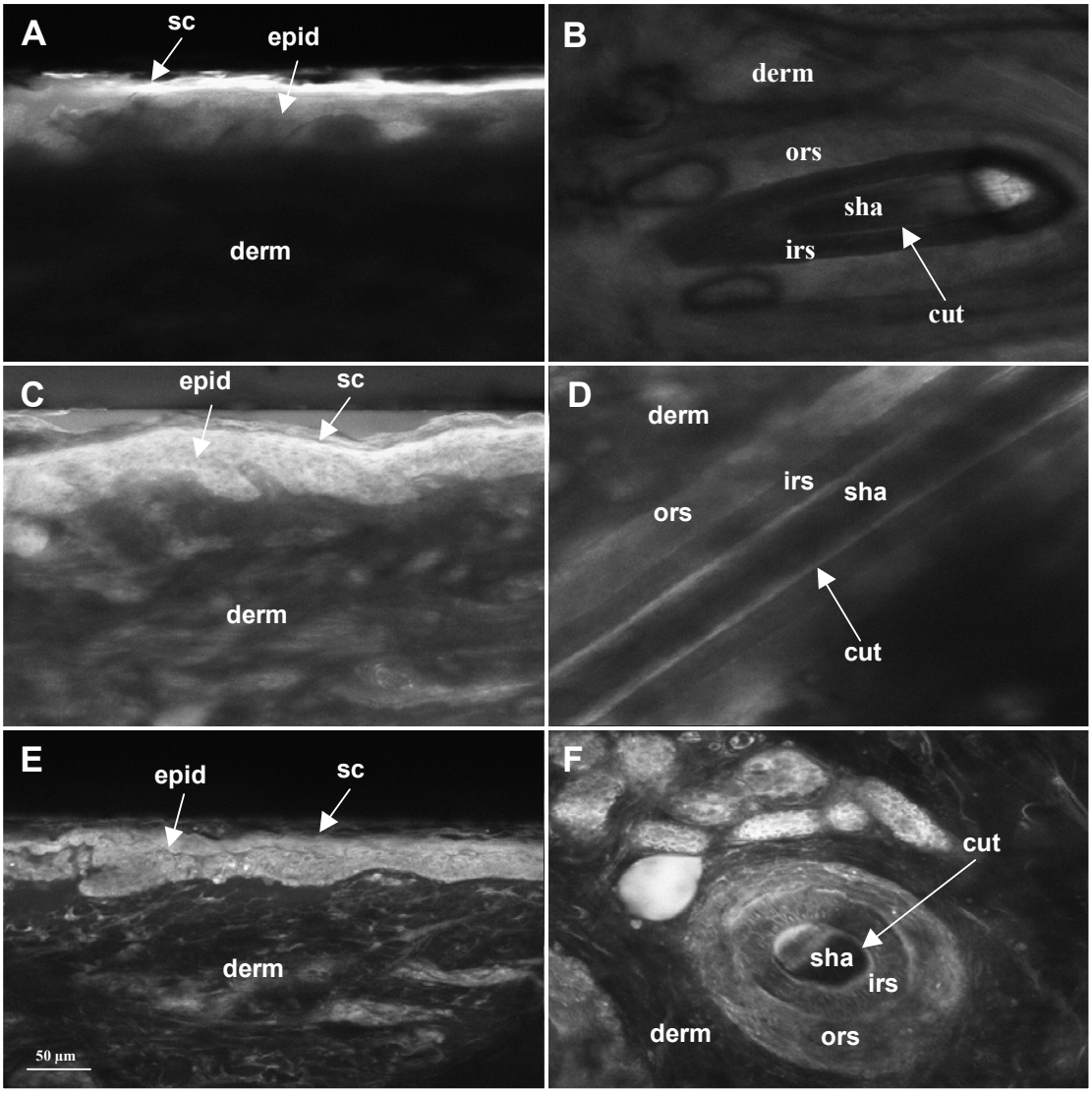

Figure 2. *Distribution of 0.25 mg/ml label from citric acid buffer pH 5.0 containing 30 % (v/v) ethanol in human scalp skin after 18 hours diffusion. A, C, E: Manual cross section of non-fixed tissue with stratum corneum (sc), epidermis (epid) and dermis (derm). Bottom view of the dermis parallel to the skin surface (B, F) and cross section view perpendicular to skin surface (D) showing a hair follicle with outer root sheath (ors), inner root sheath (irs), cuticular area (cut), hair shaft (sha) and dermis (derm). A, B: Oregon Green® 488; C, D: Bodipy® FL C5; E, F: Bodipy® 564/570 C5.*

more hydrophilic OG shows a dominating staining in the stratum corneum compared to that in the viable epidermis (Figure 2A). The dermis exhibited a less intense staining than in the viable epidermis for all fluorophores. The hair follicle, which reaches down into the dermis and subcutaneous fat reveals a characteristic and similar staining of the follicular parts for all three labels. While the outer root sheath and the cuticular area depict good labelling, staining of the inner root sheath was much weaker and hardly any label was observed in the hair shaft itself (Figure 2B, D, F). The degree of staining varied between the labels. When OG was applied to the skin the follicular region was more difficult to detect due to the low staining, not the lower quantum efficiency, in the deeper skin regions. Since after application of the Bodipy® labels, the deeper skin layers were more intense, detection of the hair follicles was easier.

Accumulation

Label lipophilicity

In the assumed skin block, less than 10 % of the fluorescence is present in the follicular volume in case of OG and BFL (Table 3) with no significant difference between the less lipophilic labels. In case of the more lipophilic dye B564, this percentage increases significantly and reaches a value of 12.4 %. Although the accumulation factors (f_{acc}) (Figure 3A) of several skin parts exhibit accumulation values above 1, only the values of OG in the stratum corneum, B564 in the epidermis, outer root sheath, inner root sheath and the cuticle revealed a significant difference. This indicates an accumulation of the labels in these skin regions. High label lipophilicity does not significantly influence the accumulation factor in the epidermis and dermis, but results in a significant decrease ($p<0.01$) of the accumulation factor in the stratum corneum.

Vehicle effect

Deeper skin layers are easier visualised when ethanol is present in the donor phase. This observation is confirmed by the F_{rel} percentages. An addition of 30 % (v/v) ethanol to the CAB vehicle has the tendency to increase the F_{rel} percentage for the hair follicle from 5.6 to 9.1. When comparing the accumulation factors (Figure 3B) of the same vehicles these values reveal that the stratum corneum contains a very high fluorescent intensity (f_{acc} value of 10.1) in the absence of ethanol. Also in the presence of ethanol the accumulation in stratum corneum is rather high (f_{acc} value of 5.2). No difference in accumulation in the presence or absence of ethanol can be observed in the dermis and epidermis, while the f_{acc} values of the outer root sheath, the inner root sheath and the cuticle reveal the trend of an increase in f_{acc} in the presence of ethanol.

Table 3. *Relative fluorescence (F_{rel}) in the non-follicular (stratum corneum, epidermis, dermis) and the follicular area (outer root sheath, inner root sheath, cuticle, hair shaft) after 18 hours of diffusion of OG, BFL and B564 in either citric acid buffer (CAB) or CAB containing 30 % (v/v) of ethanol (CAB/EtOH). The F_{rel} is a means to estimate how much of the calculated fluorescence is present in the follicular area in an assumed skin block in comparison to the non-follicular area.*

		F_{rel} (non-follicular) [%]		***F_{rel} (Follicular) [%]***	
		Average	*Standard error*	*Average*	*Standard error*
OG in CAB	*(n=3)*	*94.4*	*1.5*	*5.6*	*1.5*
OG in CAB/EtOH	*(n=4)*	*90.5*	*1.0*	*9.5*	*1.0*
BFL in CAB/EtOH	*(n=3)*	*92.0*	*0.4*	*8.0*	*0.4*
B564 in CAB/EtOH	*(n=4)*	*87.6*	*0.9*	*12.4*	*0.9*

DISCUSSION

Diffusion

During the first 10 hours the flux is low whereas after 10 hours it increases noticeable. No tendency is observed that either the more hydrophilic or the more lipophilic substance is permeating the human scalp skin faster. The most lipophilic substance (B564) exhibits extremely low fluxes, which might be due to the high $\log P_{oct/buf}$ value. Its lipophilic character will minimise the partitioning from the dermis into the acceptor phase thereby minimising the diffusion of B564. However at a pH of 5.0 (pH of the donor solution and the stratum corneum) the as hydrophilic considered OG has an affinity for the lipophilic phase. In the diffusion process, when the pH changes to values of about 7.4 in deeper skin strata, the affinity of OG for the aqueous environment dominates (hydrophilic) while the Bodipy® labels are still lipophilic (Table 1).

The diffusion profile exhibits a long lag-time. This might be due to the lipid lamellae in the stratum corneum that may act as a depot for the more lipophilic labels. Alternatively the full thickness *human* skin used in the present studies increases the permeation path length and affects the lag-time.

In pilot studies (unpublished results) skin degradation was observed after 72 h, however not after 18 hours. Since a significant difference in flux between OG and BFL is already seen after 24 hours, degradation is not expected to be the main cause for the difference in flux. This difference in flux might be due to i) a different degree of saturation of the two labels, ii) a difference in the diffusion coefficient of each label in the skin or iii) a difference in permeation pathway. Since BFL exhibits a higher flux but at the same time has a lower thermodynamic activity (saturation of ca. 50 %) than OG (saturation of ca. 80 %), either a difference in partition coefficient, diffusion coefficient and/or penetration pathway is responsible for the difference in flux.

Finally our diffusion results reveal that addition of ethanol to the donor phase results in a much higher flux of OG. This strongly indicates that ethanol is a very good penetration enhancer for OG. Whether ethanol enhances the solubility of OG in the skin or changes the lipid organisation in the stratum corneum is not known. Ghanem *et al.* [22] postulated, that smaller ethanol volume fractions (<25 %) in the donor phase resulted in a permeation enhancement due to partitioning of ethanol into the stratum corneum, while larger volume fractions (>50 %) result in a dehydration and pore formation in the skin. Berner and Liu [23] summarise the effect of ethanol as a penetration enhancer. They differentiate the enhancement effect of lipophilic and hydrophilic penetrants and mention that the primary action of ethanol for lipophilic compounds is to dissolve in the lipid regions thereby increasing the solubility of the lipophilic penetrants therein.

Accumulation

The distribution of the various labels was determined by calculating the degree of accumulation (relative accumulation factor = f_{acc}) in the various skin areas. It has to be realised that the f_{acc} value gives no indication for the total amount of fluorophore in the skin. If rather high f_{acc} values have been determined, it is still possible, that only a low total amount of label has reached the plane of imaging and vice versa. However a good measure is obtained for changes in label distribution and thus for a change in deposition in the various skin compartments.

Although the label was applied on top of the stratum corneum only low relative accumulation was observed for the more lipophilic labels in this skin barrier. This can be explained by predominant penetration of the label across the lipid domains of the stratum corneum. Since, the lipid lamellae constitute only a small region of the stratum corneum compared to the corneocytes, this will “dilute” the label concentration in the stratum corneum. The adjacent viable epidermis is much brighter stained than the stratum corneum. Since in this layer the cornified envelope has not been developed yet, the label can distribute throughout the entire epidermis, which results in a brighter appearance. The

deeper layer of the skin (dermis) shows only low labelling (Figure 2A, C, E) and no accumulation of dye (Figure 3A).

In the hair follicle the outer root sheath exhibits the highest relative accumulation whereas the adjacent inner root sheath reveals lower relative accumulation values. Compared to the outer root sheath, which is the least keratinised layer of the follicle, the inner root sheath starts its keratinisation process already shortly after cell formation in the lower part of the follicle. Therefore keratinisation is thought to protect a cell from label penetration. The cuticle of the hair shaft is keratinised in early stages as well and therefore protects the soft hair cortex from environmental influences [24]. This might lead to the accumulation of the dye in the cuticular area. Previously Kelch *et al*. [25] showed that a fluorophore accumulates in the soft endocuticle and the cell membrane complex.

Influence of permeant lipophilicity

In the stratum corneum accumulation of BFL and B564 is less than of OG. Since OG is expected to be less soluble in the lipids of the stratum corneum than the Bodipy® dyes, the high intensity of OG is most probably caused by an accumulation of this label on the surface. Generally, the relative accumulation in the follicular unit increases with high lipophilicity as seen from the F_{rel} and f_{acc} values. This can on the one hand be attributed to an increased penetration through the epidermis to the outer root sheath, since the outer root sheath is directly connected to and has similar features as the epidermis [26]. However, a second route of transport might be the gap between the skin and the hair shaft. The gap is filled with the lipophilic sebum and allows movement of the keratinised hair in the skin. Since in the deeper regions of the epidermal invagination the stratum corneum along the hair shaft becomes thinner, the permeability of the skin is expected to increase in these regions. A combination of the mentioned routes of penetration is most likely to occur since penetration via all routes includes the overcoming of a lipophilic barrier. Reviewed by Lauer *et al.* [4] and Agarwal *et al.* [18], literature reports that the follicular duct contains neutral and non-polar lipids, and that the hair follicle favours the permeation of polar compounds. Up to now no proof for either of the routes can be given from our experiments.

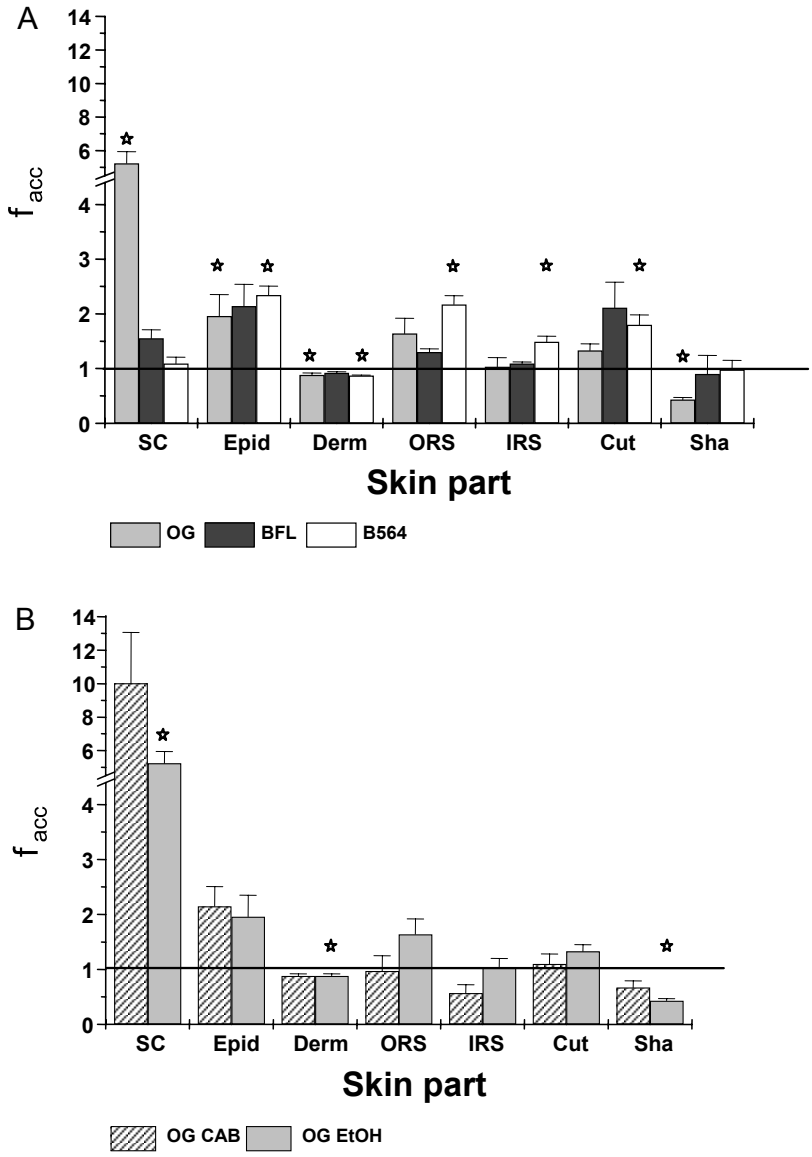

Figure 3. *Relative accumulation (f_{acc}) including standard error (n=3) of Oregon Green® 488 (OG), Bodipy® FL C_5 (BFL) and Bodipy® 564/570 C_5 (B564) in the stratum corneum (SC), epidermis (Epid), dermis (Derm), outer root sheath (ORS), inner root sheath (IRS), cuticular area (Cut) and the hair shaft (Sha). A depicts the influence of lipophilicity on the relative accumulation when the fluorophores are applied in a citric acid buffer solution containing 30 % (v/v) ethanol. B shows the f_{acc} values when a hydrophilic dye is applied in citric acid buffer with (EtOH) or without ethanol (CAB). f_{acc} values of ≤1 imply that no accumulation is present. Stars indicate a significant difference ($p<0.05$) in the specific skin part of the f_{acc} value from 1.*

Vehicle effect

Our results indicate that the presence of 30 % (v/v) ethanol targets Oregon Green® 488 to the hair follicle as indicated by the f_{acc} and F_{rel} values. There are two possible influences of ethanol on the penetration route. By increasing the relative amount of dye in the epidermis, more dye is available for the diffusion via the direct connection to the outer root sheath and thereby to the hair follicle. Simultaneously the ethanol can interact with the lipids excreted into the follicular duct by the sebaceous gland making the duct more accessible for penetration. One advantage of the penetration via the follicular duct is the decreased barrier function of the stratum corneum.

CONCLUSIONS

From the diffusion studies we conclude, that ethanol (30 % (v/v) in CAB) increases the penetration rate of Oregon Green® 488 across the skin. However no conclusion can be drawn whether this influence is due to changes in permeation pathway or stratum corneum structure. At the same time, although not significant in this study ethanol seems to promote the transport of Oregon Green® 488 into the hair follicle. Increasing permeant lipophilicity to a certain degree results in an increase in penetration rate across human scalp skin as determined by diffusion studies. Simultaneously, the relative distribution in the skin is also affected by the lipophilicity of the permeating dye. A high lipophilicity of the label promotes the deposition of the label in the hair follicle. This has clearly been demonstrated by the increased F_{rel} and f_{acc} values. Therefore, delivery to the hair follicle can be improved by the use of a lipophilic substance. No conclusions can be drawn concerning the actual route of transport across the skin and to the hair follicle since permeation is a dynamic process. Therefore time-resolved experiments have to be performed in future.

ACKNOWLEDGEMENT

The authors thank Unilever Research, Port Sunlight, UK for financing this project.

REFERENCES

[1] R.J. Scheuplein, I.H. Blank, G.J. Brauner, D.J. MacFarlane, Percutaneous absorption of steroids. J. Invest. Dermatol. 52 (1969) 63-70.

[2] R.J. Scheuplein, Mechanism of percutaneous absorption. II. Transient diffusion and the relative importance of various routes of skin penetration. J. Invest. Dermatol. Symp. Proc. 48 (1967) 79-88.

[3] J.C. Keister, G.B. Kasting, The use of transient diffusion to investigate transport pathways through skin. J. Control. Release 4 (1986) 111-117.
[4] A.C. Lauer, L.M. Lieb, C. Ramachandran, G.L. Flynn, N.D. Weiner, Transfollicular drug delivery. Pharm. Res. 10 (1995) 179-186.
[5] N. Weiner, Targeted follicular delivery of macromolecules via liposomes. Int. J. Pharm. 162 (1998) 29-38.
[6] N.G. Turner, R.H. Guy, Visualisation and quantitation of iontophoretic pathways using Confocal Microscopy. J. Invest. Dermatol. Symp. Proc. 3 (1998) 136-142.
[7] H. Schaefer, F. Watts, J. Brod, B. Illel, Follicular penetration, in: R.C. Scott, R.H. Guy, J. Hadgraft (Eds.), Prediction of Percutaneous Penetration. Methods, Measurements, Modelling, IBC Technical Services, 1989, pp. 163-173.
[8] A. Rolland, N. Wagner, A. Chatelus, B. Shroot, H. Schaefer, Site-specific drug delivery to pilosebaceous structures using polymeric microspheres. Pharm. Res. 10 (1993) 1738-1744.
[9] C.C. Sumian, F.B. Pitre, B.E. Gauthier, M. Bouclier, S.R. Mordon, A new method to improve penetration depth of dyes into the follicular duct: Potential application for laser hair removal. J. Am. Acad. Dermatol. 41 (1999) 172-175.
[10] J. Lademann, H.J. Weigmann, C. Rickmeyer, H. Barthelmes, H. Schaefer, G. Mueller, W. Sterry, Penetration of titanium dioxide microparticles in a sunscreen formulation into the horny layer and the follicular orifice. Skin Pharmacol. Appl. Skin Physiol. 12 (1999) 247-256.
[11] L.M. Lieb, C. Ramachandran, K. Egbaria, N.D. Weiner, Topical delivery enhancement with multilamellar liposomes into pilosebaceous units: I. In vitro evaluation using fluorescent techniques with the hamster ear model. J. Invest. Dermatol. 99 (1992) 108-113.
[12] S. Tata, N. Weiner, G. Flynn, Relative influence of ethanol and propylene glycol cosolvents on deposition of minoxidil into the skin. J. Pharm. Sci. 83 (1994) 1508-1510.
[13] E. Touitou, B. Godin, C. Weiss, Enhanced delivery of drugs into and across the skin by ethosomal carriers. Drug Dev. Res. 50 (2000) 405-415.
[14] F.L. Bamba, J. Wepierre, Role of the appendageal pathway in the percutaneous absorption of pyridostigmine bromide in various vehicles. Eur. J. Drug Metab. Pharmacokinet. 18 (1993) 339-348.
[15] F. Hueber, H. Schaefer, J. Wepierre, Role of transepidermal and transfollicular routes in percutaneous absorption of steroids: in vitro studies on human skin. Skin Pharmacol. 7 (1994) 237-244.
[16] F. Hueber, M. Besnard, H. Schaefer, J. Wepierre, Percutaneous absorption of estradiol and progesterone in normal and appendage-free skin of the hairless rat: lack of importance of nutritional blood flow. Skin Pharmacol. 7 (1994) 245-256.
[17] A.C. Lauer, J.T. Elder, N.D. Weiner, Evaluation of the hairless rat as a model for in vivo percutaneous absorption. J. Pharm. Sci. 86 (1996) 13-18.
[18] B. Illel, Formulation for transfollicular drug administration: Some recent advances. Crit. Rev. Ther. Drug Carrier Sys. 14 (1997) 207-219.
[19] R. Agarwal, O.P. Katare, S.P. Vyas, The pilosebaceous unit: A pivotal route for topical drug delivery. Methods Find. Exp. Clin. Pharmacol. 22 (2000) 129-133.
[20] M.E.M.J. Meuwissen, J. Janssen, C. Cullander, H.E. Junginger, J.A. Bouwstra, A cross-section device to improve visualisation of fluorescent probe penetration into the skin by Confocal Laser Scanning Microscopy. Pharm. Res. 15 (1998) 352-356.
[21] Y.Y. Grams, J.A. Bouwstra, A new method to determine the distribution of a fluorophore in scalp skin with focus on hair follicles. Pharm. Res. 19(3) (2002) 350-354.
[22] A.H. Ghanem, H. Mahmoud, W.I. Higuchi, P. Liu, W.R. Good, The effects of ethanol on the transport of lipophilic and polar permeants across hairless mouse skin: Methods/validation of a noval approach. Int. J. Pharm. 78 (1992) 137-156.
[23] B. Berner, P. Liu, Alcohols, in: E.W. Smith, H.I. Maibach (Eds.), Percutaneous Penetration Enhancers, CRC Press, Boca Raton, 1995, pp. 45-60.
[24] J.C. Kvedar, H.A. Daryanani, H.P. Baden, Cross-linked components of the cuticle of the cortex of hair. J. Invest. Dermatol. 96 (1991) 84S-85S.
[25] A. Kelch, S. Wessel, T. Will, U. Hintze, R. Wepf, R. Wiesendanger, Penetration pathways of fluorescent dyes in human hair fibres investigated by scanning near-field optical microscopy. J. Microsc. 200 (2000) 179-186.
[26] K. Hashimoto, S. Shibazaki, Ultrastructural study on differentiation and function of hair, in T. Kobori, W. Montagna, K. Toda, Y. Ishibashi, Y. Hori, F. Morikawa (Eds.), Biology and Disease of the Hair, University of Tokyo Press, Tokyo, 1976, pp. 23-57.

IV

Permeant lipophilicity and vehicle composition influence on accumulation of dyes in hair follicles of human skin

YY Grams, S Alaruikka, L Lashley, J Caussin, L Whitehead and JA Bouwstra.
Eur J Pharm Sci. ***18*** *(5): 329-36 (2003)*

ABSTRACT

In skin and hair research drug targeting to the hair follicle is of great interest. Therefore the influence of permeant lipophilicity and vehicle composition on local accumulation has been examined using Confocal Laser Scanning Microscopy (CLSM). Formulations saturated with either Oregon Green® 488, Bodipy® FL C_5 or Bodipy® 564/570 C_5 were prepared. The dyes were applied in citric acid buffer, 8% (w/v) surfactants in citric acid buffer or 8% (w/v) surfactants/20% (w/v) propylene glycol in citric acid buffer. Flow-through diffusion experiments were performed with fresh human scalp skin, after which the skin was imaged using CLSM. Diffusion studies showed for Oregon Green® 488 (low lipophilicity) a higher flux when applied in citric acid buffer compared to surfactants. In contrast the fluxes of the more lipophilic dyes (Bodipy® FL C_5 and Bodipy® 564/570 C_5) are highest when applied in surfactants/propylene glycol. CLSM studies revealed that follicular accumulation increased with i) a lipophilic dye and ii) application of lipophilic dyes in surfactants/propylene glycol. Therefore we conclude that targeting to the hair follicle can be increased by the use of lipophilic drugs in combination with surfactant solutions and PG.

INTRODUCTION

One of the major limitations in transdermal and dermal drug delivery is the barrier function of the skin. For this reason most studies are focussed on increasing the permeation rate of active substances across the skin. However local drug targeting to the pilosebaceous unit (hair follicle and sebaceous gland) and to the sweat glands is of growing importance. Increased accumulation in the pilosebaceous unit could treat alopecia, acne and skin cancer more efficiently and improve the effect of cosmetic substances and nutrients. Main target areas are the sebaceous gland of the pilosebaceous unit (acne, overproduction of sebum), the bulge area (growth activation), the hair bulb (nutrition, melanin, growth), basal cells (skin cancer) and the cuticle (strength and elasticity of the hair shaft). Recent reviews (Agarwal et al., 2000) report an increased delivery to the hair follicle when using liposomal formulations (Gupta et al., 2001; Li, Hoffman, 1995; Weiner, 1998), nanoemulsions (Wu et al., 2001), particles of 3-10 µm size (Rolland et al., 1993; Schaefer et al., 1989; Schaefer, Lademann, 2001; Sumian et al., 1999), crystals (Allec et al., 1997), iontophoresis (Turner, Guy, 1998) and formulations containing low molecular weight dextrans (Lieb et al., 1995).

In hair-care surfactant formulations are wide spread. Their frequent use as shampoo or conditioning agent makes them potential formulations not only for cleansing but also for drug delivery. However, the daily use of surfactant formulations and the stability of the formulation strongly limit the classes of surfactants to be used in these formulations. Therefore, for increasing follicular targeting the combination of selected surfactants in the formulation, the addition of non-irritating agents, and the physico-chemical parameters of the active substance need also to be optimised.

Previously we developed a method to relatively quantify the accumulation of fluorescent dyes in the hair follicle of fresh unfixed human scalp skin (Grams, Bouwstra, 2002a), in which we were able to distinguish between label accumulation in the hair, cuticle, the inner root sheet and the outer root sheet. With this method it is possible to compare the relative accumulation of dyes after different treatments. However, it is not possible to compare absolute intensities in the various skin regions after various treatments. Subsequently we hypothesised that the presence of 30% (v/v) ethanol in a buffer solution promotes the accumulation of a substance with low lipophilicity in the hair follicle (Grams, Bouwstra, 2002b). Since propylene glycol and surfactants are present in a large number of topical formulations, in the present study we aimed to examine the effect of these additives on the targeting to the hair follicle. The possible synergistic effect of propylene glycol and surfactant formulation on targeting to

the hair follicles has to our knowledge not been examined yet. For this purpose we used permeation studies and confocal laser scanning microscopy (CLSM).

The objective of this study is to investigate the effect of surfactant formulation in the presence and absence of propylene glycol on the penetration rate and distribution of drugs in human scalp skin. As active agents model dyes of similar molecular weight with increasing lipophilicity have been used. Point of special interest is the targeting potential of the formulations to the various compartments in the hair follicle.

MATERIALS AND METHODS

2',7'-difluorofluorescein (Oregon Green® 488), 4,4-difluoro-5,7-dimethyl-4-bora-3a,4a-diaza- *s*-indacene-3-pentanoic acid (Bodipy® FL C_5) and 4,4-difluoro-5-styryl-4-bora-3a,4a-diaza- *s*-indacene-3-pentanoic acid (Bodipy® 564/570 C_5) were purchased from Molecular Probes, The Netherlands. The surfactant stock solution consisted of 14% (w/v) sodium laureth sulphate, 2% (w/v) cocamidopropyl betaine, 1% (w/v) sodium chloride and 0.5% (w/v) sodium benzoate and was kindly providedby Unilever Research, Port Sunlight, UK. Fresh human scalp skin (female, average age 47 years) was obtained within 3 hours after cosmetic surgery.

Saturation

All the diffusion experiments described in this paper were performed with saturated formulations. The saturated concentration of each label in the equivalent vehicle was determined prior to the diffusion experiment. Briefly, an excess of the dye was added to the solvent. Subsequently the solution was mixed vigorously, sonicated for 1 hour and left for equilibration over night. After centrifugation (15 min, 14000 rpm, Eppendorf centrifuge) the concentration of the dye was measured in the supernatant by HPLC.

Diffusion

Diffusion studies were carried out using fluorescent dyes as model drugs with varying lipophilicity. LogP values at pH 5.0 are 1.6 (Oregon Green® 488), 2.5 (Bodipy® FL C_5) and 4.3 (Bodipy® 564/570 C_5). The logP values at pH of 7.4 are –2.5, 1.2 and 3.0 for Oregon Green® 488, Bodipy® FL C_5 and Bodipy® 564/570 C_5, respectively. Three donor solutions were prepared namely (i) citric acid buffer pH 5.0, (ii) 8% (w/v) surfactant solution in citric acid buffer and (iii) 8% (w/v) surfactant solution/20% (w/v) propylene glycol in citric acid buffer. The original surfactant solution contained a total of 16 % surfactants (sodium laureth sulphate, cocamidopropyl betaine), which was diluted 1:1 (w/w) with citric acid buffer in experimental conditions. Oregon Green® 488 and Bodipy® FL C_5 were

applied in all three formulations. Bodipy® 564/570 C_5 was not applied in the buffer solution (i) due to its lipophilic character.

Diffusion experiments were performed as described elsewhere (Grams, Bouwstra, 2002b). Briefly, fresh human scalp skin was dermatomed to a thickness of 1100 +/- 150 µm and placed in flow-through diffusion cells with a skin surface area of 0.38 cm^2. 250 µl donor solution was applied occlusively for 18 hours. Hourly fractions were collected of the acceptor phase (phosphate buffered saline, pH 7.4) and analysed by HPLC. Although in hair application, exposition times are shorter, stronger indications on differences between treatments are expected from longer exposure times. The washing process can be considered as an occlusive application since no water will evaporate from the skin and hydration is likely to occur.

Distribution

After terminating the diffusion experiment, the skin was processed immediately for the visualization studies by Confocal Laser Scanning Microscopy (CLSM). The unfixed skin was clamped in a special designed sample holder and the distribution of the various labels in the skin, including the hair follicle, was visualised by Confocal Laser Scanning Microscopy (CLSM). The CLSM consisted of a Bio-Rad MRC 600 unit, equipped with an Argon/HeNe laser combined with an inverted Zeiss IM-35. Images are obtained from the bottom (parallel to the skin surface at the dermis side) displaying the hair follicle in the dermis and the cross section (perpendicular to the skin surface) showing stratum corneum, epidermis, dermis. The latter view of the skin is obtained using a modified cutting device according to Meuwissen *et al.* (Meuwissen et al., 1998) circumventing fixation of the skin.

Laser intensities were optimised for each dye. Comparison of fluorescence intensities between images of different dyes is impossible due to the CLSM technique. Therefore images were evaluated by determination of the relative accumulation factor (f_{acc}) as described elsewhere (Grams, Bouwstra, 2002a) and tested for significance (One-way Anova or Student's T-test). Briefly, fluorescent intensities of various skin parts are normalised between the follicular and the cross sectional image. Subsequently, relative intensities of various compartments in an assumed model skin block are calculated. By comparing this relative intensity in one skin region with the relative intensity assuming a homogeneous distribution in the model skin block, a relative accumulation value (f_{acc}) for each skin compartment is calculated. Values above 1 indicate accumulation while values of 1 or lower indicate no accumulation of dye. These regional values serve to estimate the change in accumulation when label lipophilicity or donor solutions are modified and are therefore a measure for accumulation in the hair follicles. The f_{acc} values do not provide any information

about the absolute amount of fluorescent intensity in the various skin compartments.

RESULTS

Saturation

The saturation values of the dyes when dissolved in the surfactant formulations are summarized in Table 1. When dissolved in citric acid buffer pH 5.0, the saturated concentration of Oregon Green® 488 and Bodipy FL C_5 is 0.05 mg/ml and 0.02 mg/ml, respectively. A significant difference is obtained in the saturated concentrations of Oregon Green® 488, Bodipy® FL C_5 and Bodipy® 564/570 C_5 in the various donor phases. The highest saturated concentration in 8% (w/v) surfactant solution is observed for the moderate lipophilic Bodipy® FL C_5 (2.42 mg/ml) followed by most lipophilic Bodipy® 564/570 C_5 (0.61 mg/ml) and the least lipophilic Oregon Green® 488 (0.11 mg/ml). When 20% (w/v) propylene glycol is added to the surfactant solution, no significant change in saturation value is detected for each label (Oregon Green® 488=0.10 mg/ml, Bodipy® FL C_5=2.75 mg/ml and Bodipy® 564/570 C_5=0.58 mg/ml). An increase in equilibration time did not lead to a change in saturation values.

Table 1. *Solubility data of the dyes (Oregon Green® 488, Bodipy® FL C_5, Bodipy® 564/574 C_5) in the three different donor phases used in the diffusion experiments. Values are given in mg/ml.*

	Oregon Green® 488	*Bodipy® FL C_5*	*Bodipy® 564/570 C_5*
Citric acid buffer pH 5.0 (CAB)	*0.05*	*0.11*	*0.10*
8 % surfactants in CAB	*0.02*	*2.42*	*2.75*
8 % surfactants/20 % propylene glycol in CAB	*Not used*	*0.61*	*0.58*

Diffusion

Diffusion experiments (Figure 1) revealed the highest amount penetrated for the medium lipophilic Bodipy® FL C_5. Increasing or decreasing dye lipophilicity resulted in a significant decrease in penetrated amount. Since the amount of penetrated Bodipy® 564/570 C_5 in one hour is about factor 1000 smaller than the amount which can be dissolved in the acceptor phase, solubility of Bodipy® 564/570 C_5 in the acceptor phase is not critical. Furthermore, in this figure a very interesting trend is observed as far as the influence of the vehicle is concerned. For the least lipophilic dye (Oregon Green® 488) an increasing cumulative amount is observed in the order surfactant/propylene glycol<surfactant<citric acid buffer (Figure 1). The opposite tendency is observed for the more lipophilic dyes. The cumulative amount increased in the vehicle order citric acid buffer<surfactant<surfactant/propylene glycol for Bodipy® FL C_5 and in the vehicle order surfactant<surfactant/propylene glycol in case of Bodipy® 564/570 C_5.

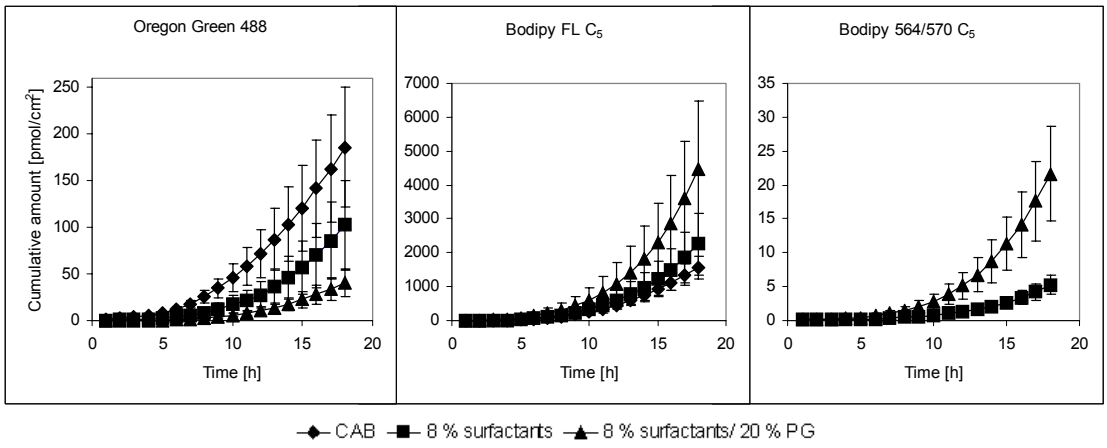

Figure 1. *Cumulative amount of Oregon Green® 488, Bodipy® FL C5 and Bodipy® 564/570 C5 when applied as a saturated solution in citric acid buffer containing 8% (w/v) of surfactants (square) or citric acid buffer containing 8% (w/v) surfactants/20% (w/v) propylene glycol (triangle) for 18 hours. Depicted is the standard error with n(Bodipy® FL C5)=5, n(Oregon Green® 488 in citric acid buffer)=3 and n(Oregon Green® 488 in surfactant or surfactant/propylene glycol)=7.*

Distribution

The CLSM images show the distribution of the dyes in the cross-section of the skin (Figure 2) and in the hair follicle (Figure 3). These figures provide already an indication of the most pronounced trends of fluorescent staining in the various skin parts. With increase in permeant lipophilicity, the relative labelling of the stratum corneum decreases and the relative labelling of the epidermis increases.

Furthermore propylene glycol promotes the presence of the more lipophilic Bodipy® 564/570 C_5 in the stratum corneum and reduces labelling of the epidermis. Focussing on the hair follicle (Figure 3), the outer root sheath and the cuticular area show the brightest staining while the hair shaft and the inner root sheath were hardly labelled for all three labels. Addition of propylene glycol to the surfactant formulation did not influence this staining pattern.

To obtain more detailed information about changes in dye distribution in the various skin regions, relative accumulation values (f_{acc}) have been calculated (Figure 4). We stress that an increase in f_{acc} value does not necessarily imply an increase in absolute amount of dye in the skin region. However, these f_{acc} values provide information on the relative distribution of the label in the various skin regions. The results provided in figure 4 suggest that Oregon Green® 488 applied in a buffer solution accumulated in the stratum corneum and the epidermis with the highest accumulation values for the stratum corneum. In the remaining skin parts (dermis, outer and inner root sheath, cuticle and hair shaft) no accumulation (values smaller than 1) was observed in any of the applied vehicles. The medium lipophilic Bodipy® FL C_5 applied in buffer solution resulted similar to Oregon Green in an accumulation in the stratum corneum and in the epidermis. When surfactants were added to the formulation the accumulation values of Oregon Green® 488 tend to decrease in the stratum corneum and to increase in the epidermis while for Bodipy® FL C_5 the f_{acc} tend to decrease in both, the stratum corneum and the epidermis. Furthermore, a trend to increasing values is also noticed for Bodipy® FL C_5 in all regions of the hair follicle. This tendency is also observed in the outer root sheath after the addition of propylene glycol to the surfactant formulation. Bodipy® 564/570 C_5 was not applied in a buffer solution due to its low solubility. Exposed to the skin in a surfactant formulation, Bodipy® 564/570 C_5 accumulated in all skin regions, except for the dermis, the inner root sheath and the hair shaft. The addition of propylene glycol to the surfactant formulation shows the trend of increasing accumulation in all skin parts except for the epidermis with significant difference in the cuticle. In Figure 5 the accumulation values are re-plotted as function of the permeant lipophilicity. For both surfactant formulations no clear trend was observed for the non-follicular part with increasing lipophilicity of the penetrant. When focussing on the hair follicle the following trends were noticed. Permeant lipophilicity appears to have a greater influence in the presence of surfactant/propylene glycol compared to surfactants only. With surfactant/propylene glycol an increase in dye lipophilicity results in a gradual increase in dye accumulation in the hair follicle with significant difference between Oregon Green® 488 and Bodipy® 564/570 C_5 in all follicular parts. With surfactant only, increased accumulation with increased lipophilicity is observed for the outer root sheath and to some degree also in the cuticle.

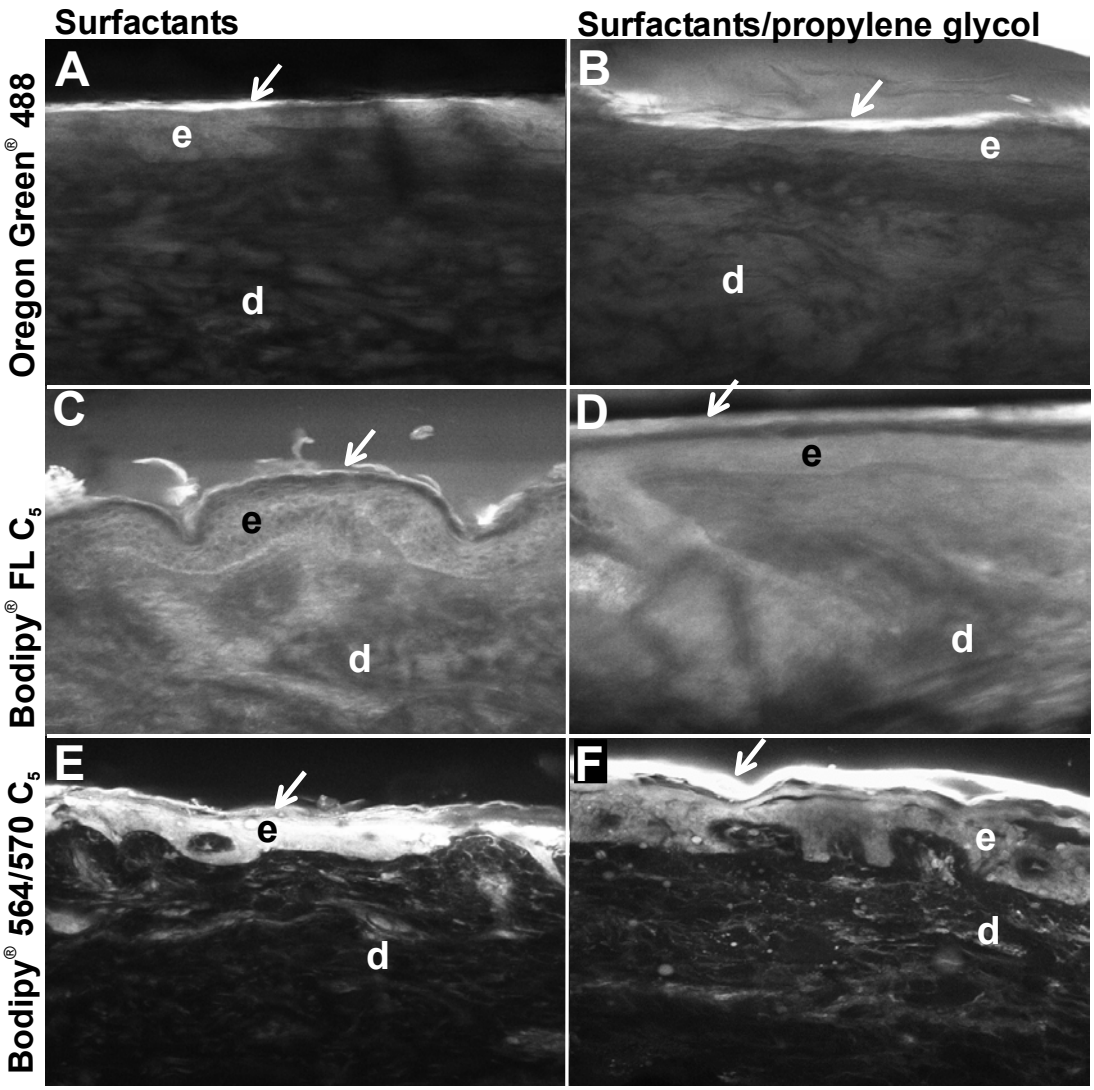

Figure 2. *Distribution of Oregon Green® 488, Bodipy® FL C5 and Bodipy® 564/570 C5 in a cross-section of fresh human scalp skin after 18 hours application of a saturated dye solution in either 8% (w/v) surfactants or 8% (w/v) surfactants/20% (w/v) propylene glycol. The cross-section depicts the stratum corneum (arrow), epidermis (e) and dermis (d). The hydrophilic Oregon Green® 488 is mainly present in the stratum corneum and to a lesser extent in the epidermis. Only low fluorescent intensity is observed in the dermis (A and B). The more lipophilic Bodipy® FL C5 results in a bright fluorescence in the epidermis and to a lower extend in the dermis (C and D). The distribution of the most lipophilic compound Bodipy® 564/570 C5 is affected by the presence of propylene glycol in the surfactant solution (E, F). Propylene glycol decreases the strong staining in the epidermis. The staining of the stratum corneum is either similar to that of the epidermis (surfactant solution) or dominating (surfactant with propylene glycol).*

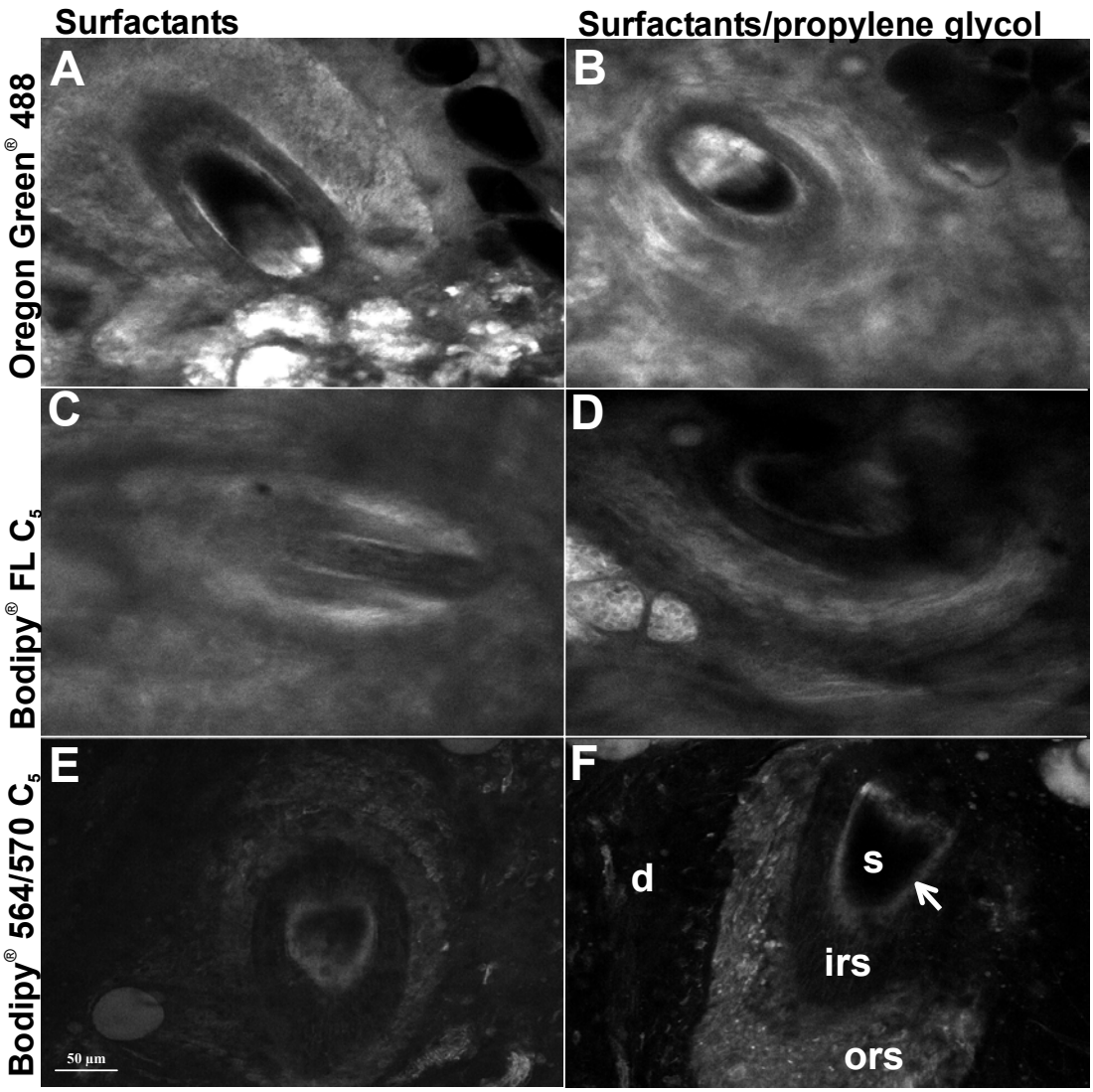

Figure 3. *Distribution of Oregon Green® 488, Bodipy® FL C_5 and Bodipy® 564/570 C_5 in fresh human scalp skin after 18 hours application of a saturated dye solution in either 8% (w/v) surfactants or 8% (w/v) surfactants/20% (w/v) propylene glycol. The bottom view parallel to the skin surface at a depth of 1100 µm depicts dermis (d), outer root sheath (ors), inner root sheath (irs), cuticle (arrow) and hair shaft (s). The general staining pattern of the hair follicles after the various treatments is very similar irrespective of the label or the vehicle composition used. The outer root sheath and the cuticular area revealed the brightest staining while the hair shaft and the inner root sheath were hardly labelled. The intensities of the images of different dyes cannot be compared due to the differences in fluorescence properties.*

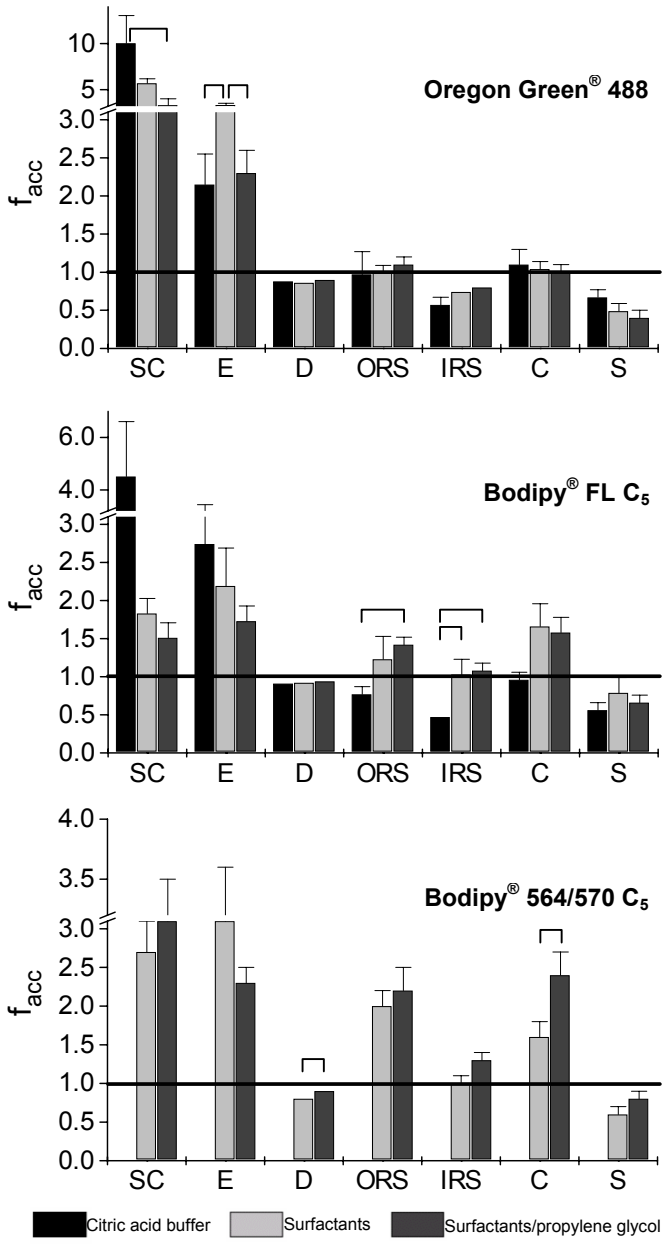

Figure 4. *Relative accumulation values of Oregon Green® 488, Bodipy® FL C_5 and Bodipy® 564/570 C_5 in the stratum corneum (SC), epidermis (E), dermis (D), outer root sheath (ORS), inner root sheath (IRS), cuticle (C) and hair shaft (S). Values above the horizontal line (f_{acc}=1) indicate accumulation. The donor phase consisted of a saturated dye solution in citric acid buffer, citric acid buffer containing 8% (w/v) of surfactant or citric acid buffer containing 8% (w/v) surfactant/20% (w/v) propylene glycol. The most lipophilic Bodipy® 564/570 C_5 was insoluble in citric acid buffer. Depicted is the standard error with n(Bodipy® FL C_5)=5, n(Oregon Green® 488 in citric acid buffer)=3 and n(Oregon Green® 488 in surfactant or surfactant/propylene glycol)=6. Significant differences between columns (p<0.05) are indicated by horizontal bars above the columns.*

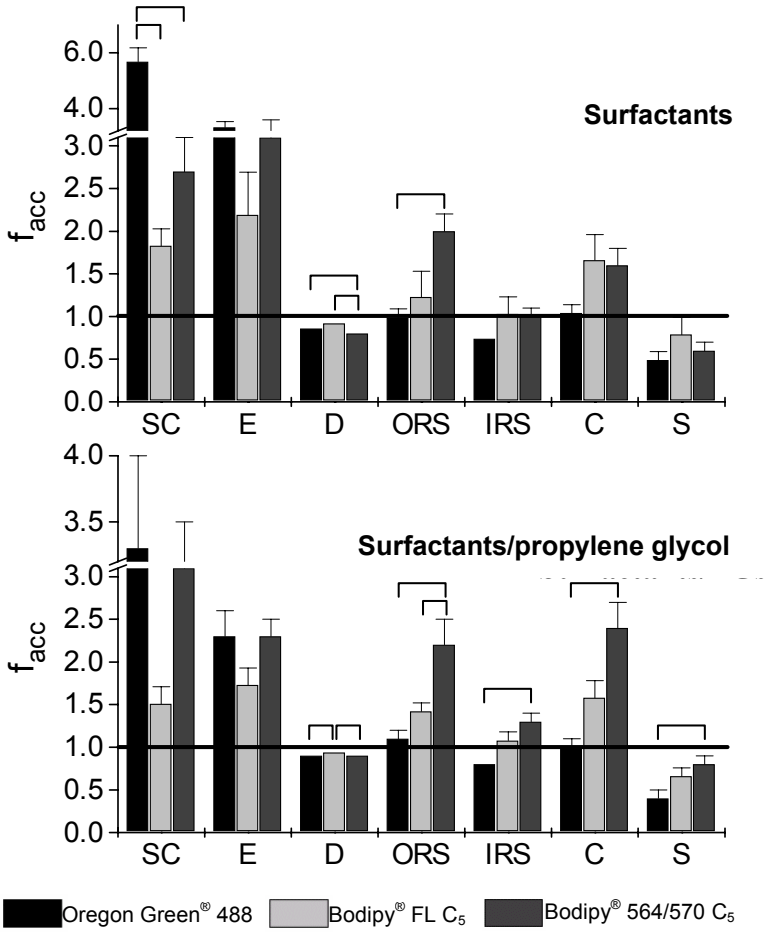

Figure 5. *Relative accumulation values of Oregon Green® 488, Bodipy® FL C_5 and Bodipy® 564/570 C_5 in the stratum corneum (SC), epidermis (E), dermis (D), outer root sheath (ORS), inner root sheath (IRS), cuticle (C) and hair shaft (S). Values above the horizontal line (f_{acc}=1) indicate accumulation. The donor phase consisted of a saturated dye solution in citric acid buffer, citric acid buffer containing 8% (w/v) surfactant or citric acid buffer containing 8% (w/v) surfactant/20% (w/v) propylene glycol. The most lipophilic Bodipy® 564/570 C_5 is insoluble in citric acid buffer only. Depicted is the standard error with n(Bodipy® FL C_5)=5, n(Oregon Green® 488 in citric acid buffer)=3 and n(Oregon Green® 488 in surfactants or surfactants/propylene glycol)=6. Significant differences between columns ($p<0.05$) are indicated by horizontal bars above the columns.*

DISCUSSION

Since as observed in previous studies degradation of the skin is observed after longer diffusion periods we decided to study the flux for 18 hours only. However as a consequence no steady state situation was reached yet, which is most probably due to the thickness of the skin (1100 µm +/- 150 µm). We chose for this skin thickness, since it is crucial for the visualisation of the hair follicle in deeper skin layers.

Diffusion - Influence of permeant lipophilicity

For Oregon Green® 488 the strong labelling of the stratum corneum (Figure 2), which might also be attributed to the label at the surface of the stratum corneum, indicates that the stratum corneum with its lipid lamellae is the main barrier for the diffusion of Oregon Green® 488. When Bodipy® FL C_5 is applied the labelling of the stratum corneum is less dominating compared to application of Oregon Green® 488. This suggests that the more lipophilic dye Bodipy® FL C_5 permeates faster across the stratum corneum explaining the higher flux and accumulate less at the surface of the stratum corneum. In contrast, the decrease in flux of Bodipy® 564/570 C_5 compared to Bodipy® FL C_5 can be attributed to its low partitioning into the hydrophilic dermis and the acceptor phase rather than the barrier function of the stratum corneum. This is demonstrated in Figure 2, which shows a strong labelling of the epidermis after application of Bodipy® 564/570 C_5. Since the dermis is a more hydrophilic environment (connective tissue embedded in an amorphous ground substance containing mucopolysaccarides) than the epidermis, the affinity of Bodipy® 564/570 C_5 for the dermis is expected to be lower than for the epidermis.

Diffusion - Influence of vehicle composition

With increasing permeant lipophilicity, the addition of propylene glycol to the surfactant formulation appears to be more effective in enhancing the permeation rate of the dye. This is clearly demonstrated in figure 1, in which it is shown that the addition of propylene glycol increases the flux of the most lipophilic Bodipy® 564/570 C_5 significantly, while propylene glycol has the tendency to reduce the flux of the most hydrophilic dye, Oregon Green®. The large variation in flux for each dye is most likely due to the use of full thickness skin and is the reason that even an increase by 100% of the accumulated amount in the presence of propylene glycol is not significant. The increased flux of the most lipophilic dye in the presence of propylene glycol can be explained by various mechanisms. i) Due to their lipophilic nature Bodipy® dyes are expected to be located in the micelles. Propylene glycol facilitates the partitioning of these

lipophilic dyes from the micelles into the buffer phase. This increases the availability of the dye for the skin interaction. ii) The co-solvent propylene glycol modifies the micelles or interacts with the skin acting as penetration enhancer or increasing the solubility of the dye in the skin. This might be more effective for the lipophilic than for the hydrophilic dye.

Distribution - Influence of vehicle composition

The addition of surfactants with or without propylene glycol does not only influence the permeation of the dyes across the skin, but also changes the distribution of the dyes in the skin. For the least lipophilic Oregon Green® 488 the main influence is a decrease of accumulation in the stratum corneum. In the absence of surfactants, absorption processes on the skin surface most likely explain the high relative accumulation value for this dye. The decrease in relative accumulation value in the presence of surfactants can therefore be due to a decrease in affinity to the stratum corneum surface and barrier integrity.

The decrease in the relative accumulation of the more lipophilic label Bodipy® FL C_5 in stratum corneum and epidermis in the presence of surfactants with and without propylene glycol can be explained by alteration of the stratum corneum as a barrier and depot. Once in the epidermis the dye can diffuse into the dermis or via the direct connection from the epidermis into the outer root sheet. An increase in the accumulation of the outer root sheet is indeed observed. The increase in relative accumulation for Bodipy® FL C_5 in the follicular area in the presence of the surfactant formulation can additionally be explained by interaction of the surfactant formulation with the lipophilic sebum in the opening of the hair making the hair duct more accessible for the dye. The stratum corneum in the duct becomes gradually thinner thereby facilitating the diffusion through the skin barrier. The addition of PG resulted for Bodipy® FL C_5 and Bodipy® 564/570 C_5 in an increase in accumulation in the outer and inner root sheath of the hair follicle. This indicates that propylene glycol either affects the lipids in the follicular opening or increases the diffusion from the epidermis to the outer root sheath (see above).

Distribution - Influence of permeant lipophilicity

The donor phases influence the effect of permeant lipophilicity on the accumulation in the various skin compartments. Previously it has been hypothesised that the presence of 30% ethanol (v/v) in citric acid buffer (Grams, Bouwstra, 2002b) promotes the partitioning of the lipophilic dye in the hair follicle regions. From the results in this study it is clear that also for a surfactant vehicle the accumulation in the hair follicle regions is stronger promoted for the more lipophilic dyes than for the less lipophilic Oregon Green® 488. An even stronger accumulation of the lipophilic dyes in the hair follicles is observed when the

surfactant formulation is combined with propylene glycol indicating a synergistic effect for lipophilic dyes.

CONCLUSION

The relative accumulation values do not give any indications on the absolute accumulation. However by comparing the relative accumulation values of two labels in the hair follicle, the influence of donor phase composition on the label distribution can be accessed. Therefore from our results we can conclude that a substance with low lipophilicity hardly accumulates in the hair follicle and that this accumulation is not enhanced in the presence of surfactants. With an increase in permeant lipophilicity, an increase in follicular accumulation is achieved. This accumulation of lipophilic permeants in the follicular area is enhanced in the presence of surfactants and PG. The increased accumulation can be achieved in two ways: i) Increased penetration through the stratum corneum resulting in an increased transport via the epidermis to the outer root sheet. ii) Interaction between formulation and the sebum lipids in the infundibulum, thereby facilitating the access to the thinner stratum corneum and the penetration along the hair shaft into deeper skin regions. Overall we conclude that lipophilic substances can be accumulated in the hair follicle by means of surfactant solutions. However from this study no conclusion can be drawn regarding the most likely mechanism, since no information is available about the permeation pathway of the dye. For this reason on-line diffusion studies are initiated.

ACKNOWLEDGEMENTS

We gratefully thank Unilever Research, Port Sunlight, UK for financing this project.

REFERENCES

Agarwal, R., Katare, O.P., Vyas, S.P., 2000. The pilosebaceous unit: A pivotal route for topical drug delivery. Methods Find. Exp. Clin. Pharmacol. 22, 129-133.

Allec, J., Chatelus, A., Wagner, N., 1997. Skin distribution and pharmaceutical aspects of adapalene gel. J. Am. Acad. Dermatol. 36, S119-S125.

Grams, Y.Y., Bouwstra, J.A., 2002a. A new method to determine the distribution of a fluorophore in scalp skin with focus on hair follicles. Pharm. Res. 19, 350-354.

Grams, Y.Y., Bouwstra, J.A., 2002b. Penetration and distribution *in vitro* of three lipophilic probes in human skin focussing on the hair follicle. J. Control. Release submitted.

Gupta, S., Domashenko, A., Cotsarelis, G., 2001. The hair follicle as a target for gene therapy. Eur. J. Dermatol. 11, 353-356.

Li, L., Hoffman, R.M., 1995. The feasibility of targeted selective gene therapy of the hair follicle. Nat. Med. 1, 705-706.

Lieb, L.M., Liimatta, A.P., Bryan, R.N., Krueger, G.G., 1995. Description and definition of a transfollicular route of permeation for topically applied agents to human scalp skin. J. Invest. Dermatol. 104, 655.

Meuwissen, M.E.M.J., Janssen, J., Cullander, C., Junginger, H.E., Bouwstra, J.A., 1998. A cross-section device to improve visualization of fluorescent probe penetration into the skin by Confocal Laser Scanning Microscopy. Pharm. Res. 15, 352-356.

Rolland, A., Wagner, N., Chatelus, A., Shroot, B., Schaefer, H., 1993. Site-specific drug delivery to pilosebaceous structures using polymeric microspheres. Pharm. Res. 10, 1738-1744.

Schaefer, H., Lademann, J., 2001. The role of follicular penetration - A differential view. Skin Pharmacol. Appl. Skin Physiol. 14 Suppl. 1, 23-27.

Schaefer, H., Watts, F., Brod, J., and Illel, B., 1989. Follicular penetration. In: Scott, R.C., Guy, R.H., and Hadgraft, J. (Eds.), Prediction of Percutaneous Penetration; Methods, Measurements, Modelling. IBC Technical Services, pp. 163-173.

Sumian, C.C., Pitre, F.B., Gauthier, B.E., Bouclier, M., Mordon, S.R., 1999. A new method to improve penetration depth of dyes into the follicular duct: Potential application for laser hair removal. J. Am. Acad. Dermatol. 41, 172-175.

Turner, N.G., Guy, R.H., 1998. Visualization and quantitation of iontophoretic pathways using confocal microscopy. J. Invest. Dermatol. Symp. Proc. 3, 136-142.

Weiner, N., 1998. Targeted follicular delivery of macromolecules via liposomes. Int. J. Pharm. 162, 29-38.

Wu, H.L., Ramachandran, C., Weiner, N.D., Roessler, B.J., 2001. Topical transport of hydrophilic compounds using water-in-oil nanoemulsions. Int. J. Pharm. 220, 63-75.

V

On-line visualisation of dye diffusion in fresh unfixed human skin

YY Grams, L Whitehead, P Cornwell and JA Bouwstra. Pharm Res. 21 (2004) 851-859.

ABSTRACT

Purpose. The purpose of the present study was to develop a new method to examine the diffusion in fresh unfixed human skin *on-line*.

Methods. Full thickness skin samples were cut perpendicular to the skin surface (cutting plane facing upwards) with a new cutting device forming part of the final diffusion cell. The donor solution contained 0.1 mg/ml Bodipy® FL C_5 (moderately lipophilic,) dissolved in citric acid buffer pH 5.0 while the acceptor phase consisted of phosphate buffered saline pH 7.4. Images were taken with confocal laser scanning microscopy (CLSM) every 10 minutes for 8 hours.

Results. This new method enabled for the first time visualisation of concentration profiles in different skin layers simultaneously as a function of time. For this model penetrant, Bodipy® FL C_5, showed that, the lower stratum corneum layer constitutes the greatest barrier to diffusion. Furthermore there is preferred partitioning of this probe in epidermis versus either stratum corneum or dermis.

Conclusions. The on-line diffusion cell in combination with CLSM is a promising tool to study diffusion processes of dyes in fresh unfixed skin on-line. The method has the potential to access deeper skin layers as well as to visualise diffusion processes in cells.

INTRODUCTION

In pharmaceutical and cosmetic research the distribution of penetrating probes is of great interest for understanding and improving drug efficacy. This distribution is accessible by visualisation of the skin, focussing either on the stratum corneum, the epidermis or on deeper layers of the skin including its appendages. The latter is especially of interest for local delivery to the sweat glands or to the pilosebaceous unit (sebaceous gland and the hair follicle).

Recently, techniques used so far in skin imaging (1) or in quantification of substance distribution within the skin have been reviewed elsewhere (2). In summary, local targeting of a drug and its distribution in the skin can be investigated using (i) only one-time-point or (ii) multiple-time-point or even continuous visualisation in one piece of skin. In the first case visualisation methods including post-experimental processing like fixation or staining are feasible (1,2). However they bear the danger of artefact formation or delocalisation of the label. In the second case post-experimental processing of the skin (cutting or chemical fixation) is not acceptable, since it would influence the diffusion process of the substance. Additionally minimisation of the variation between time points by using skin of the same donor is an advantage.

In literature various techniques have been described which are feasible for real-time visualisation of skin namely video fluorescence imaging (3), video microscopy (4-7), magnetic resonance imaging (8-10), electron paramagnetic resonance (11), ultrasound backscatter microscopy (12), Raman spectroscopy (13,14) and various modifications of confocal microscopy (15-21). While techniques like fluorescence imaging, magnetic resonance imaging and ultrasound backscatter microscopy have a limited resolution; techniques like fluorescence imaging and video microscopy are limited to the visualisation of the upper layers. Confocal microscopy and confocal Raman spectroscopy can access deeper layers such as the upper dermis due to optical sectioning even *in vivo*.

In our studies Confocal Laser Scanning Microscopy (CLSM) in combination with fluorophores has been used. This has the advantage that the skin can be visualised without fixation and that the resolution is sufficient to visualise the various layers of the hair follicle. However the deeper layers of the dermis are not accessible due to scattering and absorption processes of the fluorescence signal. For this reason a method has been developed in our group limiting the artefact formation by cross-sectioning *fresh* human skin (22). More recently, this technique was extended to full-thickness skin (23). This method allows examining the distribution of fluorophores in the various skin compartments after a pre-determined period of diffusion. Although this provides detailed information on the fluorophore accumulation in the various skin

compartments, it is not possible to gain information on the permeation pathways of the active agents. For information on permeation pathways on-line visualisation of diffusion processes is required. Therefore the aim of our present study is to develop a visualisation method enabling real-time image acquisition in the same donor using human skin. Since future studies will be focused on target areas in deeper skin layers such as the pilosebaceous unit, the subcutaneous tissue is also included.

MATERIALS AND METHODS

Model substance

Two fluorophores were selected to develop the diffusion cell used for on-line CLSM visualisation, subsequently named 'on-line diffusion cell'. Oregon Green 488®, a low molecular weight molecule with a $logP_{octanol/buffer}$ of 1.6 at pH 5.0 and -2.5 at pH 7.4, was selected for leakage tests due to poor penetration in the skin. Bodipy® FL C_5, a low molecular weight compound with a $logP_{octanol/buffer}$ of 2.5 at pH 5.0 and 1.2 at pH 7.4, was used for the on-line experiments due to its good staining properties. Both fluorophores were purchased from Molecular Probes, The Netherlands. Impregum F was obtained from Espe, Germany and the pioloform from Agar Scientific Ltd., UK.

Confocal Laser Scanning Microscopy

The visualisation of the fluorophores in the *non-fixed* scalp skin (3 donors) was carried out using a Bio-Rad MRC 600 unit equipped with an Argon laser with an emission line at 488 nm. The microscopic unit consisted of an inverted Zeiss IM-35 using a PlanApo 20 or PlanApo 63 oil immersion objective. The cross sectional view of the skin is obtained by using a modified cutting device according to Meuwissen *et al*. (22), which is used as a sample holder at the same time.

Donor and acceptor phase

The donor solutions contained 0.1 mg/ml Oregon Green 488® or 0.1 mg/ml Bodipy® FL C_5in citric acid buffer, pH 5.0. The donor compartment was completely filled with the donor solution, which was approximately 100 µl, with slight variations due to the dental clay usage. Care was taken to circumvent air enclosure in the donor compartment. The acceptor phase consisted of phosphate buffered saline pH 7.4 (139 mM NaCl, 2.5 mM KCl, 8 mM Na_2HPO_4, 1.5 mM KH_2PO_4, 25 mg/L Streptomycin and 25000 U/l Penicillin). The acceptor compartment was a static compartment of approximately 100 µl with small variations in size due to the dental clay sealing.

Preparation of on-line diffusion cell

The design and the preparation procedure of the on-line diffusion cell are depicted in Figure 1. Briefly, the stratum corneum surface of a fresh human scalp skin square (8x8 mm) including the subcutaneous fat is wiped with PBS and 70 % (v/v) ethanol to remove any contaminants and placed in the equivalent space of the cutting device (Figure 1, II). A silicone square with a pre-cut smaller square (4 x 2.5 mm) is supporting the skin at the stratum corneum side thereby preventing artefact formation during the cutting procedure (Figure 1, II). After cutting perpendicular to the skin surface only one half of the cutting device is used (Figure 1, III). The smaller square is removed carefully and a drying protection is placed above the cutting surface not touching the skin (not shown). Mounting the donor compartment to the cell completes the assembly (Figure 1, IV). A thin layer of dental clay (Impregum F) surrounds the skin and the cell compartments in the cutting plane (not shown). A pioloform-coated cover glass (0.5 % (w/v) pioloform in Chloroform, not shown) is placed on top of the dental clay and the skin, thereby sealing the on-line diffusion cell. After complete hardening of the dental clay, the acceptor phase is injected through the dental clay and the pioloform is removed from the accessible side of the cover glass with 70 % (v/v) ethanol. The on-line cell is now placed in a holder and subsequently in an adapter for the microscope (Figure 1, V-VI).

Image acquisition

The cross section is localised using its low autofluorescence with sensitive CLSM settings. Images were collected every 10 minutes starting 10 minutes after application of the donor phase for a period of 8.5 hours. Obvious leaking on-line preparations were immediately discarded from investigation. When the swelling appeared to have a severe influence on the movement of the point of focus the results were discarded as well. During the experiment, the temperature of the skin is not monitored. All measurements have been carried out at room temperature.

Test for leakage

In a pilot experiment the on-line diffusion cell was checked for leakage between the cover glass and the skin. For this purpose skin from the same donor was visualised after a 2-hour application in a flow-through diffusion cell from PermeGear and for 2 hours in an on-line diffusion cell.

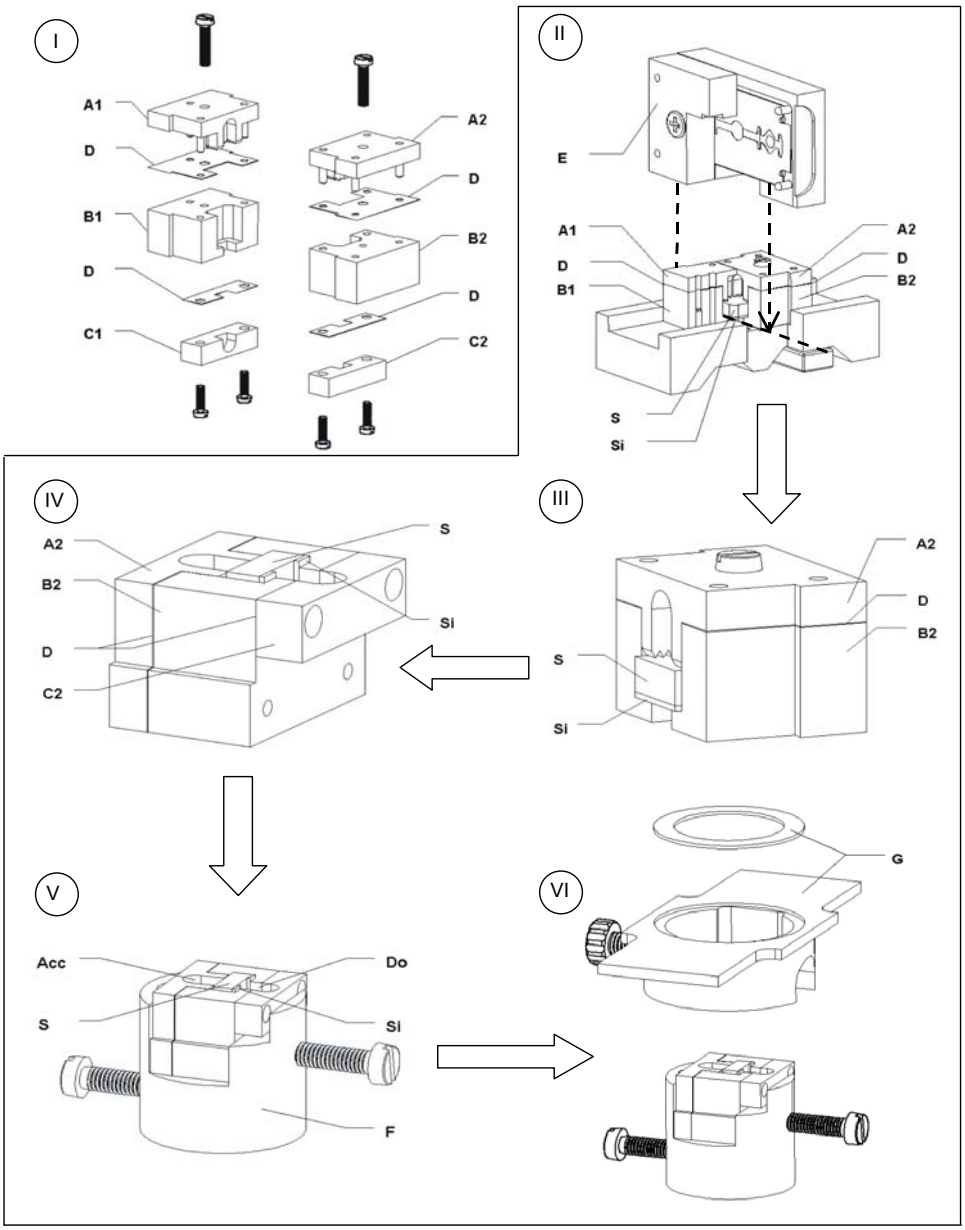

Figure 1. *Composition and preparation of the on-line diffusion cell with A - acceptor phase compartment, B - skin compartment, C - donor phase compartment, D - teflon sheet, E - cutting knife containing razor blade, S - Skin, Si - silicone square, Acc - acceptor phase, Do - donor phase, F - diffusion cell holder, G - microscope adapter. I shows the combined cutting and visualisation device, while II-VI depicts the preparation process of the on-line diffusion cell. A piece of skin including the subcutaneous fat is placed in the equivalent compartment of the cutting device with the stratum corneum side facing down (II). After cutting perpendicular to the skin surface (II) one half of the cutting device will be used for further processing (III). The donor compartment (C2) will be attached to the cutting device resulting in a cross sectional view of the skin with the adjacent donor and acceptor compartment (IV). The cross section is sealed with cover glass and dental clay (not shown) and subsequently placed in diffusion cell holders to enable visualisation in the CLSM (V and VI).*

Image analysis

In the image analysis of the on-line series it has to be assumed that the fluorescence of one molecule is independent of the skin part. Therefore a model drug has been chosen which is reported to be insensitive to pH and solvent polarity (24). Although the measurement of the fluorescence results in a two-dimensional image, the actual focal plane is three-dimensional. Therefore the obtained fluorescence is the integrated fluorescence from a constant volume around the focal plane. The images of the time series were analysed using Image J software. A grey scale displays fluorescence intensities in one image with 0 (black) as the minimal and 254 (white) as the maximal value. In order to obtain an average value for the fluorescence intensity of a pixel in depth, a box of 50 pixels wide and a length determined by the cross section (>300 pixels) was chosen and placed across the image perpendicular to the stratum corneum (Figure 3). The analysed box is displayed above each distribution profile. The change of fluorescence in time (dF/dt) and in depth from the skin surface (dF/dx) was recorded. The stratum corneum was divided into three layers (top, middle and deep) and the viable epidermis in two layers (top, deep) while only the upper layers of the dermis could be analysed.

Fick's law describes that the transported mass dm [g] per time unit dt [h] through a defined area A [cm^2] is directly proportional to the diffusion coefficient D [cm^2/s], the size of the area and the concentration change dc [g/cm^3]. However it is reverse proportional to the thickness of the membrane dx [cm].

$$\frac{dm}{dt} = -DA\frac{dc}{dx} \qquad \text{Equation 1}$$

The change of concentration with depth (dc/dx) in a defined time period is proportional to the change of fluorescence in depth (dF/dx) in the same time period. The proportionality is unknown in CLSM however can be expressed by introducing a proportionality factor K_c.

$$\frac{dc}{dx} = K_c\frac{dF}{dx} \qquad \text{Equation 2}$$

In a steady state situation, the mass transported across the stratum corneum, the viable epidermis and the dermis are equal, since no accumulation in each of the skin layers occurs. Therefore a relation between the diffusion coefficients of the various skin layers can be estimated and consequently the influence of different skin layers on the diffusion of a dye through the skin can be compared. However it has to be realised, that using Fick's law of diffusion is an approximation in our experimental set-up as the donor and acceptor phase were both static.

RESULTS

Test for leakage

To ensure that the observed diffusion is not due to leakage of label between the cutting surface and the cover glass the set up was checked for leakage. Neither a preliminary test with a methylene blue solution (not shown) nor the comparison of 2 hours penetration of a hydrophilic Oregon Green 488® in skin of the same donor using the static (Figure 2 IA) and the on-line mode (Figure 2 IB) revealed any indication of leakage. With identical microscopic settings, comparable images were obtained. In both cases neither the epidermis nor the dermis revealed significant staining.

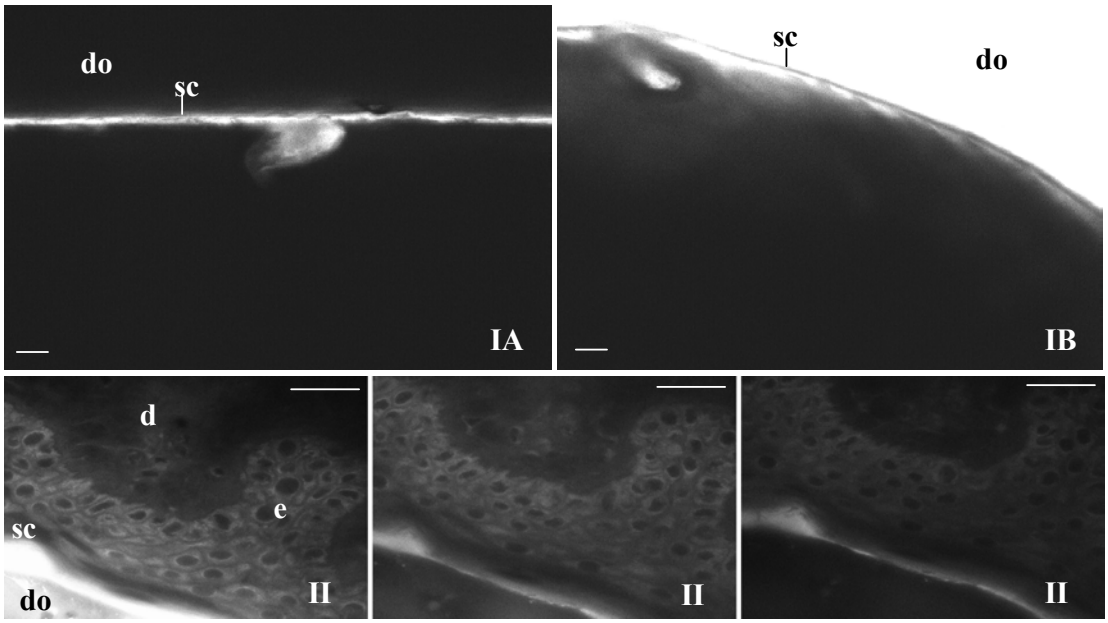

***Figure 2**. Tests for leakage of the on-line diffusion cell. IA shows the distribution of 0.1 mg/ml Oregon Green® 488 in citric acid buffer pH 5.0 after 2 hours application in a PermeGear flow-through diffusion cell after post-experimental cross sectioning. IB is the view of the skin cross section in the on-line diffusion cell after 2 hours application of the same donor solution. The donor solution is still present in the on-line diffusion cell. No indication of leakage is present. Do - donor phase compartment, sc - stratum corneum. Images II show the distribution of 0.1 mg/ml Bodipy® FL C_5 in citric acid buffer pH 5.0 in the on-line diffusion cell after 10 min (IIA), 4 h 10 min (IIB) and 8 h 20 min (IIC). This time series is a positive example of leakage. If leakage was observed, the on-line preparation was discarded immediately. d - dermis, e - epidermis. The scale bar represents 25 µm.*

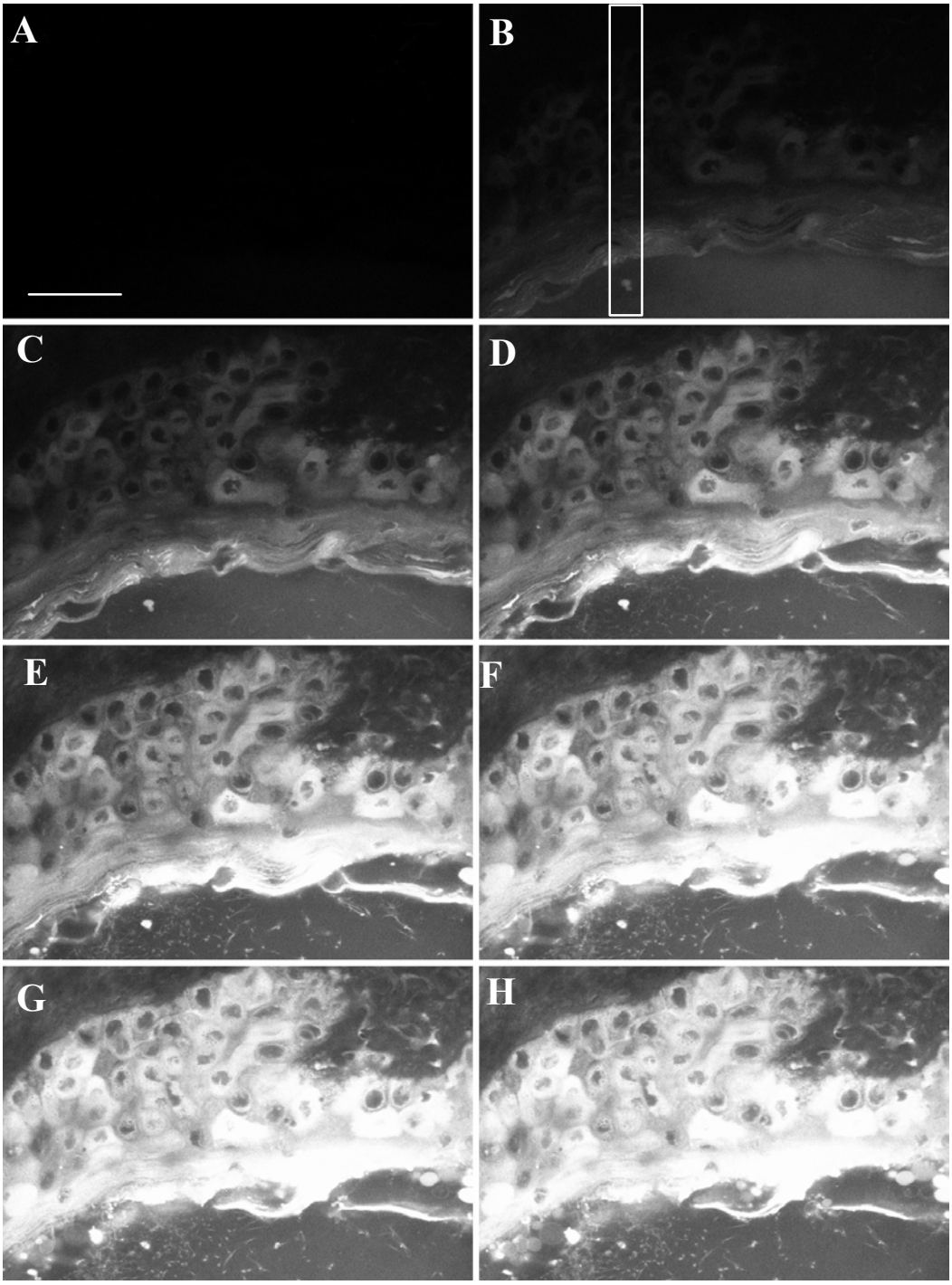

Figure 3. *A typical example of on-line visualisation of the distribution of 0.1 mg/ml Bodipy® FL C_5 in citric acid buffer applied at time point 0 in the donor compartment. Images were obtained every 10 minutes from which time points 10 min (A), 50 min (B), 1 h 30 min (C), 2 h 10 min (D), 2 h 50 min (E), 3 h 30 min (F), 4 h 10 min (G) and 4 h 50 min (H) are displayed. The box depicted in B resembles the quantified area at all time points that are provided in Figure 5. The scale bar is equivalent to 25 µm.*

On-line experiments were started using Bodipy® FL C_5. Figure 2 IIA-IIC depict one skin preparation where leakage of the Bodipy® FL C_5 along the cover glass is obvious. The images reveal an immediate presence of label in the epidermal layer. Furthermore no increase in label intensity could be observed. A decrease in fluorescence intensity up to the end of image acquisition took place. In on-line experiments where leakage was suspected as in Figure 2 IIA-C, the prepared skin was discarded.

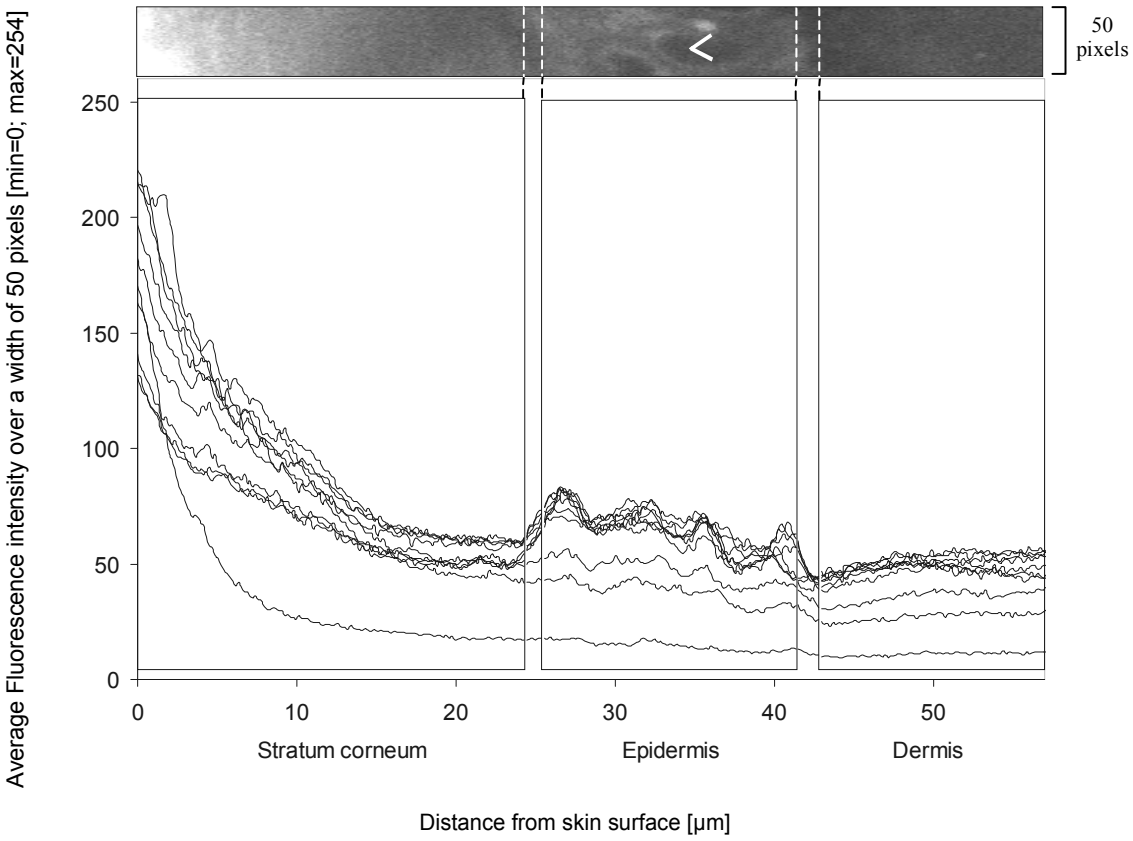

***Figure 4**. Distribution profiles of 0.1 mg/ml Bodipy® FL C5 in citric acid buffer pH 5.0 displayed as average fluorescence intensity against depth of one representative donor as detected by confocal laser scanning microscopy. The average intensity was measured by selecting a 50-pixel wide box (depicted above the donor profile) over the whole thickness of the imaged skin and averaging the value of 50 pixels for every pixel in the depth. Images were recorded every 10 minutes. To increase clarity of the figure, only distribution profiles of every 40 minutes are depicted with the lowest line representing 10 minutes after application. For the complete set of distribution profiles for this donor, see donor 2 of Figure 5. The area of the respective stratum corneum, epidermis and first part of the dermis is marked in the graph and as dashed lines in the confocal picture above the graph. Inhomogeneities in the distribution profile of the viable epidermis can be correlated to the nuclei as seen in the confocal image (arrow).*

On-line diffusion

With the on-line diffusion cell and the described method of preparation it is possible to examine the diffusion of a fluorophore in unfixed fresh human skin from the stratum corneum across the viable epidermis into the dermis (Figure 3). Shortly after the application of the donor solution only the donor phase and the skin interface can be distinguished. In the diffusion process, the stratum corneum is labelled first, with strong labelling at the surface, followed by the epidermis and the dermis. At late time points the staining of the epidermis is stronger than in the lower part of the stratum corneum and the dermis. Additionally details of the epidermis such as the cell nuclei can be monitored as well.

Distribution profile in time

Due to the Image J analysis of the time series, a distribution profile of the fluorescence in a 10-minute time-interval at pixel resolution is obtained (Figure 4 and Figure 5). The distribution profiles in time vary between the three donors (Figure 5). Differences are observed in thickness of the stratum corneum and the viable epidermis as well as in the average fluorescence intensity values (maximum values in the raw data range from 110 for donor 1 up to >254 for donor 3). However gradients within one skin layer and relative fluorescence differences between the layers are comparable between the various donors. Focussing at the profile itself, at early time points label is detected only in the stratum corneum where the intensity increases fast with time. After 8 hours it appears that within the stratum corneum the fluorescence gradient in depth is dependent on the position and not constant throughout the stratum corneum. The region close to the surface is characterised by a steep fluorescence gradient in the stratum corneum, while a less steep fluorescence gradient is observed in the stratum corneum region close to the viable epidermis. In the viable epidermis low fluorescence intensity is observed at early time points and increases with time. At late time points an abrupt increase in fluorescence intensity is observed for donor 1 and 2 at the junction between the stratum corneum and the viable epidermis. At the same time a significant decrease ($p<0.001$) in fluorescence intensity in the second half of the epidermis is observed for all three donors up to the epidermal-dermal junction. Local fluctuations in the profile of the epidermis correspond to smaller structures such as nuclei as seen in the analysed box (Figure 4). At the junction of viable epidermis and dermis the intensity drops significantly for all three donors. The dermis reveals in all three donors a constant increase in fluorescence intensity in time until a maximum is reached. However nothing can be said about the distribution within the dermis since due to the microscopic settings only the first few micrometers are accessible in these time series. Although no differences between the stratum corneum and the viable epidermis

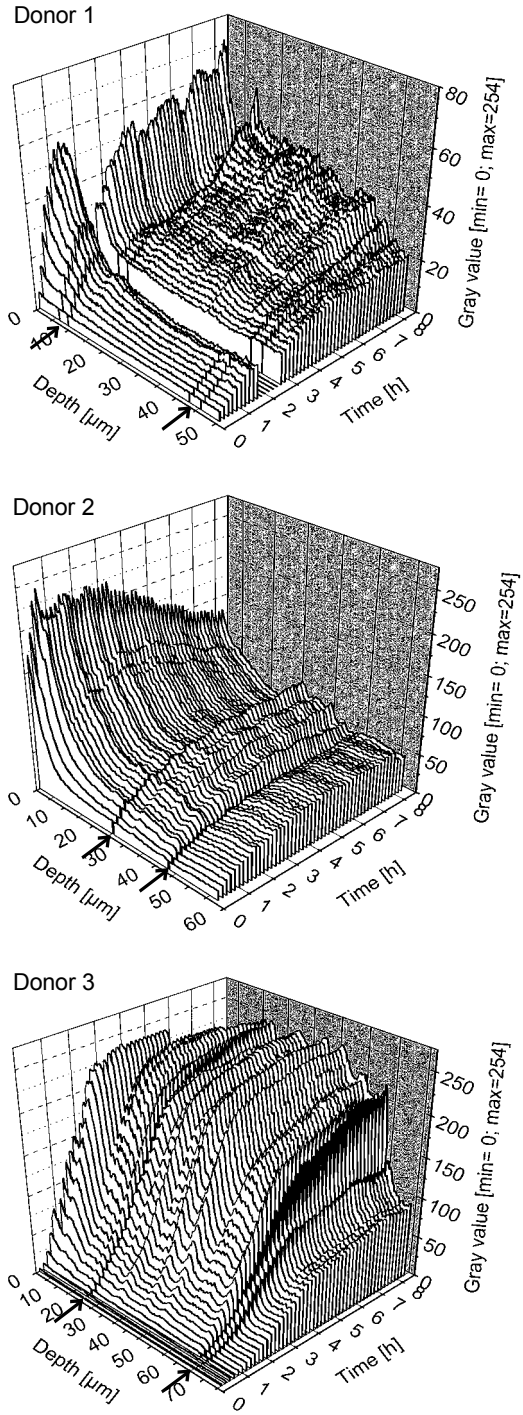

Figure 5. 3-dimensional distribution profiles of 0.1 mg/ml Bodipy® FL C5 in citric acid buffer pH 5.0 displayed as average fluorescence intensity against depth and time of 3 donors as detected by confocal laser scanning microscopy. The average intensity was measured by selecting a 50-pixel wide box over the whole thickness of the imaged skin and averaging the value of 50 pixels for every pixel in the depth. Images were recorded every 10 minutes with the lowest line representing 10 minutes after application. The transition from the stratum corneum to the epidermis and from the epidermis to the first part of the dermis is marked in the graph by arrows.

at late time points were observed for donor 3 due to saturation of the signal, at early time points similar profiles were observed as with donor one and two. Regarding the difference between the viable epidermis and the dermis at late time points this observation is also in agreement with donor 1 and donor 2.

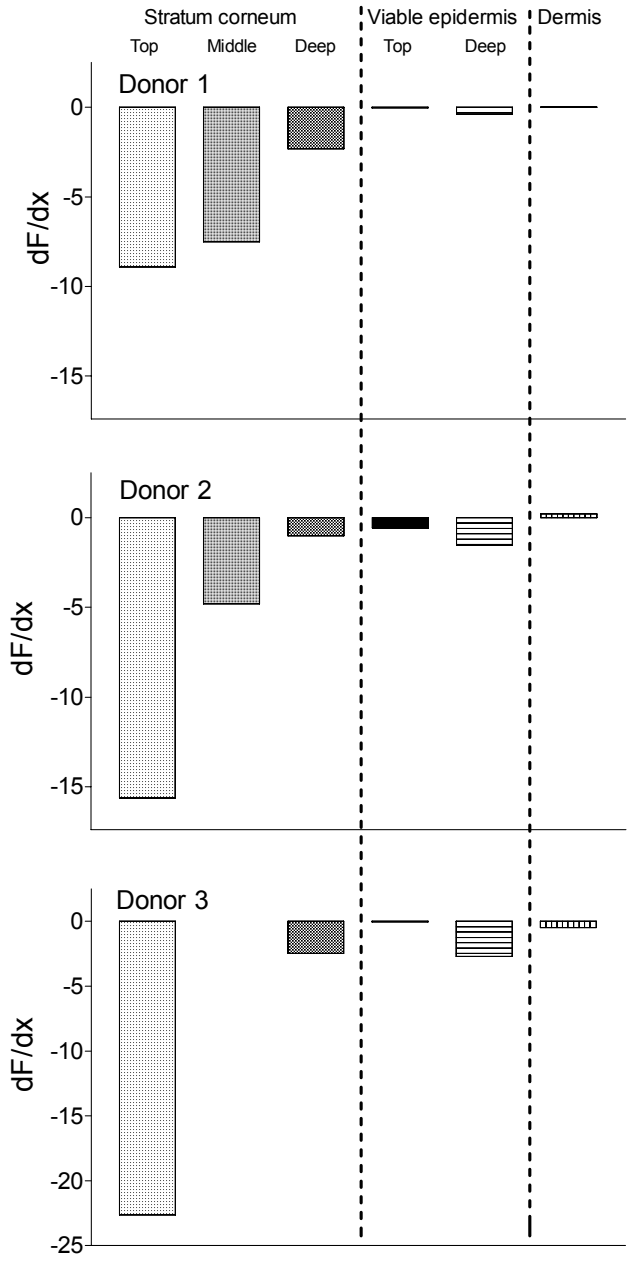

***Figure 6**. Fluorescence gradient (dF/dx) in the stratum corneum (top, middle, deep), the viable epidermis (top, deep) and the upper part of the dermis after application of 0.1 mg/ml Bodipy® FL C5 in citric acid buffer pH 5.0. The fluorescence gradient has been determined from Figure 5 selecting time points close to steady state. Pre-steady state diffusion and influences due to dye degradation and donor phase depletion were not included. In donor 3 only two layers of the stratum corneum could be clearly distinguished.*

Figure 6 displays the fluorescence gradient in depth of the various skin layers. Values of different donors were treated separately due to variations in the detected fluorescence signal despite the same settings of the microscope for all the on-line experiments. The stratum corneum reveals the highest fluorescence gradients; however the gradients decrease with depth. In the viable epidermis, rather low gradients are observed which increase in the lower half of the viable epidermis. The dermis reveals hardly any fluorescence gradient in the visualised layers. Comparing the fluorescence gradient of one skin layer with the fluorescence gradient of a second skin layer, information about the diffusion can be obtained.

DISCUSSION

Variability within distribution profile

The observed variation in the thickness of the stratum corneum and the viable epidermis is due to the local differences within one individual (e.g. desquamating stratum corneum and undulating epidermal-dermal junction) and to the inter-individual variations. The obvious deviation in profile of donor 3 compared to donor 1 and 2 is due to pre-selected settings of the CLSM. In pilot studies standard settings for the CLSM were chosen to obtain an adequate signal from the time series since signal optimisation cannot be carried out during the diffusion process. When a fluorescence value of 254 is reached, no further increase in fluorescence intensity can be detected although higher fluorescence might be present. Since the intensity in the stratum corneum of donor 3 reaches the maximum after two hours, no difference with the high value in the epidermis is obtained. The elevated fluorescence of the epidermis however results in a clearer difference of fluorescence intensity between the epidermis and the dermis.

Care should be taken as much as possible to avoid photobleaching, since within one time series this can lead to inconsistencies. One of the reasons for selecting Bodipy® FL C_5 is the improved photostability making the dye less sensitive to photobleaching. Bodipy® FL C_5 is also reported to be insensitive to solvent polarity and pH (24) and therefore is a suitable model compound for the evaluation of the diffusion pathway. A photobleaching experiment of labelled skin (150 scans) revealed only a minor decrease in fluorescence intensity. Since we did not observe any decrease of fluorescence intensity within time in the experiment, photobleaching is not expected to influence the presented on-line diffusion results.

Distribution profiles

Although the donor phase was not stirred and exhibited depletion after longer diffusion times and the acceptor phase was static, the obtained curves resemble the ones of the two-layer skin model as reported earlier (25-27). In CLSM, fluorescence intensities of different donors cannot be averaged. Therefore the fluorescence gradient of Bodipy® FL C_5 have been summarised as displayed in Figure 6. The gradient within the stratum corneum is not constant but varies in depth. The steepest gradient is observed in the upper part of the stratum corneum, where most of the fluorescent label is accumulated. The sudden increase in fluorescence intensity from the dead to the viable epidermis can originate from the absence of cornified envelope and the easy partitioning into the viable epidermis. In the epidermis, the fluorescent intensity gradient is less than in stratum corneum and also varies in depth. The dermis contains fibrous, filamentous and amorphous connective tissue with a high water retaining capacity (28) making the dermis rather hydrophilic. The sudden decrease of the fluorescence from the epidermis to the dermis can therefore be explained by the lower affinity of the dermis for a lipophilic substance as Bodipy® FL C_5.

Time- and Depth-resolution

Several studies have been performed to obtain depth profiles of substances within the epidermis and dermis. Caspers *et al.* (14) has obtained a depth profile of Raman active compounds of the skin in vivo. Although no diffusion profiles in time have been reported yet, the authors propose that this technique has the potential to achieve time and depth resolution. Yu *et al.* (29) published distribution profiles of two fluorescent dyes using two-photon CLSM up to a depth of 32 µm. In this case the on-line diffusion was not studied. Previously Hoogstraate *et al.* (20) reported concentration gradients of a fluorescent dye in buccal epithelium observed for 2 hours. Profiles were measured using narrow boxes parallel to the skin surface. The method presented in this article extends the method from Hoogstraate *et al.* (20) in 3 ways. Since in the combined cutting/on-line cell the skin is not moved from the cutting device to the on-line diffusion cell, damage of the freshly obtained cutting surface is prevented. Furthermore, in the present studies only very small variations in the volumes of the acceptor and of the donor phase occur. In the previous studies by Hoogstraate *et al.* these compartments were created solely by dental clay and varied between the various experiments. Another advantage of this technique is that the measurement of the fluorescence intensity in time is specific per pixel rather than limited to the shape of boxes parallel to the skin surface. Additionally this new technique has the potential to visualise fluorophores in deeper layers of the skin such as appendages (sweat glands, sebaceous glands, and hair follicles) and the subcutaneous fat.

By estimating the fluorescence gradient for the different skin layers, valuable information can be gained about the diffusion process of substances in intact skin. As mentioned above the stratum corneum does not reveal a linear fluorescence gradient over the full stratum corneum thickness. It appears that the stratum corneum is not a homogeneous membrane as considered in the various models but that layers at different depths have different diffusion properties. In order to further optimise the experimental set-up, a flow-through acceptor and donor phase can be created to rule out depletion and accumulation in any of the phases.

Importantly, the maximum fluorescent gradient in the upper layers of the stratum corneum is formed over a considerate time period. This can be explained as follows. If the deepest layers in the stratum corneum are almost impermeable for the dye, only a limited amount of dye will cross this layer. This will cause, due to its favourable partitioning, an accumulation of the lipophilic dye in the more superficial layers in the stratum corneum, which in turn causes a steep concentration gradient within the stratum corneum. The low fluorescence gradient in the viable epidermis and the fact that the steady state gradient is reached in a rather short time period proves the absence of a physical barrier function in this layer. Although the lower part of the viable epidermis reveals a higher fluorescence gradient, it is still lower than the fluorescence gradient of the upper 2/3 of the stratum corneum. Once reaching the dermis, the fluorescence gradient is slightly lower implying that the diffusion from the epidermis to the dermis is not rate limiting. Focusing on the partitioning of the lipophilic dye from one skin layer to the adjacent skin layer it is striking, that the partitioning of the dye from the lower stratum corneum to the viable epidermis is high, while the partitioning from the epidermis further into the dermis is not favoured. This supports the earlier finding of high affinity of the epidermis for this lipophilic label (30, 31). Early publications reviewed by Kim *et al.* (32) state that the penetration of highly lipophilic compounds from the epidermis into the dermis can be rate limiting. In case of our lipophilic substance the rate-limiting step is still within the stratum corneum.

The presented study is the first study in which a fluorescence gradient is measured on-line in fresh and unfixed human skin. Using this method it is not only possible to measure fluorescent gradients in the main skin layers (stratum corneum, viable epidermis and dermis) but fluorescent intensities can even be distinguished between areas within these layers. However in this study the fluorescent gradient for the dermis is limited to the first few micrometers and cannot give any information about the deeper layers. Decrease in the magnification would improve the information obtained for the dermal area, but will limit the information on the stratum corneum. In future studies this technique can be improved by designing a flow-through donor and acceptor phase to create a steady state situation. Pilot studies performed in our laboratory give indications

that a flow-through construction of the donor and acceptor compartment is a feasible modification.

CONCLUSION

The presented method enables the visualisation and evaluation of time resolved diffusion into the skin. Fixation and thereby alteration of skin structures and the danger of delocalisation of the dye can be circumvented. Due to the cross-sectional view, visualisation of structures as far in the skin as the subcutaneous fat can be possible without loss of resolution or sensitivity. Cell structures like nuclei and membranes can be distinguished which provides the opportunity to observe diffusion processes not only at the skin layer level but as well at the cellular level in the epidermis. This would be of interest to study DNA transfer in cell nuclei. Taking advantage of this time-resolved visualisation technique, transport processes can be investigated and delivery systems developed and optimised. In spite of its limitation to fluorophores and *in vitro* studies the combined cutting device/on-line diffusion cell with CLSM is a promising tool for skin transport studies due to its high resolution, use of non-fixed skin and access to subcutaneous fat.

ACKNOWLEDGEMENTS

We would like to thank Jan Janssen and Henk Verpoorten for the co-operation in the development of the on-line diffusion cell. Furthermore we acknowledge Unilever Research, Port Sunlight, UK for financing this project.

REFERENCES

1. P. Corcuff and G. E. Pierard. Skin imaging: State of the art at the dawn of the year 2000. *Skin Bioeng.* ***26*****:**1-11 (1998).
2. E. Touitou, V. M. Meidan and E. Horwitz. Methods for quantitative determination of drug localized in the skin. *J. Control. Rel.* ***56*****:**7-21 (1998).
3. F. Lund and T. Jogestrand. Video fluorescein imaging of the skin: description of an overviewing technique for functional evaluation of regional cutaneous blood perfusion in occlusive arterial disease of the limbs. *Clin. Physiol.* ***17*****:**619-633 (1997).
4. R. H. Bull, D. O. Bates and P. S. Mortimer. Intravital video-capillaroscopy for the study of the microcirculation in psoriasis. *Br. J. Dermatol.* ***126*****:**436-445 (1992).
5. J. L. Morris. Cotransmission from sympathetic vasoconstrictor neurons to small cutaneous arteries in vivo. *Am. J. Physiol. Heart Circ. Physiol.* ***46*****:**H58-H64 (1999).
6. T. Salmon, R. A. Walker and N. K. Pryer. Advances in Microscopy-Part III; Video-Enhanced Differential Interference Contrast Light Microscopy. *BioTechniques* ***7*****:**624-633 (1989).
7. A. W. B. Stanton, H. S. Patel, J. R. Levick and P. S. Mortimer. Increased dermal lymphatic density in the human leg compared with the forearm. *Microvasc. Res.* ***57*****:**320-328 (1999).
8. S. Richard, B. Querleux, J. Bittoun, I. Idy-Peretti, O. Jolivet, E. Cermakova and J. L. Leveque. In vivo proton relaxation times analysis of the skin layers by magnetic resonance imaging. *J. Invest. Dermatol.* ***97*****:**120-125 (1991).

9. H. K. Song, F. W. Wehrli and J. F. Ma. In vivo MR microscopy of the human skin. *Magn. Reson. Med.* ***37*****:**185-191 (1997).
10. M. Szayna and W. Kuhn. In vivo and in vitro investigations of hydration effects of beauty care products by high-field MRI and NMR microscopy. *Eur Acad Dermatol Venereol.* ***11*****:**122-128 (1998).
11. T. Herrling, J. Fuchs and N. Groth. Kinetic measurements using EPR imaging with a modulated field gradient. *J. Magn. Reson.* ***154*****:**6-14 (2002).
12. D. H. Turnbull, B. G. Starkoski, K. A. Harasiewicz, J. L. Semple, L. From, A. K. Gupta, D. N. Sauder and F. S. Foster. 40-100 MHz B-SCAN ultrasound backscatter microscope for skin imaging. *Ultrasound Med. Biol.* ***21*****:**79-88 (1995).
13. P. J. Caspers, G. W. Lucassen, R. Wolthuis, H. A. Bruining and G. J. Puppels. In vitro and in vivo Raman spectroscopy of human skin. *Biospectroscopy* ***4*****:**S31-S39 (1998).
14. P. J. Caspers, G. W. Lucassen, E. A. Carter, H. A. Bruining and G. J. Puppels. In vivo confocal Raman microspectroscopy of the skin: Noninvasive determination of molecular concentration profiles. . *J. Invest. Dermatol.* ***116*****:**434-442 (2001).
15. D. Aghassi, R. R. Anderson and S. Gonzalez. Time-sequence histologic imaging of laser-treated cherry angiomas with in vivo confocal microscopy. *J. Am. Acad. Dermatol.* ***43*****:**37-41 (2000).
16. C. Bertrand and P. Corcuff. In vivo spatio-temporal visualization of the human skin by real-time confocal microscopy. *Scanning* ***16*****:**150-154 (1994).
17. P. Corcuff, C. Bertrand and J. L. Leveque. Morphometry of human epidermis in vivo by real-time confocal microscopy. *Arch. Dermatol. Res.* ***285*****:**475-481 (1993).
18. C. Cullander. Light microscopy of living tissue: the state and future of the art. *J. Invest. Dermatol. Symp. Proc.* ***3*****:**166-171 (1998).
19. B. S. Grewal, A. Naik, W. J. Irwin, G. Gooris, G. J. de-Grauw, H. G. Gerritsen and J. A. Bouwstra. Transdermal macromolecular delivery: Real-time visualization of iontophoretic and chemically enhanced transport using two-photon excitation microscopy. *Pharm. Res.* ***17*****:**788-795 (2000).
20. A. J. Hoogstraate, C. Cullander, J. F. Nagelkerke, F. Spies, J. Verhoef, A. H. G. J. Schrijvers, H. E. Junginger and H. E. Bodde. A novel in-situ model for continuous observation of transient drug concentration gradients across buccal epithelium at the microscopical level. *J. Control. Rel.* ***39*****:**71-78 (1996).
21. M. Rajadhyaksha, S. Gonzalez, J. M. Zavislan, R. R. Anderson and R. H. Webb. In vivo confocal scanning laser microscopy of human skin II: Advances in instrumentation and comparison with histology. *J. Invest. Dermatol.* ***113*****:**293-303 (1999).
22. M. E. M. J. Meuwissen, J. Janssen, C. Cullander, H. E. Junginger and J. A. Bouwstra. A cross-section device to improve visualization of fluorescent probe penetration into the skin by Confocal Laser Scanning Microscopy. *Pharm. Res.* ***15*****:**352-356 (1998).
23. Y. Y. Grams and J. A. Bouwstra. A new method to determine the distribution of a fluorophore in scalp skin with focus on hair follicles. *Pharm. Res.* ***19*****:**350-354 (2002).
24. J. Karolin, L. B. A. Johansson, L. Strandberg and T. Ny. Fluorescence and absorption spectroscopic properties of Dipyrrometheneboron difluoride (BODIPY) derivatives in liquids, lipid membranes, and proteins. *J. Am. Chem. Soc.* ***116*****:**7801-7806 (1994).
25. H. Okamoto, F. Yamashita, K. Saito and M. Hashida. Analysis of drug penetration through the skin by the two-layer skin model. *Pharm. Res.* ***6*****:**931-937 (1989).
26. R. J. Scheuplein and L. W. Ross. Mechanism of percutaneous absorption. V. *J. Invest. Dermatol.* ***62*****:**353-360 (1974).
27. F. Yamashita, H. Bando, Y. Koyama, S. Kitagawa, Y. Takakura and M. Hashida. In vivo and in vitro analysis of skin penetration enhancement based on a two-layer diffusion model with polar and nonpolar routes in the stratum corneum. *Pharm. Res.* ***11*****:**185-191 (1994).
28. H. Schaefer and T. E. Redelmeier. *Skin Barrier: Principles of Percutaneous Absorption,* Karger, Basel,1996.
29. B. Yu, C. Y. Dong, P. T. So, D. Blankschtein and R. Langer. In vitro visualization and quantification of oleic acid induced changes in transdermal transport using two-photon fluorescence microscopy. *J. Invest. Dermatol.* ***117*****:**16-25 (2001).
30. Y. Y. Grams and J. A. Bouwstra. Penetration and distribution of three lipophilic probes in vitro in human skin focusing on the hair follicle. *J. Control. Rel.* ***83*****:**253-262 (2002).
31. Y. Y. Grams, S. Alaruikka, L. Lashley, J. Caussin, L. Whitehead and J. A. Bouwstra. Permeant lipophilicity and vehicle composition influence accumulation of dyes in hair follicles of human skin. *Eur. J. Pharm. Sci.* **18:**329-336 (2003).
32. Y. H. Kim, A. H. Ghanem and W. I. Higuchi. Model studies of epidermal permeability. *Semin. Dermatol.* ***11*** **:**145-156 (1992).

VI

Time and depth resolved visualisation of the diffusion of a lipophilic dye into the hair follicle of fresh unfixed human scalp skin

YY Grams, L Whitehead, P Cornwell and JA Bouwstra. J Control Release, in press (2004)

ABSTRACT

Visualising the penetration pathway of a lipophilic model dye into the hair follicle of fresh unfixed human skin would facilitate optimisation of drug formulations for local delivery to the pilosebaceous unit. A block of fresh human scalp skin was mechanically fixed in a newly designed combination of cutting device/on-line diffusion cell, manual cross-sectioned perpendicular to the skin surface and sealed to create the donor and acceptor compartment. The donor phase consisted of a saturated solution of Bodipy® FL C_5 in a citric acid buffer solution. Images were obtained on-line by confocal laser scanning microscopy every 30 minutes for 16 hours. For each time point and each skin region relative intensity values were calculated. The on-line visualisation showed a fast diffusion of the label into the gap of the hair follicle followed by a fluorescent staining in the gap itself. The data strongly indicate that the fluorescence in the cuticle originates mainly from the dye of the gap and not from the surrounding epidermis. The on-line visualisation provides a new and excellent tool to monitor simultaneous changes in distribution profiles in the various skin layers including the hair follicle. This information can be used to determine penetration pathways in the skin.

INTRODUCTION

Investigation of the hair follicle as a local target is of special interest for pharmaceutical and cosmetic applications with regard to treatment of skin diseases and improvement of the hair condition. Optimised local targeting would decrease the necessary amount of the active drug in the formulation and has the potential to decrease toxicity. Additionally gene delivery to local targets would be feasible.

Several techniques have been applied to study the deposition of a penetrant in the follicular regions. These techniques have been summarised by Lauer et al [1], Touitou et al [2], Corcuff and Pierard [3]. Most of the techniques include fixation of the skin by freezing or embedding followed by slicing into thin sections and visualisation. During these procedures artefact formation due to cell damaging and delocalisation of the substance might occur. Additionally visualisation of diffusion processes *on-line* is impossible once the skin is fixated. Chemical fixation of the skin is unnecessary in conventional Confocal Laser Scanning Microscopy (CLSM) and enables the use of fresh skin. CLSM in combination with optical sectioning allows the visualisation of depth profiles reaching the epidermal-dermal junction [4] *in vitro*[5-9]. More recently new microscopic techniques have been developed taking advantage of reflected light, which can be used for in vivo real-time visualisation of non-stained skin [10] reaching similar depth levels[11-18]. These visualisation techniques of the skin have been reviewed by Cullander [19].

When fluorophores are used to investigate diffusion processes by CLSM, scattering and re-absorption of emitted fluorescence limits the possibility of intensity comparison between different depths. A manual cross section perpendicular to the skin surface preceding the visualisation circumvents this problem and allows the visualisation of the fluorophore in epidermis and dermis in one image. Most importantly, since the epidermis and the dermis (z-direction) are imaged at identical depths parallel to the cross-section, the fluorescence distribution can therefore be determined in a relative manner [20,21]. This cross-sectional imaging has previously been extended by Grams *et al.* [22] to resolve for the first time the visualisation of the diffusion of a model penetrant into non-fixed fresh skin on-line. That study has been focussed on the visualisation of diffusion processes in the epidermis and the upper part of the dermis. At steady state conditions where the transported amount in time through sequential skin layers has to be equal, the presence of a high concentration gradient in depth correlates to a lower diffusion coefficient in that layer. That study revealed the highest fluorescence gradient in the top layers of the stratum corneum, consequently corresponding to a low diffusion coefficient, while the top part of the epidermis revealed the lowest gradient and therefore a high diffusion coefficient.

The aim of the present study is to visualise the diffusion process of a model dye *on-line* into the upper part of the hair follicle in real time and in depth. Images of the diffusion process were taken every 30 minutes for a period of 16 hours. Changes in intensity distribution in time are of interest and might provide information regarding the follicular contribution to the diffusion process in vitro.

MATERIALS AND METHODS

Materials

Bodipy® FL C_5 was obtained from Molecular Probes, The Netherlands. Fresh human scalp skin from cosmetic face lift surgery was transported on filter paper soaked with phosphate buffered saline pH 7.4 (139 mM NaCl, 2.5 mM KCl, 8 mM Na_2HPO_4, 1.5 mM KH_2PO_4, 25 mg/L Streptomycin and 25000 U/l Penicillin) and stored at 4°C until used. Within 4 hours after face-lift surgery, the experiment was started thereby avoiding alteration of the skin due to extended storage and freezing. The dental clay Impregum F (Espe) for sealing of the on-line diffusion cell was purchased from Dental Union BV, The Netherlands.

Methods

Preparation for the diffusion experiment

The acceptor phase consisted of phosphate buffered saline pH 7.4, with the same buffer composition as has already been used for transport and storage. The donor phase consisted of saturated solution (0.1 mg/ml) of Bodipy® FL C_5 (excitation/emission = 505/511 nm) in 50 mM citric acid buffer (CAB) at a pH of 5.0, equivalent to that of the skin surface.

Upon arrival in our laboratory, the scalp skin was gently cleaned with tissue and the surface was wiped with PBS followed by 70 % ethanol to remove any contaminants of the subcutaneous fat from the skin surface. The hair was cut with surgical scissors to a length of 2 mm above the surface. Subsequently a skin square of 8x8 mm with the hair follicles parallel to two sides of the square is cut with a stanza for later use. The skin square included the epidermis (viable and non-viable), dermis and subcutaneous fat.

Preparation of the on-line diffusion cell

Previously the preparation of the on-line diffusion cell has been described in detail [22]. Basically, the on-line diffusion cell is part of a combined

cutting device/on-line diffusion cell. The skin block is mounted into the cutting device with the stratum corneum being supported by a silicone square to avoid artefact formation during sectioning. After mechanical fixation the skin is cut from the dermis side to the stratum corneum side resulting in a flat cross sectional cutting plane with the acceptor compartment at the dermis side. Subsequently the donor compartment is screwed onto the mechanically fixed skin with the acceptor compartment. In order to seal donor and acceptor compartments and to prevent any leakage along the cutting plane, the on-line diffusion cell is completed by fixing a pioloform-coated (0.5 % (w/v) pioloform in Chloroform) cover glass with dental clay (Impregum F) to the diffusion compartments. The dental clay seal allows injection of the acceptor and donor phase at the start of the experiment. A schematic drawing of the on-line diffusion cell is provided in **Figure 1**A. A more detailed explanation is provided in our recent publication [22].

Image acquisition using Confocal Laser Scanning Microscopy (CLSM)

The confocal microscope was a Bio-Rad MRC 600 set-up, equipped with a Argon/HeNe laser with an excitation wavelength of 488 nm. The microscopic unit was an inverted Zeiss IM-35 with a PlanApo 20 and PlanApo 60 objective. Fixed microscopic settings of the CLSM were used and determined in pilot experiments. At these fixed settings autofluorescence did not interfere with our measurements. However autofluorescence was visible at the most sensitive setting which is an essential tool for the location of the hair follicle prior to the application of the donor phase. A hair follicle, which can be analysed, has to emerge from the skin a few micrometers below the cutting plane however at sufficient distance to avoid visualisation of damaged cells due to the mechanical cutting procedure.

After injection of the donor phase into the equivalent compartment, images were collected every 30 minutes starting 10 minutes after application for a period of 16 hours. Possible leakage of donor phase between the cover glass and cross-section plane of the skin has previously been studied. If there was evidence for leakage, the study has been excluded from further investigation. When swelling of the skin appeared to have a severe influence on the movement of the point of focus the series of images obtained were excluded as well.

Data analysis

Skin regions of interest were the stratum corneum, viable epidermis, dermis, gap, outer root sheath, cuticle and the hair shaft. The inner root sheath is not present in the infundibulum of the hair follicle and could therefore not be visualised. Using the Image J software, circular areas were marked being representative for a specific skin region and the average intensity was measured.

With slight modifications to the previously published relative quantification method [20], relative fluorescence values (F_{rel}) and relative accumulation values (f_{acc}) were determined from these average intensities as described below. In order to be able to calculate these accumulation values, a model skin block measuring 400 µm on all three sides (Figure 1C) was taken to calculate the appropriate volumes of the various skin parts. For the determination of the volumes, the skin block was divided into 3 horizontal sections (Figure 1B). The first section extended from the stratum corneum up to the epidermal-dermal junction and the second up to the point where the gap ends. The basic dimensions of key elements within the model skin block were obtained from the time series images: hair shaft (diameter = 49.4 µm), gap opening (diameter = 121.5 µm), gap (depth = 222.8 µm), upper outer root sheath (width = 49.0 µm), lower outer root sheath (width = 33.1 µm), cuticle (width = 2.8 µm), stratum corneum (depth = 9.6 µm) and viable epidermis (depth = 76.8 µm). The mean number of the hair follicles (160/cm^2) was counted and also included into the model skin block. The obtained volumes are summarised in Table 1.

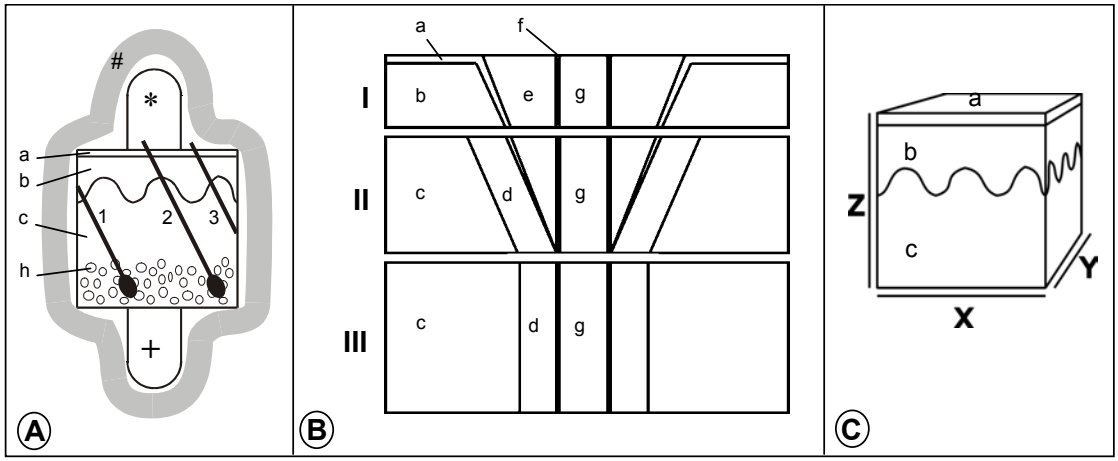

Figure 1. *(A) View of cross-section with donor compartment (*), acceptor compartment (+), stratum corneum (a), epidermis (b), dermis (c), subcutaneous fat (h) and hair follicles (1-3) sealed with dental clay (#). Hair follicles 1 and 3 do not have access to the donor phase. Therefore only hair follicle 2 can be investigated. Images B and C depict the model skin block from which the volumes of the selected skin areas have been calculated. (C) The overall dimensions of the model skin block were 400 µm on all three sides (x, y, z). The model block contained the stratum corneum (a), the viable epidermis (b), the dermis (c) and 260 hair follicles/cm^2. (B) X-z view displaying the subdivision in the various skin areas: stratum corneum (a), the viable epidermis (b), the dermis (c), outer root sheath (d), gap (e), cuticle (f) and hair shaft (g). In order to facilitate the calculation of each volume, the model block was divided into 3 sections parallel to the skin surface. Section I starts at the skin surface and stops and the epidermal-dermal junction. Section II goes from this junction to the end of the gap leaving the rest for section III. Volumes of a skin area was calculated for each section and subsequently added up to obtain the volume in the model skin block.*

The calculation of the relative accumulation in a time resolved experiment is similar to the previous published method to determine the relative accumulation [20] in a static experiment. Briefly, for every selected area the average fluorescence intensity (I_{av}), the analysed area (A) in μm^2 and the number of pixels (n_{pix}) are obtained by the Image J software. The intensity density (ID) is the fluorescence intensity per unit area and is calculated as follows (equation 1).

$$ID = I_{av} * n_{pix} / A \qquad \textbf{Equation 1}$$

The relative intensity density ($ID_{rel\ i}$) of each skin part (i) expresses the relative distribution of the fluorescence in the images without including the equivalent volumes of each skin part with ID_{tot} being the sum of all ID_i's (equation 2). That means the ID_{rel} is a means of comparing the fluorescence distribution assuming the same volume for all skin areas.

$$ID_{rel\ i} = ID_i / ID_{tot} * 100\% \qquad \textbf{Equation 2}$$

Now the actual volume of each skin part (Table 1) is included into the calculation by multiplying the $ID_{rel\ i}$ by the volume of each skin part (V_i). The relative fluorescence distribution ($F_{rel\ i}$) in the model skin block is obtained by dividing this product by the sum of all $ID_{rel\ i} * V_i$ (equation 3).

$$F_{rel\ i} = \frac{ID_{rel\ i} * V_i}{\Sigma(ID_{rel\ i} * V_i)} \qquad \textbf{Equation 3}$$

The relative fluorescence values give access to distribution changes of the fluorescence in the model skin block; however, not to changes in the relative accumulations. For this reason the relative accumulation factor (f_{acc}) was introduced. This factor expresses the actual relative fluorescence compared to the relative fluorescence at homogeneous distribution. The latter is equal to the relative volumes ($V_{rel\ i}$) of each skin part (Table 1, equation 4). Therefore the $f_{acc\ i}$ is independent of the volume of each skin part and is a better means to compare accumulation changes within the skin than the $F_{rel\ i}$ values.

$$f_{acc\ i} = \frac{F_{rel\ \ i} \quad (in\ \%)}{V_{rel\ \ i} \quad (in\ \%)} \qquad \textbf{Equation 4}$$

If the relative distribution value ($F_{rel\ i}$) is higher than the equal distribution value (expressed in $V_{rel\ i}$ [%]), i.e. a value for $f_{acc\ i}$ above 1, label accumulation in the selected part is present.

The F_{rel} values were calculated for the non-follicular (stratum corneum, epidermis, dermis), the gap and the follicular (outer root sheath, cuticle, hair shaft) area while the facc values were determined for all of the mentioned areas separately.

***Table 1**. Volume and relative volume of various skin areas in a model skin block of 400 µm side length. The density of hair follicles was determined (160 follicles per cm^2) and incorporated in the skin model. The volumes of the gap and the cuticle of section I and II/III are already incorporated in the total volume of the equivalent skin part and are therefore not part of the total skin block as indicated by the brackets.*

	Volume (V) [10^6 µm^3]	Relative Volume (V_{rel}) [%]
Stratum corneum	**1.56**	**2.44**
Viable epidermis	**12.19**	**19.05**
Dermis	**48.99**	**76.55**
Gap total	**0.21**	**0.33**
Gap section I	(0.13)	(0.20)
Gap section II	(0.08)	(0.13)
Outer root sheath	**0.80**	**1.25**
Cuticle total	**0.05**	**0.07**
Cuticle section I	(0.01)	(0.01)
Cuticle section II/III	(0.04)	(0.06)
Hair shaft	**0.20**	**0.31**
TOTAL SKIN BLOCK	**64.00**	**100.00**

RESULTS

On-line diffusion

Figure 2A depicts images at a 1.5-hour time interval of the diffusion of Bodipy® FL C_5 into fresh unfixed human scalp skin combined with the quantification of the fluorescence in time (Figure 2B). Directly after application (10 min) of the dye, the label is only present in the donor phase. Penetration into the skin occurs via the whole surface however in the initial diffusion process, interestingly, the deepest regions are reached fastest via the gap (Figure 2A, 1 hour 40 minutes) of the hair follicle. After 3 hours the cuticle shows intense staining as well. Figure 2B shows that fluorescence intensity increases fastest in the cuticle and the upper gap. The lower gap reveals the fastest increase of fluorescence intensity of the skin parts situated below the epidermal-dermal junction. In all other skin parts of the deeper skin regions (lower cuticle, dermis and hair shaft) a slow increase of fluorescence intensity is observed. As the diffusion process proceeds the intensity of the gap decreases together with a reduction in fluorescence intensity in the donor phase while the intensity of the cuticle is not decreasing yet (Figure 2A and B). At later time points, also the intensity of the cuticle decreases. Staining of the epidermis increases in the initial phase and remains nearly constant throughout the diffusion process with slight

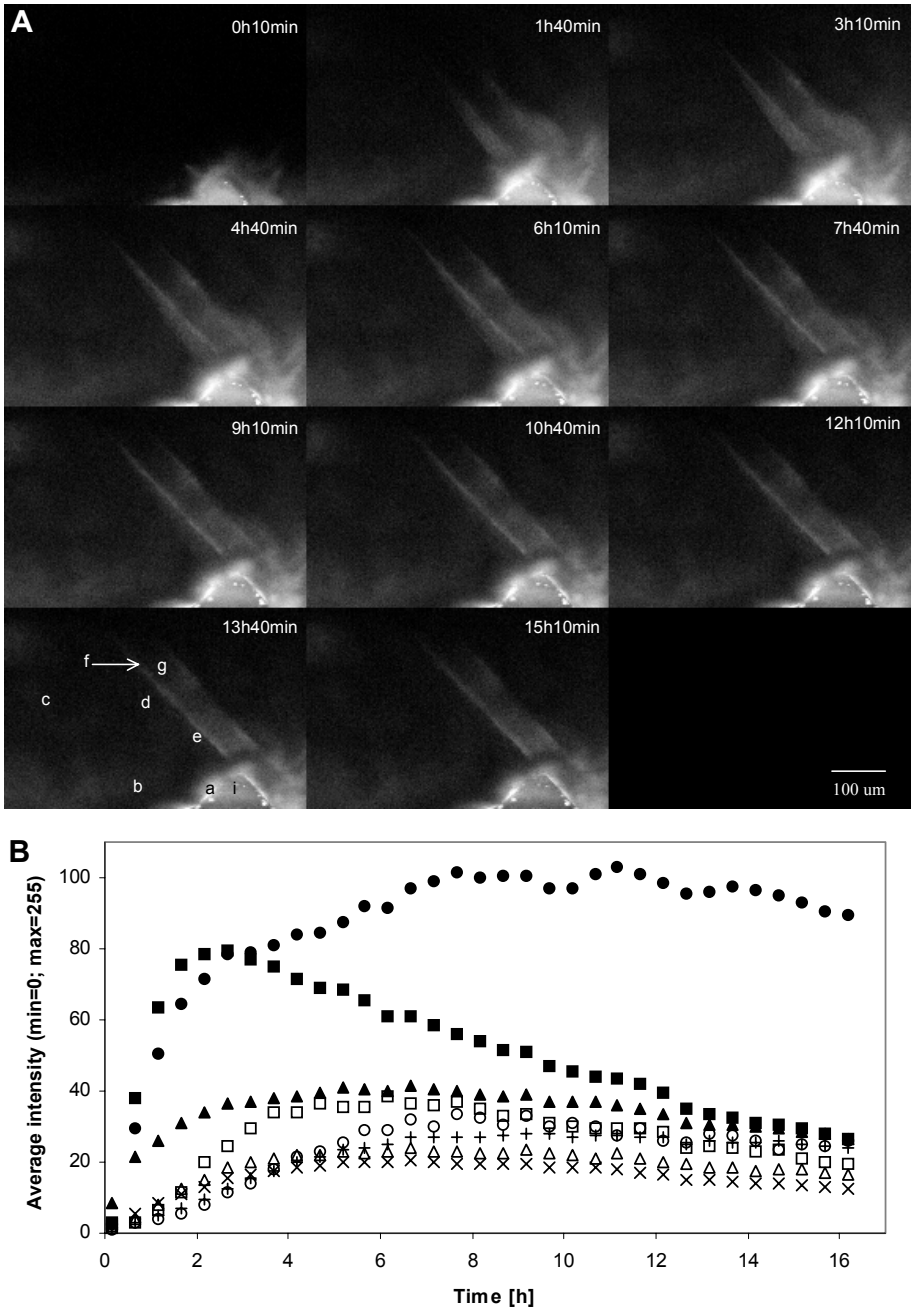

Figure 2. On-line visualisation (confocal laser scanning microscopy) of the diffusion of 0.1 mg/ml Bodipy® FL C_5 applied in citric acid buffer pH 5.0. Changes in distribution in a cross-sectional view can be followed over time by use of a newly developed on-line visualisation device. (A) Confocal laser scanning microscopy images are depicted in a 1-hour 30-minutes time interval starting 10 minutes after application. (a) stratum corneum, (b) viable epidermis, (c) dermis, (d) outer root sheath, (e) gap, (f) cuticle, (g)hair shaft and (i) donor phase. Figure (B) displays the average fluorescence intensity analysed by Image J of the selected areas over 16 hours. Upper gap (■), lower gap (□), upper cuticle (●), lower cuticle (○), outer root sheath (△), hair shaft (+), epidermis (▲) and dermis (x).

decrease at late time points as seen in the images and the figure. The outer root sheath cannot be distinguished from the surrounding tissue in the initial period of the diffusion process, however the outer root sheath is stained at later time points.

A higher magnification of the gap area of the hair follicle after the on-line time series revealed more detailed information on the location of the fluorophore (Figure 3). At the skin surface (Figure 3D) strong staining of the top layers of the stratum corneum are observed with less labelling of the same structure a few micrometers deeper (mainly in the intercellular regions). In the epidermis, nuclei appear as dark areas with indications of staining of their nucleus membrane whereas the cytosol shows homogeneous staining. The dermis contains little label. Figure 3B displays an enlarged hair shaft where cells start to form a close contact with the hair shaft. The lower left hand corner (closest to the surface)

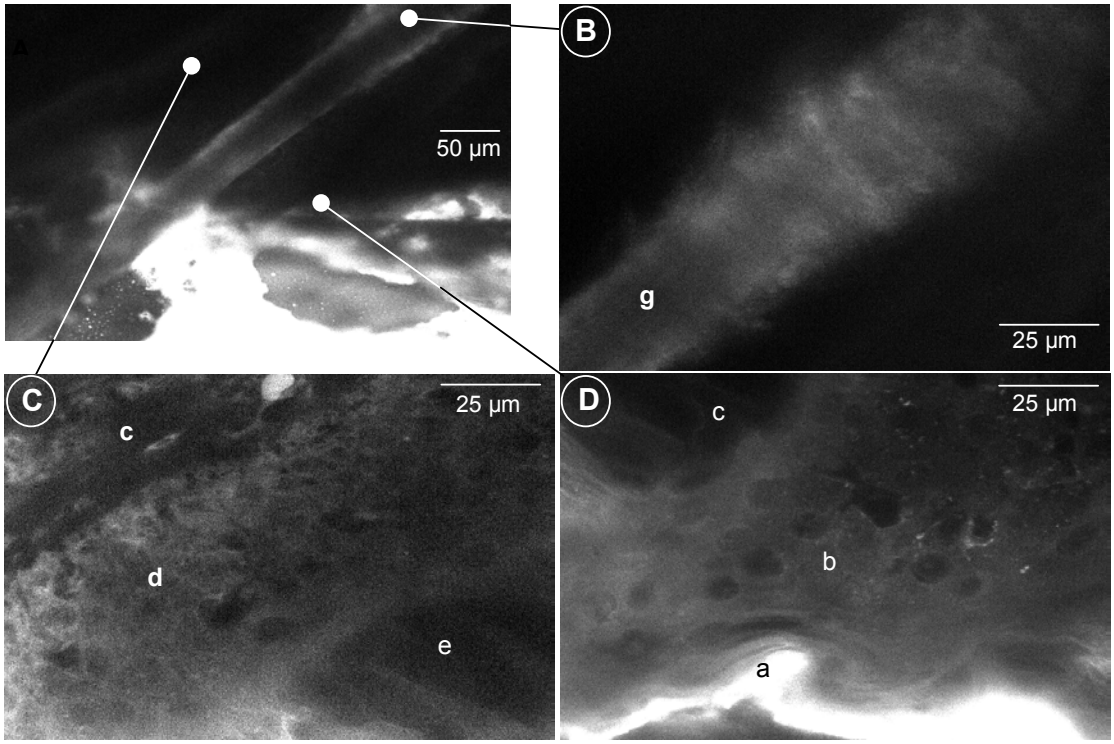

Figure 3. 0.1 mg/ml Bodipy® FL C_5 applied in citric acid buffer pH 5.0 in a newly developed on-line visualisation device. Distribution of Bodipy® FL C_5 visualised by confocal laser scanning microscopy in a cross-sectional view of human scalp skin after 16 hours on-line visualisation. (A) Last image of an on-line series visualised with a PlanApo 20 objective. Images (B-D) display details of image (A) indicated by lines using a PlanApo 60 objective closer to the cross-sectional cutting surface. (B) Enlargement of the hair shaft (g) at the point where a tighter contact is formed with the skin, (C) enlargement of the area of the outer root sheath (d), dermis (c) and gap (e), (D) focus on the stratum corneum (a), epidermis(b), and dermis.

shows straight outlines while the upper right hand corner (deeper in the skin) reveals less sharp outlines of the hair shaft. Close to the cross-sectional surface where scattering and absorption of the fluorescence is lowest, details of the outer root sheath are visible (Figure 3C). At the end of the experiment the outer root sheath shows stronger labelling than the dermis and the hair gap with similar stained features as the epidermis. However absolute intensities of skin areas of two different enlargements cannot be compared quantitatively.

Relative fluorescence values

The fluorescence intensity of the images has been measured every half-hour and analysed for several skin areas. In order to gain insight in the relative distribution of the fluorescence in the follicular region within the model skin block, a distinction has been made between the non-follicular part, the follicular part and the gap. From Figure 4 it is clear that the initial relative fluorescence values after 10 minutes show high variations in the follicular and the non-follicular region. However, already after 40 minutes these variations are strongly reduced. The F_{rel} values reveal that the relative fluorescence in the non-follicular part does not drop below 97.5 % in a time period from 0 up to 16 hours. However a decrease

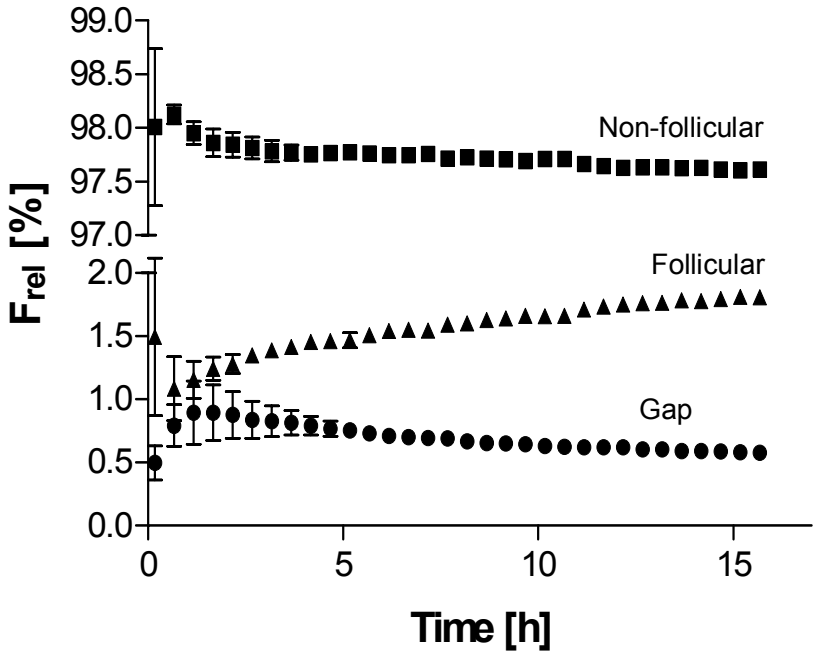

Figure 4. *Relative fluorescence values of Bodipy® FL C_5 (saturated solution in citric acid buffer pH 5.0) in a model skin cube of with side length of 400 µm. The values were obtained after quantification of the average fluorescence intensity of selected skin areas in the CLSM on-line time series using the Image J software. Subsequently the average intensities had to be transformed as explained in the methods section. Depicted values are averages of n=3 of the non-follicular (■), the follicular (▲) and the gap region (●).*

of the relative contribution of the non-follicular part in time is observed. Consequently, the total contribution of the area of the hair follicle and gap does not exceed 2.5 %. Interestingly, a difference is observed for these two skin regions. In the initial stage of diffusion the relative contribution of the gap to the total fluorescence intensities in the model skin block increases, followed by a decrease after two hours. In the follicular region the opposite is observed where an initial drop of the relative fluorescence contribution is followed by a continuous increase. After two hours the relative fluorescence contribution in the hair follicle is significantly higher than in the gap with $p<0.05$. Due to the absence of fluorescence immediately after the start of the diffusion experiment and the larger volume of the follicular region compared to the gap, the rather high F_{rel} is observed for the follicular region.

Relative accumulation values

To obtain information regarding the actual accumulation in certain skin parts, the relative accumulation values were determined in various parts of the skin and of the hair follicle (Figure 5, donor 1-3). This figure shows that f_{acc} values between the donors vary to a certain extent. However the change in the f_{acc} values within time and within one skin area is similar. Summarising all three donors the overall change in the relative accumulation of the fluorescence is provided in Figure 5. In the stratum corneum the highest f_{acc} is observed in the initial diffusion period and decreases in the first hours to reach a constant level. In the epidermis, a similar trend is observed with two differences. In the first hour, the f_{acc} value increases, after which the f_{acc} subsequently decreases, but to a lesser extent than in the stratum corneum. In the dermis all relative accumulation values in time are below a value of 1 indicating that this is a skin area with low fluorescence intensity. An increase is observed in the first hours reaching a constant value during the remaining diffusion process. Focussing on the area of the hair follicle starting with the gap close to the surface, a sudden increase (twice the initial value) within the first 1.5 hours of the f_{acc} value is determined. After reaching this maximum value, a fast decrease is observed. However, the relative accumulation values in the lower part of the gap show another trend in time. The initial increase of the f_{acc} is threefold, but extends over 7-8 hours. However, the overall f_{acc} values are lower than the values calculated for the upper part of the gap. After 7-8 hours only a slight decrease occurs with time in the lower part of the gap. Focussing at the hair cuticle, which is in direct contact with the gap, a different observation is made. Overall the lower part of the cuticle reaches lower f_{acc} values than the upper part of the cuticle indicating a fluorescent intensity gradient. This gradient remains for the remaining diffusion period. In the upper as well as lower part of the cuticle, f_{acc} values increase 4-fold compared to the initial value, however, the time schedules at which this 4-fold increase is reached is completely different. The increase in the upper part of the

cuticle is very fast in the first 1.5 hours and slows slightly down in the following time period. In the lower part of the cuticle, the increase is more gradually reaching a constant level after 12 hours diffusion. In the outer root sheath of the infundibulum and in the hair shaft f_{acc} values are very low. Within the outer root sheath after a moderate initial increase, a constant value of 1 is reached. In the hair shaft the increase is continuous. Overall in the initial period of the diffusion process relative accumulation values above 1 are only determined for the stratum corneum and the upper gap. At later time points the stratum corneum, viable epidermis, the upper/lower gap and the upper/lower cuticle reveal f_{acc} values >1 as well.

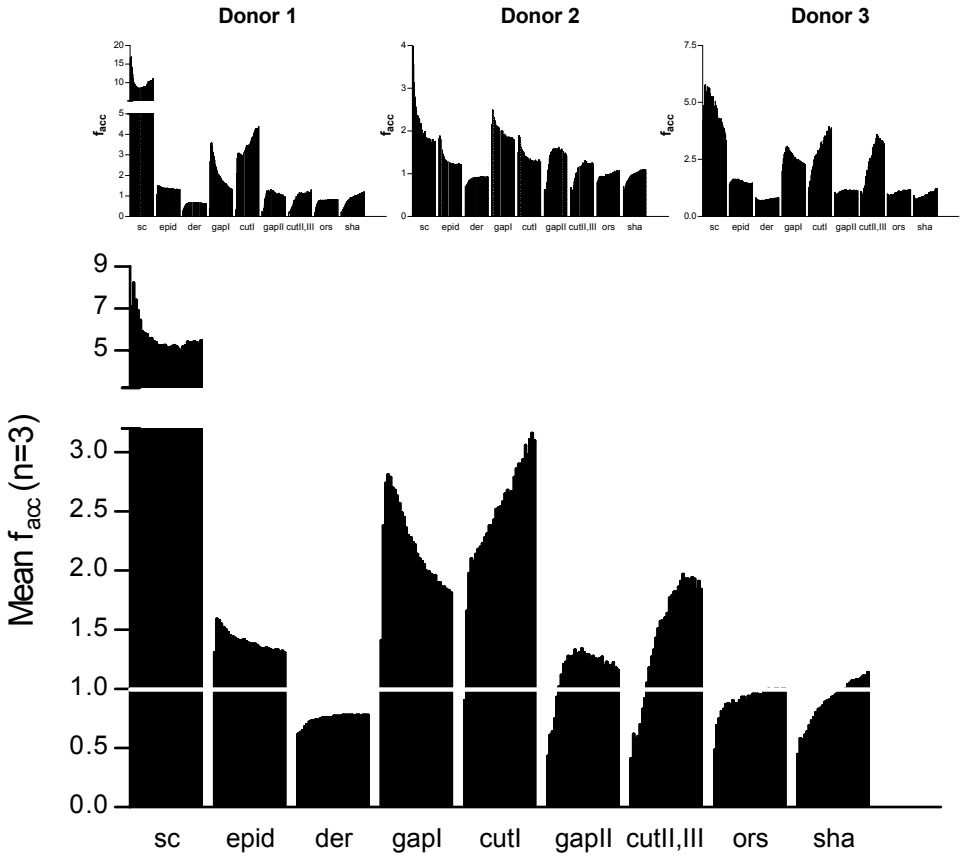

Figure 5. *Relative accumulation factors (f_{acc}) of 3 different donors (donor 1-3) and their average (Mean f_{acc}) for selected skin regions in the previously mentioned sections of the model skin block (Fig.1). The f_{acc} was determined for stratum corneum (sc), epidermis (epid), dermis (der), upper gap (gapI) and the upper cuticle in section I (cutI). Furthermore it was determined for the lower gap in section II (gapII), the lower cuticle representative of sections II/III (cutII,III), outer root sheath (ors) and hair shaft (sha). For each skin area f_{acc} values are displayed as bars in a 30 minute time interval starting 10 minutes after application of a saturated Bodipy® FL C_5 solution in citric acid buffer up to 16 hours. A white line indicates the f_{acc} value of one. Values >1 imply accumulation in that specific area with regard to homogeneous distribution.*

DISCUSSION

On-line diffusion

Previously Hoogstraate and co-workers have visualised on-line diffusion in buccal tissue [23]. In that study, the size donor and acceptor compartments varied substantially since the compartments were created solely by dental clay. Furthermore diffusion processes into the buccal tissue was visualised for less than 2 hours. Since no stratum corneum is present in the buccal tissue fast diffusion was expected and a short time period was sufficient. However in the case of intact skin, where the diffusion is much slower, the diffusion process has to be examined over a longer period of time. We were able to visualise diffusion processes over time periods as long as 16 hours in a 30-minute time interval. Acquisition intervals of 2 minutes can be achieved if necessary. In the present construction the donor and acceptor phases are static without flow-through mechanism to replace either of the solutions. Very recent studies have shown the possibility of creating flow-through mechanisms for either compartment thereby ensuring infinite penetrant concentration in the donor phase and sink conditions in the acceptor phase. This will be an aim of our future research.

From the images obtained on-line it is obvious that the gap presents a low resistance for the diffusion of a lipophilic label from an aqueous donor solution into hairy skin. The lipophilic nature of the sebum paired with an absence of a tight cell structure such as present in the stratum corneum provides a favourable environment for the penetration of the Bodipy® dye. After entering the gap, the cuticle of the hair shaft appears to have a high affinity for the applied dye. Even after the fluorescence intensity of the gap decreases, the cuticle retains the fluorophore for a longer time period. This implies that the cuticle has a high up-take of the fluorophore, however it does not release the dye at the same speed.

In the donor phase, the gap and at a later stage in the diffusion process also in the cuticle, a decrease of fluorescence intensity is observed. Photobleaching has been tested previously. With more scans than used in this experiment only weak photobleaching was observed which could not be accounted for the degree of fluorescence decrease observed in our images. Furthermore photobleaching would be expected to occur simultaneously in the gap and the cuticle instead of shifted in time like observed in our time series. Therefore it is more likely for the dye to diffuse most likely further into deeper skin regions along the concentration gradient.

Relative fluorescence values

It is generally known that the surface area of the hair follicle is 0.1-1 % of the total skin surface [24]. In our study, this results in a relative fluorescence of 2.4 % in the follicular region (gap and hair follicle) of the model skin block. Assuming that the diffusion coefficient in the hair follicle is of a similar order of magnitude as in the inter-follicular area one might conclude that for this dye the overall contribution of the follicular region to the transport through the skin might therefore be limited. Compared to in vivo studies where the vascularisation of the hair follicle is intact, in vitro studies might underestimate the contribution of the hair follicle to the overall transport due to the lack of blood circulation and the decreased follicular opening.

Relative accumulation values

Focussing first on the f_{acc} values of the individuals it can be concluded, that the skin of donor 2 reveals the least variation of f_{acc} between different skin areas. The fluorescence intensities of the time series of donor 2 were very low reaching only 17 % of the maximum intensities detectable with the settings we used. This reduces the sensitivity for changes in intensity. This implies that the in pilot experiments determined optimal settings for the on-line detection of the label were excellent for donor 1 and 3, but less suitable for donor 2. This phenomenon stresses also the high variability of skin permeability particularly in scalp skin, which has also been observed by another group [25]. Scalp skin is more exposed to various treatments like fixatives, colouring agents, cleansing and conditioning products which might have an effect on the barrier function. Additionally differences between individuals are expected to be higher than for normal skin due to different styling behaviour.

Initially the increase in relative accumulation factors is strongest in the top section of the gap and the upper part of the cuticle. This indicates that the diffusion of the dye is dominating in these regions at early time points. The fact that the stratum corneum has a very high accumulation factor can be attributed to a certain amount of label, which is attached to the skin surface. Since Bodipy® FL C_5 is a lipophilic dye (log P 2.5 at pH 5.0) of a small size, penetration is expected to be relatively high. This has been shown previously for a buffer phase containing 30 % ethanol [26] or 8 % surfactants [27]. Our finding is therefore in agreement with the model of Scheuplein [28]. He stated that in the initial period the follicular pathway is of greater importance for the diffusion process than the pathway via the skin surface especially for a substance penetrating the stratum corneum very slowly. However from our studies it is clear that diffusion of this particular dye occurs via the stratum corneum and via the follicular duct. In some regions of the deeper skin layers such as the outer root sheath, the dermis and the hair shaft the f_{acc} increase slower than other regions in the same depth such

as the lower gap and the lower cuticle. This implies that label in the deeper parts of the cuticle can originate from the hair canal and from the upper cuticle, but not from the outer root sheath, dermis or hair shaft. This is also supported by the fact that the f_{acc} values of the outer root sheath, the dermis and the hair shaft do not reach values above 1 implying that no accumulation is present. The stratum corneum is the main barrier at the surface and the upper part of the gap where it thins out up to a depth of approximately 200 µm [29]. This is in agreement with the strong labelling of the gap and the cuticle.

The results of the present experiments strongly indicate that the high amount of fluorophore, which is present in the hair duct, diffuses into the cuticle. This is based on the fact that the relative accumulation in the cuticle follows with a certain delay the development of the fluorescence in the gap. This does not exclude diffusion from other parts such as along the hair shaft and from the outer root sheath of the infundibulum to the cuticle or any diffusion from the gap into the outer root sheath.

CONCLUSION

On-line CLSM is a recently developed tool to visualise the diffusion of a dye in a cross sectional view of fresh unfixed piece of skin including subcutaneous fat. From these studies we conclude that this technique can visualise the diffusion of a dye into the upper hair follicle at different time points. Thereby the two disadvantages of (i) increased scattering and absorption in deeper layers of the skin from conventional depth scans and (ii) the limitation in depth due to optical sectioning is avoided. We can conclude that a lipophilic dye penetrates at early time points via the stratum corneum and the gap. Since the diffusion into the gap is fast and reaches deeper skin layers, we conclude that the diffusion resistance for a lipophilic compound is lower in the gap than in the stratum corneum/epidermis of the same thickness. From the gap label diffuses into the cuticle where it accumulates. However it cannot be excluded that diffusion also takes place to some extent in the other directions as well. Since the hair follicle is highly vascularised, the follicular contribution to the overall transport in vivo might be underestimated. For local delivery the here presented method is of great value to study the influence of parameters on the accumulation in regions of interest such as hair follicles and sweat ducts. Deeper skin regions e.g. sebaceous gland, sweat gland and non-infundibulum area of the hair follicle will be examined in the future.

ACKNOWLEDGEMENT

We would like to thank Jan Janssen and Henk Verpoorten for the co-operation in the development of the on-line diffusion cell. Furthermore we acknowledge Unilever Research, Port Sunlight, UK for financing this project.

REFERENCES

[1] A. C. Lauer, L. M. Lieb, C. Ramachandran, G. L. Flynn, N. D. Weiner, Transfollicular drug delivery. Pharm. Res. 12 (1995) 179-186.

[2] E. Touitou, V. M. Meidan, E. Horwitz, Methods for quantitative determination of drug localized in the skin. J. Control. Rel. 56 (1998) 7-21.

[3] P. Corcuff, G. E. Pierard, Skin imaging: State of the art at the dawn of the year 2000. Curr. Probl. Dermatol. 26 (1998) 1-11.

[4] P. Corcuff, G. Gonnord, G. E. Pierard and J. L. Leveque, In vivo confocal microscopy of human skin: A new design for cosmetology and dermatology. SCANNING. 18:351-355 (1996).

[5] A. J. Hoogstraate, S. Senel, C. Cullander, J. Verhoef, H. E. Junginger, H. E. Bodde, Effects of bile salts on transport rates and routes of FITC-labelled compounds across porcine buccal epithelium in vitro. J. Control. Rel. 40 (1996) 211-221.

[6] B. R. Masters, G. Gonnord, P. Corcuff, Three-dimensional microscopic biopsy of in vivo human skin: a new technique based on a flexible confocal microscope. J. Microsc. 185 (1997) 329-338.

[7] S. Senel, A. J. Hoogstraate, F. Spies, J. C. Verhoef, H. E. Junginger, H. E. Bodde, Visualization of enhancing effects of bile salts on buccal penetration. Eur. J. Morphol. 31 (1993) 35-41.

[8] O. Simonetti, A. J. Hoogstraate, W. Bialik, J. A. Kempenaar, A. H. G. J. Schrijvers, H. E. Bodde, M. Ponec, Visualization of diffusion pathways across the stratum corneum of native and in-vitro-reconstructed epidermis by confocal laser scanning microscopy. Arch. Dermatol. Res. 287 (1995) 465-473.

[9] N. G. Turner, R. H. Guy, Visualization and quantitation of iontophoretic pathways using confocal microscopy. J. Invest. Dermatol. Symp. Proc. 3 (1998) 136-142.

[10] D. Aghassi, R. R. Anderson, S. Gonzalez, Confocal laser microscopic imaging of actinic keratoses in vivo: A preliminary report. J. Am. Acad. Dermatol. 43 (2000) 42-48.

[11] D. Aghassi, E. Gonzalez, R. R. Anderson, M. Rajadhyaksha, S. Gonzalez, Elucidating the pulsed-dye laser treatment of sebaceous hyperplasia in vivo with real-time confocal scanning laser microscopy. J. Am. Acad. Dermatol. 43 (2000) 49-53.

[12] D. Aghassi, R. R. Anderson, S. Gonzalez, Time-sequence histologic imaging of laser-treated cherry angiomas with in vivo confocal microscopy. J. Am. Acad. Dermatol. 43 (2000) 37-41.

[13] C. Bertrand, P. Corcuff, In vivo spatio-temporal visualization of the human skin by real-time confocal microscopy. Scanning 16 (1994) 150-154.

[14] P. Corcuff, J. L. Leveque, In vivo vision of the human skin with the tandem scanning microscope. Dermatol. 186 (1993) 50-54.

[15] P. Corcuff, C. Bertrand, J. L. Leveque, Morphometry of human epidermis in vivo by real-time confocal microscopy. Arch.Dermatol.Res. 285 (1993) 475-481.

[16] S. Gonzalez, G. Rubinstein, V. Mordovtseva, M. Rajadhyaksha, R. R. Anderson, In vivo abnormal keratinization in Darier-White's disease as viewed by real-time confocal imaging. J. Cutan. Pathol. 26 (1999) 504-508.

[17] M. Rajadhyaksha, R. R. Anderson, R. H. Webb, Video-rate confocal scanning laser microscope for imaging human tissues in vivo. Appl. Opt. 38 (1999) 2105-2115.

[18] W. M. White, M. Rajadhyaksha, S. Gonzalez, R. L. Fabian, R. R. Anderson, Noninvasive imaging of human oral mucosa in vivo by confocal reflectance microscopy. Laryngoscope 109 (1999) 1709-1717.

[19] C. Cullander, Light microscopy of living tissue: the state and future of the art. J. Invest. Dermatol. Symp. Proc. 3 (1998) 166-171.

[20] Y. Y. Grams, J. A. Bouwstra, A new method to determine the distribution of a fluorophore in scalp skin with focus on hair follicles. Pharm. Res. 19 (2002) 350-354.

[21] M. E. M. J. Meuwissen, J. Janssen, C. Cullander, H. E. Junginger, J. A. Bouwstra, A cross-section device to improve visualization of fluorescent probe penetration into the skin by Confocal Laser Scanning Microscopy. Pharm. Res. 15 (1998) 352-356.
[22] Y. Y. Grams, L. Whitehead, G. L. Li, P. Cornwell, J. A. Bouwstra, On-line visualisation of dye diffusion in fresh unfixed human skin. Pharm. Res. in preparation (2002).
[23] A. J. Hoogstraate, C. Cullander, J. F. Nagelkerke, F. Spies, J. Verhoef, A. H. G. J. Schrijvers, H. E. Junginger, H. E. Bodde, A novel in-situ model for continuous observation of transient drug concentration gradients across buccal epithelium at the microscopical level. J. Control. Rel. 39 (1996) 71-78.
[24] H. Schaefer, T. E. Redelmeier, Skin Barrier, Karger AG, Basel, 1996.
[25] T. Ogiso, T. Shiraki, K. Okajima, T. Tanino, M. Iwaki, T. Wada, Transfollicular drug delivery: Penetration of drugs through human scalp skin and comparison of penetration between scalp and abdominal skins in vitro. J. Drug Target. 10 (2002) 369-378.
[26] Y. Y. Grams, J. A. Bouwstra, Penetration and distribution of three lipophilic probes in vitro in human skin focusing on the hair follicle. J Control. Rel. 83 (2002) 253-262.
[27] Y. Y. Grams, S. Alaruikka, L. Lashley, J. Caussin, L. Whitehead, J. A. Bouwstra, Permeant lipophilicity and vehicle composition influence accumulation of dyes in hair follicles of human skin. Eur. J. Pharm. Sci. submitted (2002).
[28] R. J. Scheuplein, Mechanism of percutaneous absorption. II. Transient diffusion and the relative importance of various routes of skin penetration. J. Invest. Dermatol. Symp. Proc. 48 (1967) 79-88.
[29] G. F. Odland, Skin, in: R. O. Greep, (Ed.), Histology, McGraw-Hill Company, New York, 1966.

VII

On-line diffusion profile of a lipophilic model dye in different depth of a hair follicle in human scalp skin

YY Grams, L Whitehead, G. Lamers, N. Stuurman and JA Bouwstra. J Invest Dermatol (submitted)

ABSTRACT

In skin and hair research drug targeting to the hair follicle is of great interest in the treatment of skin diseases. The aim of this study is to visualise on-line the diffusion processes of a model fluorophore into the hair follicle at different depths using fresh human scalp skin and Confocal Laser Scanning Microscopy.

Up to a depth of 500 µm in the skin a fast increase of fluorescence is observed in the gap followed by accumulation of the dye in the hair cuticle. Penetration was also observed via the stratum corneum and epidermis. Very little label reached depths greater than 2000 µm. Fat cells accumulated the label fastest followed by the cuticular area and the outer root sheath of the hair follicle. Sweat glands revealed very low staining while the bulb at a depth of 4000 µm was visualised only by autofluorescence.

From this study we conclude that the on-line visualisation is a promising technique to access diffusion processes in deep skin layers even on a cellular level. Furthermore we conclude that the gap and the cuticle play an important role in the initial diffusion period with the label in the cuticle originating from the gap. Imaging full thickness skin, diffusion of a lipophilic dye into the hair bulb could not be detected.

INTRODUCTION

Investigations of transport and delivery processes in skin aim at systemic or local delivery of drugs in order to improve their efficacy. Follicular delivery is one main area of interest when treating skin diseases originating in the pilosebaceous unit (hair follicle and sebaceous gland). Therefore it is crucial to measure increases and decreases of a drug in the target area.

Reviews of the hair follicle as a route for drug delivery have been published (Agarwal *et al*, 2000; Lauer *et al*, 1995; Weiner, 1998) and summarise the status of pilosebaceous drug delivery. Numerous studies have been performed studying the role of follicular contribution to the transport of which only a selection is cited here (Hueber *et al*, 1994; Illel *et al*, 1991; Kao *et al*, 1988). These studies focus on the comparison of diffusion profiles over time between hairless or follicle free skin with normal skin. The general conclusion is that the follicular route plays an important role, however it is not the only route for penetration.

Visualisation of follicular penetration in the upper hair follicle has also been examined. This has been achieved by fluorescence or laser scanning microscopy (Allec *et al*, 1997; Lademann *et al*, 1999; Lauer *et al*, 1995; Rolland *et al*, 1993; Schaefer *et al*, 1989), autoradiography (Chu *et al*, 1996; Fabin and Touitou, 1991), scanning electron microscopy (Schaefer *et al*, 1989), microphotography in combination with UV-light (Foreman et al, 1979) and light microscopy (Meidan *et al*, 1998).

Penetration into deeper hair follicle regions have been reported by only three authors (Genina *et al*, 2002; Lieb *et al*, 1997; Serizawa *et al*, 1995) of which the studies of Lieb et al are very detailed. The latter reported transport of oligomers (24 and 25 mer) into the hair bulb. In previous studies an on-line visualisation technique was used to examine fluorophore penetration in non-fixed skin containing the subcutaneous fat. In these studies we focused on either permeation in the epidermis (Grams *et al*, 2004a) or the hair follicle (Grams *et al*, 2004b). The aim of the present study is to visualise on-line the penetration in the hair follicle with special focus on deep follicular regions in the dermis and the subcutaneous fat. An attempt has been made to visualise the diffusion into the hair bulb.

MATERIALS AND METHODS

Bodipy® FL C_5 was obtained from Molecular Probes, The Netherlands. Fresh human scalp skin from cosmetic face lift surgery was transported on filter paper soaked with phosphate buffered saline pH 7.4 (139 mM NaCl, 2.5 mM KCl,

8 mM Na_2HPO_4, 1.5 mM KH_2PO_4, 25 mg/L Streptomycin and 25000 U/l Penicillin) and stored at 4°C until used. Within 4 hours after face-lift surgery, the experiment was started thereby avoiding alteration of the skin due to extended storage and freezing. The dental clay Impregum F (Espe) for sealing of the on-line diffusion cell was purchased from Dental Union BV, The Netherlands.

Preparation for the diffusion experiment

The acceptor phase consisted of phosphate buffered saline pH 7.4, with the same buffer composition as already used for transport and storage. The donor phase consisted of a saturated solution (0.1 mg/ml) of Bodipy® FL C_5 (excitation/emission = 505/511 nm) in 50 mM citric acid buffer (CAB) at a pH of 5.0, equivalent to that of the skin surface.

Upon arrival in our laboratory, the scalp skin was gently cleaned with tissue and the surface was wiped with PBS followed by 70 % ethanol to remove any contaminants of the subcutaneous fat from the skin surface. The hair was cut with surgical scissors to a length of 2 mm above the surface. Subsequently a skin square of 8x8 mm with the hair follicles parallel to two sides of the square is cut with a stanza for later use. The skin square included the epidermis (viable and non-viable), dermis and subcutaneous fat.

Preparation of the on-line diffusion cell

Previously the preparation of the on-line diffusion cell has been described in detail (Grams *et al*, 2004a). Basically, the on-line diffusion cell is part of a combined cutting device/on-line diffusion cell. The skin block is mounted into the cutting device with the stratum corneum being supported by a silicone square to avoid artefact formation during sectioning. After mechanical fixation the skin is cut from the dermis side to the stratum corneum side resulting in a flat cross sectional cutting plane with the acceptor compartment at the dermis side. Subsequently the donor compartment is screwed onto the mechanically fixed skin with the acceptor compartment. In order to seal donor and acceptor compartments and to prevent any leakage along the cutting plane, the on-line diffusion cell is completed by fixing a pioloform-coated (0.5 % (w/v) pioloform in Chloroform) cover glass with dental clay (Impregum F) to the diffusion compartments (Figure 1). The dental clay seal allows injection of the acceptor and donor phase at the start of the experiment.

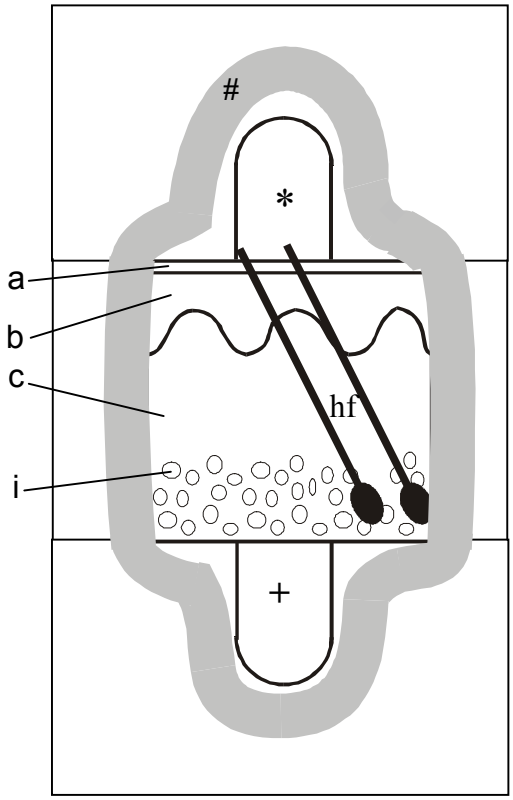

Figure 1. *View of the cross sectional cutting surface displaying the stratum corneum (a), the viable epidermis (b), the dermis (c), the subcutaneous fat tissue (i) and the hair follicle (hf) in the combined cross section/on-line device. The cross section is sealed by dental clay (#) to create closed donor (*) and acceptor compartment (+). After sealing, hair follicle parts are imaged by confocal laser scanning microscopy.*

Image acquisition using Confocal Laser Scanning Microscopy (CLSM)

The confocal microscope (Leica DM IRBE) was equipped with an Argon laser of an excitation wavelength of 488 nm and a Leica HC PL APO 20x objective. Fixed microscopic settings of the CLSM were used and determined in pilot experiments. At these fixed settings autofluorescence did not interfere with our measurements. However autofluorescence was visible at the most sensitive settings, which is an essential tool for the location of the hair follicle prior to the application of the donor phase. A hair follicle, which can be analysed, has to emerge from the skin a few micrometers below the cutting plane however at sufficient distance to avoid visualisation of damaged cells due to the mechanical cutting procedure.

After injection of the donor phase into the equivalent compartment, images were collected every 60 minutes starting 10 minutes after application for a period of 15 hours. In case of leakage, the study has been excluded from further investigation. Time series at different depths have been obtained from

different on-line cell preparations and different donors. Of course for each time series a new cross-section with another hair follicle is required.

RESULTS

Several time series (on-line) of the diffusion of BFL focussing on the hair follicle at various depths have been recorded. Figure 2 displays a schematic drawing of a hair follicle in human scalp skin and the approximate location of the various time series from the skin surface up to the subcutaneous fat.

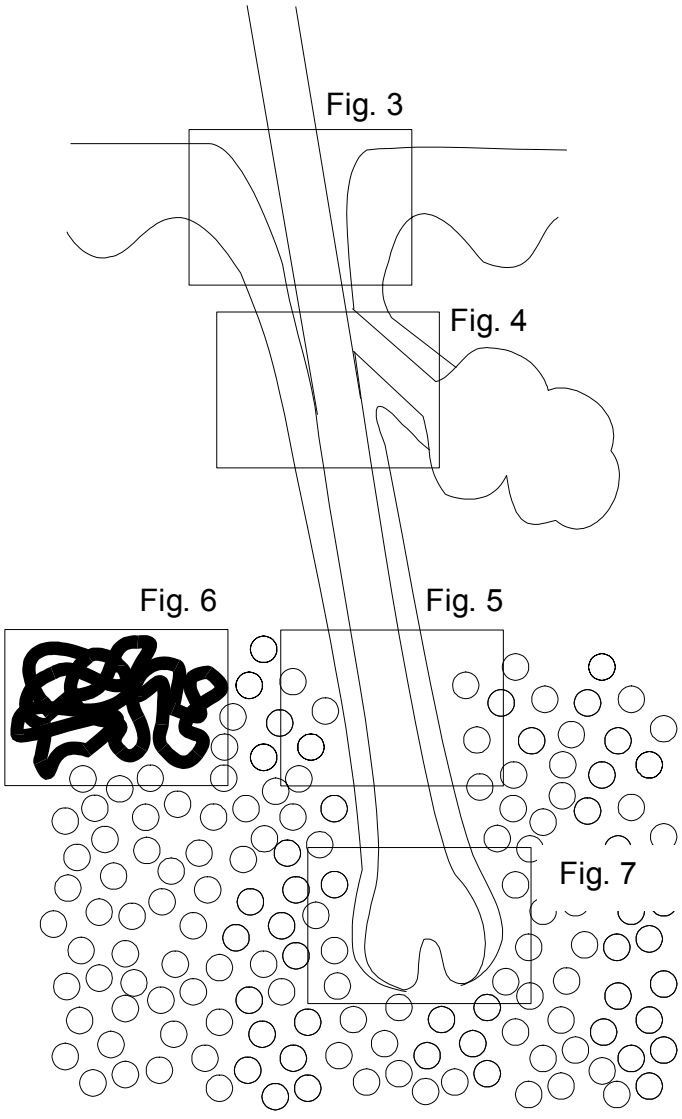

Figure 2. *Cross-sectional overview of the hair follicle in human scalp skin. The deeper regions of the hair follicle are located in the subcutaneous fat. Marked areas are indicating the position of the various time series selected in this study. Each time series requires a new hair follicle cross section.*

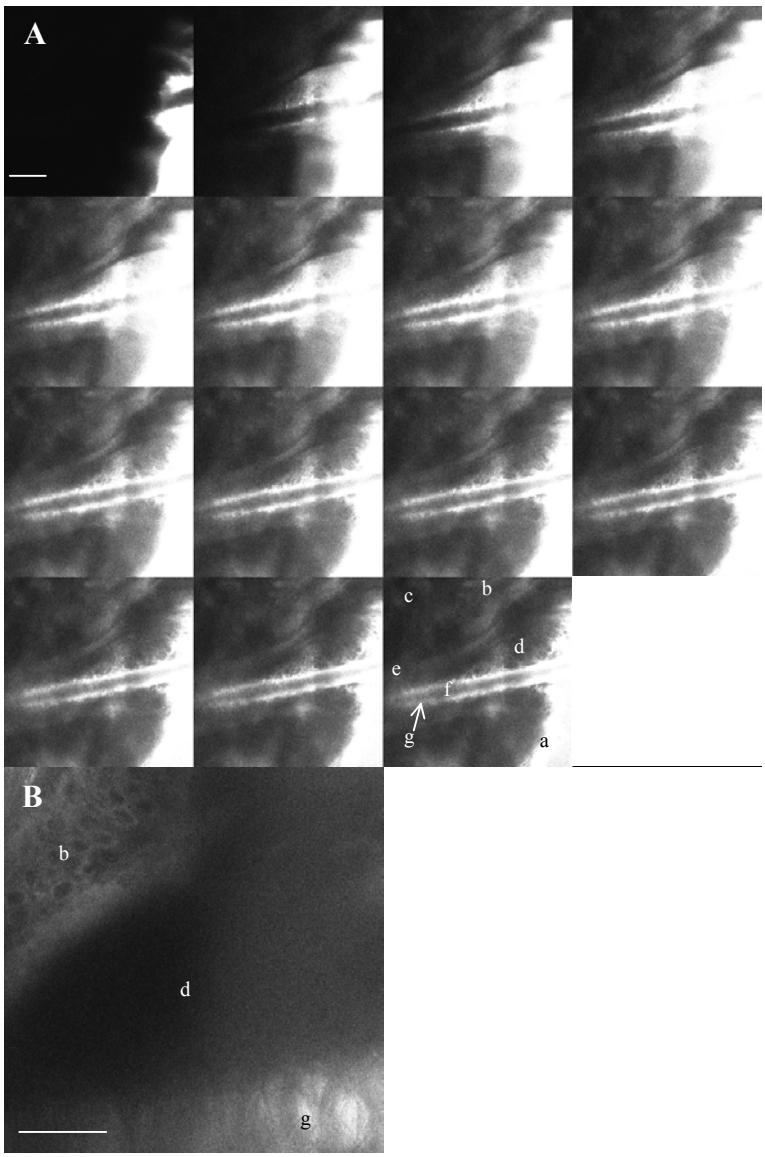

Figure 3. *On-line diffusion of Bodipy® FL C_5 (saturated solution in citric acid buffer pH 5.0) from the donor compartment into unfixed human scalp skin at the surface in a cross-sectional view. The location of the image series is illustrated in Figure 2. (A) The first image depicts the dye distribution 10 minutes after application of the donor phase followed by images in an hourly interval. In the initial time period, the gap and the cuticle of the hair follicle are stained very bright and the fluorescence reaches deeper regions as compared to the staining in the non-follicular route. In the gap the fluorescence intensity increases followed by a decrease up to the end of the experiment while the fluorescence intensity was strong in the cuticle and did not decrease. The epidermis is weakly labelled after 1 hour, while fluorescence enters the dermis after 2 hours. However the fluorescence intensity of these non-follicular regions remain lower than the intensities in the gap and in the cuticle. The bar represents 100 µm. (B) Enlargement of the gap area after the 16-hour on-line image acquisition. In this image the cells in the viable epidermis are clearly depicted. The bar indicates 50 µm. (a) Stratum corneum, (b) viable epidermis, (c) dermis, (d) gap, (e) outer root sheath, (f) hair shaft and (g) cuticle.*

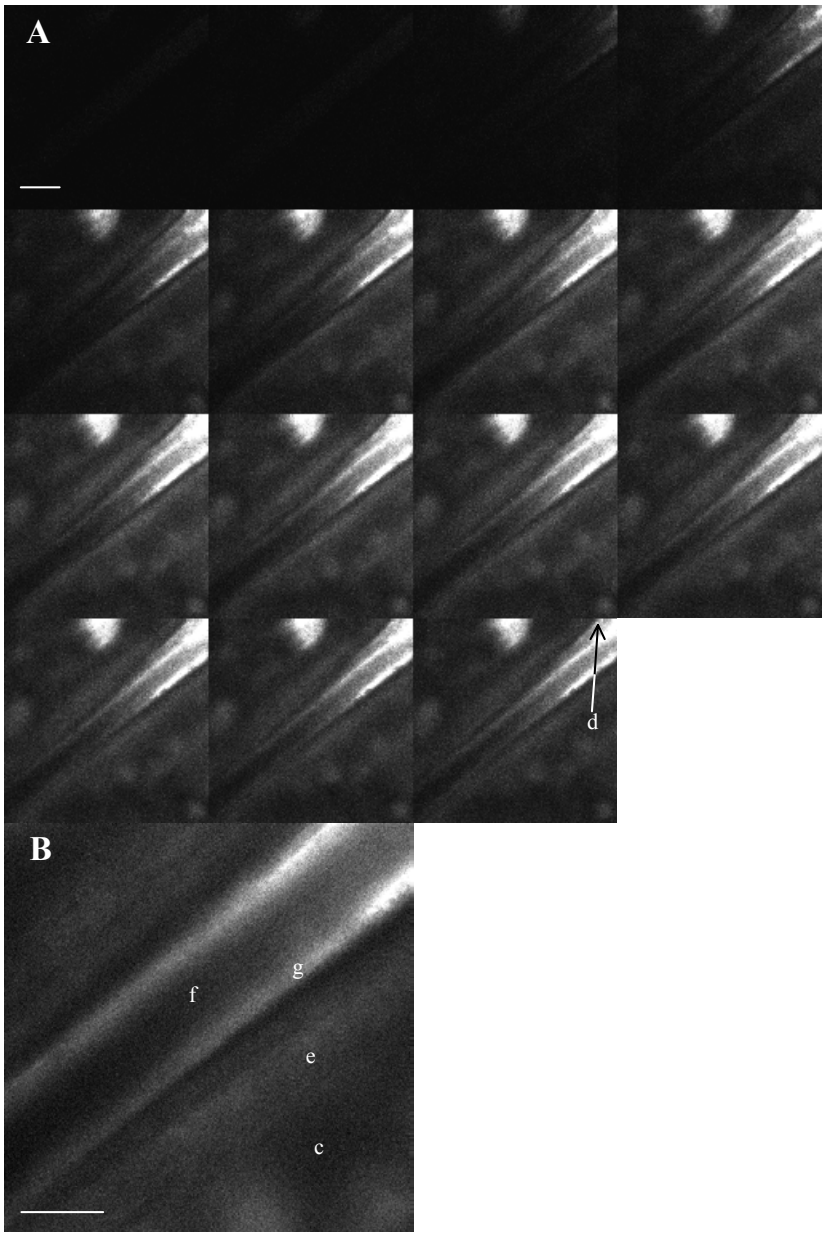

Figure 4. *On-line diffusion of Bodipy® FL C_5 (saturated solution in citric acid buffer pH 5.0) from the donor compartment (right of image) into unfixed human scalp skin at 800 µm distance from the skin surface (cross-sectional view). The location of the image series is illustrated in Figure 2. (A) The first image depicts the dye distribution 10 minutes after application of the donor phase followed by images in an hourly interval. After 2 hours fluorescence appears in the area of the gap and cuticle. After 3 hours fluorescence is also detected in the outer root sheath simultaneously with the dermis, however, the labelling is less bright than in the gap and cuticle. The intensity gradient in the gap and cuticle is much higher than in the surrounding tissue. The bar represents 50 µm. (B) Enlargement of the follicular area after the end of the 16-hour on-line image acquisition. The bar indicates 100 µm. (c) Dermis, (d) gap, (e) outer root sheath, (f) hair shaft and (g) cuticle.*

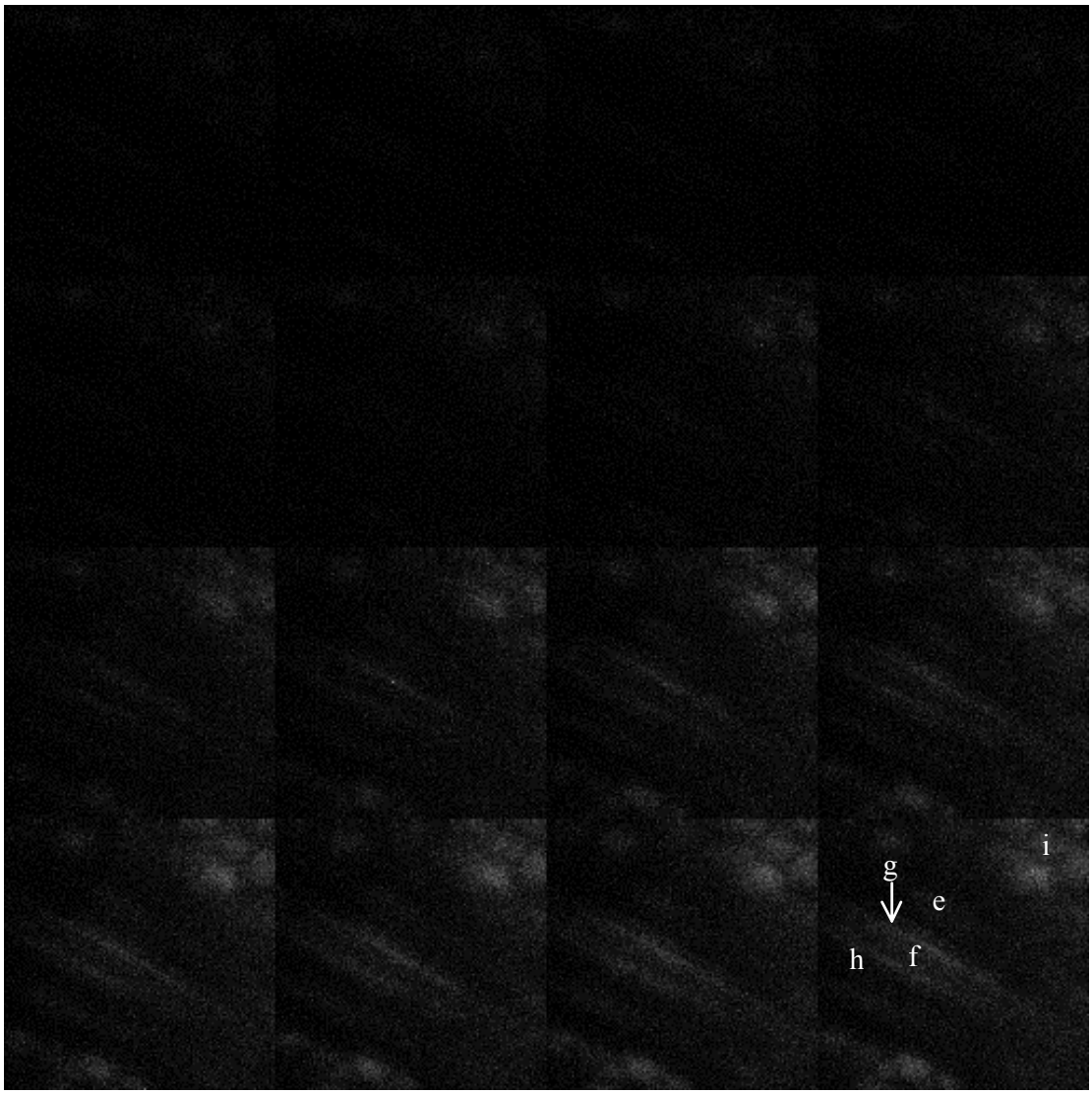

Figure 5. *On-line diffusion of Bodipy® FL C_5 (saturated solution in citric acid buffer pH 5.0) from the donor compartment (right of image) into unfixed human scalp skin at 2100 µm distance from the skin surface (cross-sectional view). The location of the image series is illustrated in Figure 2. Contrast and brightness of the image series was optimised due to weak labelling. The first image depicts the dye distribution 10 minutes after application of the donor phase followed by images in an hourly interval. Despite of low fluorescence intensity the first staining of skin structures namely the subcutaneous fat cells are visible 5 hours after the start of the experiment. After 7 hours and 9 hours the cuticle and the outer root sheath of the hair follicle is stained and increases in fluorescence intensity over time. The inner root sheath and the hair shaft are hardly stained. The bar represents 50 µm. (e) Outer root sheath, (f) hair shaft, (g) cuticle, (h) inner root sheath and (i) subcutaneous fat cells.*

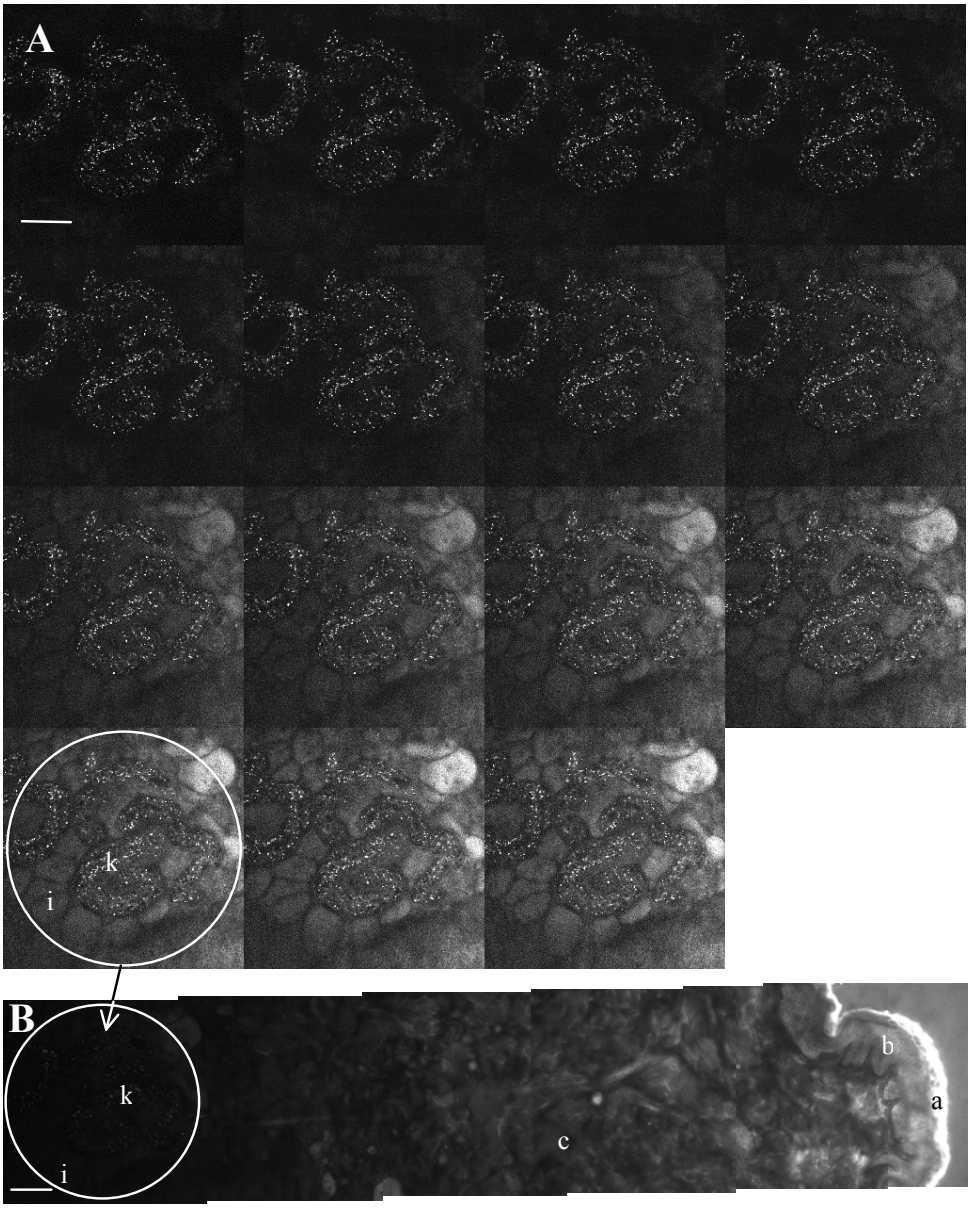

Figure 6. *On-line diffusion of Bodipy® FL C_5 (saturated solution in citric acid buffer pH 5.0) from the donor compartment (right of image) into the sweat gland of unfixed human scalp skin at 2040 µm distance from the skin surface (cross-sectional view). The location of the image series is illustrated in* ***Figure 2****. (A) The first image depicts the dye distribution 10 minutes after application of the donor phase followed by images in an hourly interval. Contrast and brightness of the image series was optimised due to little labelling. Dot-like autofluorescence are visible in the sweat glands. The first fluorescence staining is observed after 4-5 hours in the fat cells surrounding the sweat gland. As the diffusion proceeds, the autofluorescence-free area of the sweat glands also retains the dye with black non-stained areas remaining. (B) After 16 hours of on-line diffusion, a cross-section the skin was taken to determine the depth of the on-line time series indicated by a white circle. Contrast and brightness were not optimised due to the strong labelling of the stratum corneum. Both scale bars represent 100 µm. (a) Stratum corneum, (b) viable epidermis, (c) dermis, (i) subcutaneous fat cells and (k) sweat gland.*

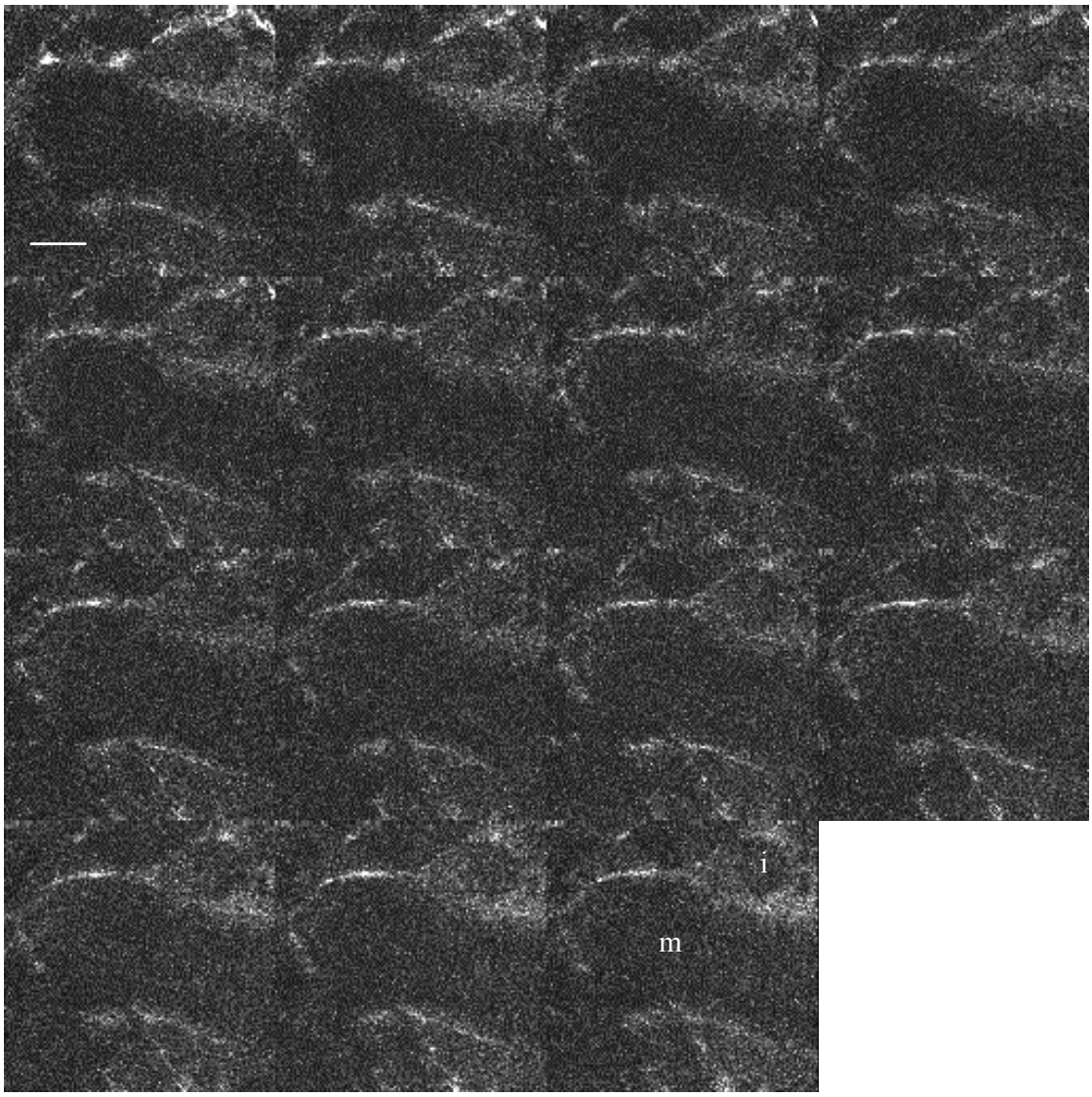

Figure 7. *On-line diffusion of Bodipy® FL C_5 (saturated solution in citric acid buffer pH 5.0) from the donor compartment (right of image) into the hair bulb of unfixed human scalp skin at 4000 µm distance from the skin surface (cross-sectional view). The location of the image series is illustrated in Figure 2. Contrast and brightness of the image series was optimised due to little labelling. The first image depicts the dye distribution 10 minutes after application of the donor phase followed by images in an hourly interval. Only autofluorescence could be detected. (i) subcutaneous fat cells and (m) hair bulb.*

In the initial diffusion period the fluorescence of the dye is primarily located along the gap and the cuticle. At the skin surface a diffusion pattern as previously reported (Grams et al, 2004b) is obtained (Figure 3A). 10 minutes after application of the donor phase, no dye was detected in the hair follicle and in the skin. Within the next hour, diffusion commenced via the hair follicle and the stratum corneum. The images (Figure 3A, 1h) show that in the initial time period, the gap and the cuticle of the hair follicle are stained very bright and that the fluorescence reaches deeper as compared to the staining in the non-follicular route. This strongly indicates permeation of the dye via the gap and cuticle. Up to 3 hours after application, the fluorescence intensity of the follicular gap increases. Then a decrease in fluorescence intensity in the gap up to the end of the experiment is observed. This fluorescence decrease is not detected in the cuticle where strong staining remains. The epidermis is weakly labelled after 1 hour, while fluorescence enters the dermis after 2 hours. However the fluorescence intensity of these non-follicular regions remain lower than the intensities in the gap and in the cuticle. After termination of the on-line experiment, an image with higher magnification was taken of the gap area (Figure 3B). The dark area in the centre of the image shows the gap area while the brighter part in the lower right hand corner is the outer layer of the hair shaft, the cuticle. The epidermis with stained cells and unstained nuclei is clearly depicted as well.

At a skin depth of 800 µm (Figure 4A) an intensity gradient is observed between the cuticle (high intensity) and the outer root sheet (low intensity), which remains during the entire diffusion period of 16 hours. Additionally, the onset of the appearance of the fluorescence is delayed compared to the superficial layers (Figure 3A). Only after 2 hours fluorescence appears in the area of the gap and cuticle. After 3 hours (Figure 4A, image 4) fluorescence is also detected in the outer root sheath simultaneously with the dermis, however, the labelling is less bright than in the gap and cuticle. The more intense staining of the gap and the cuticle compared to the surrounding tissue remains even after 16 hours. Furthermore, the intensity gradient in the gap and cuticle is much higher than in the surrounding tissue. That means that focusing on deeper areas of the hair follicle, the observed difference in fluorescence intensity between the cuticle and the outer root sheath is decreased. A higher magnification image at the end of the diffusion experiment (Figure 4B) confirms that the cuticle is still stained stronger than the outer root sheath with a higher difference in intensity closer to the skin surface. The hair shaft, the dermis and a region where the inner root sheath is disintegrating is hardly labelled at all.

Deep in the skin the fluorescent intensity remains low (Figure 5). 5 hours after starting the diffusion, the first staining occurs in the fat cells. Figure 5 depicts the diffusion of BFL at a depth of 2100 µm. Generally, at this depth the detected label intensity is very low. Therefore the contrast and the brightness of

the images had to be adjusted to obtain information about changes in label distribution. The first staining of skin structures namely the subcutaneous fat cells are visible 5 hours after the start of the experiment. After 7 hours the cuticle of the hair follicle is stained and increases in fluorescence intensity over time. Furthermore the outer root sheath is weakly stained after 9 hours and also the fluorescence intensity in this region increases with time. As has already been observed in the previous images, the inner root sheath and the hair shaft are hardly stained at this depth.

Only a very low staining is observed in the sweat glands (Figure 6A). At 2030 µm, a similar depth as the previous time series, the change in distribution of the fluorophore in a sweat gland was visualised over time. Since only very little fluorescence was detected, image adjustments (contrast and brightness) was required. Immediately after starting the experiment typical dot-like autofluorescence in the sweat glands are visible which did not seem to change over time. The first staining is observed after 4-5 hours in the fat cells surrounding the sweat gland. As the diffusion proceeds, the autofluorescence-free area of the sweat glands also retains the dye with black non-stained areas remaining. Over time the fluorescence intensity continues to increase. In Figure 6B a cross-section is depicted to illustrate the location of the sweat gland.

Proceeding even into deeper regions of the skin, no fluorescent staining was observed in the hair bulb. The follicular bulb is situated in the subcutaneous fat at a depth of 4000 µm. Also in this case contrast and brightness had to be adjusted to visualise the hair bulb (Figure 7). The detected signal in the image represented autofluorescence and did not change in time. Not even the fat cells around the hair bulb show increase in fluorescence intensity.

DISCUSSION

The technique of on-line visualisation has already been proven to be effective for time-dependent visualisation of diffusion processes (i) in stratum corneum, epidermis and dermis (Grams *et al*, 2004a) and (ii) in the hair follicle at the skin surface (Grams *et al*, 2004b). This study aimed at visualising diffusion processes in deeper areas of the skin. Our studies indicate that the technique is suitable for 'in depth visualisation' of diffusion processes over time however care has to be taken in the positioning of the skin piece to visualise an appropriate hair follicle. Figure 8A depicts the ideal positioning of a hair follicle to obtain good quality images. The donor phase has to be in direct contact with the hair follicle opening. Furthermore the follicle should be located close to the skin surface however not too close to the cutting plane which would result in damaged follicular structures. Therefore a parallel positioning of the hair follicle to the cutting plane is crucial. A divergence from the parallel orientation can result in a too large distance from the cutting plane (Figure 8B) and therefore insufficient

fluorescence intensity for image detection in the area of the hair bulb. Figure 8C shows a non-parallel orientation of the hair follicle, in which the bulb might be close enough to the cutting surface, however the hair follicle does not reach the skin surface. This preparation cannot be used for on-line visualisation purposes. The situation in Figure 8D allows visualisation of the intact follicle only in the upper half of the skin. This technique gives access to diffusion processes in deeper follicular structures of non-fixed human skin including the subcutaneous fat. However using this technique one has to be critical about the usage of every preparation.

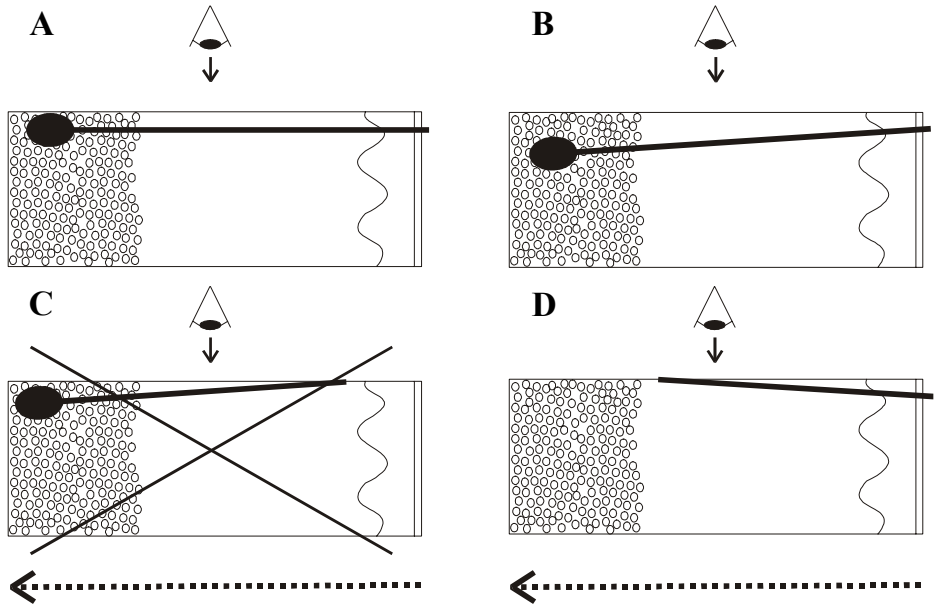

Figure 8. *Positioning of the hair follicle in the skin to enable visualisation using the on-line cutting device. The eye indicates the direction of visualisation while the dashed arrow indicates the direction of diffusion after application in the donor compartment. (A) Optimal positioning of the hair follicle namely with the opening in the donor compartment, parallel and close to the cross section. (B) Sub-optimal positioning where the fluorescence of the deeper follicle section will be substantially decreased due to scattering and absorption processes. This positioning is only suited for visualisation in the middle and eventually upper section. (C) A follicle positioned without an opening into the donor compartment results in erroneous diffusion profiles. (D) Sub-optimal positioning where the hair bulb is removed during the cutting procedure. This positioning is only suited for visualisation in the upper section where the hair follicle is still intact.*

Scheuplein (Scheuplein, 1967) has already predicted the importance of the follicular pathway in the initial diffusion processes. However this diffusion process has not been visualised on-line up to now. In the on-line time series at the skin surface and at the depth of 800 µm the gap of the hair follicle exhibits very early strong staining followed by the staining of the cuticle. These images

strongly indicate that the labelling of the cuticle originates from the dye present in the gap. Since the epidermis is weakly stained shortly after the gap and the cuticle, BFL also penetrates through the stratum corneum at early time points. This is in agreement with the general opinion, that small (BFL: 300 g/mol) and medium lipophilic compounds (BFL: logP = 2.5) penetrate relatively fast through the stratum corneum (Barry, 2001; Flynn, 1990; Guy, 1996; Hadgraft and Pugh, 1998). Keeping in mind that the gap and the cuticle are stained strongly while the epidermis is stained moderately in the beginning of the diffusion process, the origin of the label in the outer root sheath is not clear. The direct connection from the epidermis to the outer root sheath and their similarities in cell structures make this a possible route of penetration. On the other hand the label can penetrate from the gap through the thinner stratum corneum of the infundibulum into the outer root sheath. The inner root sheath is not present yet at the level of the infundibulum and starts to appear below the sebaceous gland (isthmus). Since the lipophilic dye penetrates the stratum corneum relatively fast and is detected in a high amount in the follicular gap, none of the two routes can be excluded. However since the dermis is labelled after the outer root sheath, the observations indicate strongly that the dye in the outer root sheath originate from the gap or the epidermis and not from the dermal tissue. Deeper in the hair follicle where the gap disappears, the fluorescent gradient in de cuticle is much stronger than the gradient in the surrounding tissue (Figure 4B). This strongly indicates that at this depth in the hair follicle label is diffusing from the cuticle to the surrounding tissue, subsequently being the inner, outer root sheet and the dermis.

In even deeper skin regions little label was observed which made post-experimental optimisation of the images essential. This implies that even in vitro in the absence of active blood vessels only a small amount of applied drug reaches skin structures at a depth of 2000 µm or more, which is observed for the hair follicle and the sweat glands. While in the upper part of the skin first staining was always observed in the gap and the cuticle, in the deeper skin regions the fat cells of the subcutaneous tissue were labelled first. Since this is observed in regions surrounding the hair follicle as well as in regions surrounding the sweat gland it is very likely that the fat cells retrieve their label from the dermis. Structures of the appendages (cuticle and outer root sheath of the hair follicle and sweat gland cells) can be stained by label from appendageal structures closer to the surface or via the dermis. Since the inner root sheath is hardly stained throughout time and depth, we suggest that the cuticular structures of the hair follicle obtain their label from the cuticle further up in the skin. The bulb of the hair follicle provides a target for drugs and nutrients since the hair follicle starts developing in this region. The images suggest that insufficient label molecules reach a skin depth of 4000 µm for the CLSM detection. Not even fat cells are stained suggesting that the majority of the label is captured and retained by fat cells at a depth of 2 mm. This subcutaenous fat might function as a depot for the

lipophilic label. This on-line visualisation uses skin in vitro and therefore lacks blood flow at depths of 200 µm, around the sweat gland and the around the hair follicle. If blood flow would be present, clearance of the drug by the bloodstream in the dermis and the hair follicle close to the epidermal-dermal junction is likely to occur. That would reduce the amount reaching the fat cells and deeper layers of the hair follicle. However simultaneously, the blood vessels also might provide a fast transport system to the highly vascularised hair bulb and redistribute the previously gathered drug molecules to the hair bulb.

The decrease of fluorescence over time in the gap is due to a depletion of the dye in the donor phase. In this early on-line diffusion cell design, a static set-up was chosen to prove the general usage. In future experiments a flow-through diffusion system should be established to maintain a constant donor phase concentration and circumvent the depletion of the donor phase. Pilot studies have shown the technical feasibility of a flow-through on-line set-up.

CONCLUSION

This technique allows the visualisation of the diffusion process of a fluorescent dye in deeper layers of the skin up to a depth of the subcutaneous fat. This is crucial for monitoring the penetration pathway of the dye in follicular delivery since the terminal hair follicle extends into the subcutaneous fat tissue. We conclude that for a medium lipophilic drug the initial diffusion occurs via the gap and the cuticle of the hair follicle. From the cuticle label most probably diffuses into the surrounding tissue rather than from the surrounding tissue into the cuticle. Diffusion also occurs via the stratum corneum and the epidermis. The label source of the outer root sheath is not clear since it can originate from the gap via the thinner stratum corneum of the infundibulum or from the direct connection of the epidermis with the outer root sheath. Furthermore we conclude that the label in the subcutaneous fat does not originate from the appendages but more likely from the label in the dermis. Additionally the subcutaneous fat has the potential to function as a depot for lipophilic compounds with the possibility of constant release over time. Using saturated BFL buffer solution, no detectable amount of label reached the hair bulb within in vitro conditions.

REFERENCE LIST

Agarwal R, Katare OP, and Vyas SP: The pilosebaceous unit: A pivotal route for topical drug delivery. Methods Find Exp Clin Pharmacol 22:129-133, 2000

Allec J, Chatelus A, and Wagner N: Skin distribution and pharmaceutical aspects of adapalene gel. J Am Acad Dermatol 36:S119-S125, 1997

Barry BW: Novel mechanisms and devices to enable successful transdermal drug delivery. Eur J Pharm Sci 14:101-114, 2001

Chu I, Dick D, Bronaugh R, and Tryphonas L: Skin reservoir formation and bioavailability of dermally administered chemicals in hairless guinea pigs. Food Chem Toxicol 34:267-276, 1996

Fabin B and Touitou E: Localization of lipophilic molecules penetrating rat skin in vivo by quantitative autoradiography. Int J Pharm 74:59-65, 1991

Flynn GL: Physicochemical determinants of skin absorption. In: Principles of Route-to-Route Extrapolation for Risk Assessment. New York: Elsevier, 1990, pp.98-127

Foreman MI, Picton W, Lukowiecki GA, and Clark C: The effect of topical crude coal tar treatment on unstimulated hairless hamster skin. Br J Dermatol 100:707-715, 1979

Genina EA, Bashkatov AN, Sinichkin YP, Kochubey NA, Lakodina NA, Altshuler GB, and Tuchin VV: In vitro and in vivo study of dye diffusion into the human skin and hair follicles. J Biomed Optics 7:471-477, 2002

Grams YY, Whitehead L, Cornwell P, and Bouwstra JA: On-line visualisation of dye diffuion in fresh unfixed human skin. Pharm Res accepted: 2004a

Grams YY, Whitehead L, Cornwell P, and Bouwstra JA: Time and depth resolved visualization of the diffusion of a lipophilic dye into the hair follicle of fresh unfixed human scalp skin. J Control Release submitted: 2004b

Guy RH: Current status and future prospects of transdermal drug delivery. Pharm Res 13:1765-1769, 1996

Hadgraft J and Pugh WJ: The selection and design of topical and transdermal agents: a review. J Invest Dermatol Symp Proc 3:131-135, 1998

Hueber F, Schaefer H, and Wepierre J: Role of transepidermal and transfollicular routes in percutaneous absorption of steroids: in vitro studies on human skin. Skin Pharmacol 7:237-244, 1994

Illel B, Schaefer H, Wepierre J, and Doucet O: Follicles play an important role in percutaneous absorption. J Pharm Sci 80:424-427, 1991

Kao J, Hall J, and Helman G: In vitro percutaneous absorption in mouse skin: Influence of skin appendages. Toxicol Appl Pharmacol 94:93-103, 1988

Lademann J, Weigmann HJ, Rickmeyer C, Barthelmes H, Schaefer H, Mueller G, and Sterry W: Penetration of titanium dioxide microparticles in a sunscreen formulation into the horny layer and the follicular orifice. Skin Pharmacol Appl Skin Physiol 12:247-256, 1999

Lauer AC, Lieb LM, Ramachandran C, Flynn GL, and Weiner ND: Transfollicular drug delivery. Pharm Res 12:179-186, 1995

Lieb,LM, Liimatta AP, Bryan RN, Brown BD, and Krueger GG: Description of the intrafollicular delivery of large molecular weight molecules to follicles of human scalp skin in vitro. J Pharm Sci 86:1022-1029, 1997

Meidan VM, Docker M, Walmsley AD, and Irwin WJ: Low intensity ultrasound as a probe to elucidate the relative follicular contribution to total transdermal absorption. Pharm Res 15:85-92, 1998

Rolland A, Wagner N, Chatelus A, Shroot B, and Schaefer H: Site-specific drug delivery to pilosebaceous structures using polymeric microspheres. Pharm Res 10:1738-1744, 1993

Schaefer H, Watts F, Brod J, and Illel B. 1989. Follicular penetration. 163-173.

Scheuplein RJ: Mechanism of percutaneous absorption. II. Transient diffusion and the relative importance of various routes of skin penetration. J Invest Dermatol 48:79-88, 1967

Serizawa T, Onodera T, and Oba K: Percutaneous absorpiton of a drug into hair follicles. Curr Probl Dermatol 22:195-200, 1995

Weiner N: Targeted follicular delivery of macromolecules via liposomes. Int J Pharm 162:29-38, 1998

VIII

Summary and future perspectives

INTRODUCTION

Local drug delivery in the skin is important for the efficacy of a drug or a nutrient. Optimisation of the physical and chemical properties of the penetrant itself and the vehicle can improve the efficacy of the delivery to a certain skin region. Target regions of interest are for example sweat glands, pilosebaceous units, the basal lamina of the epidermis and the Langerhans cells within the epidermis. The pilosebaceous unit consists of a sebaceous gland and a hair follicle with the duct of the sebaceous gland joining the follicular duct in the upper part of the dermis. In terminal hair, the bulb of the hair follicle is located in the subcutaneous fat. The hair follicle moves upwards from the bulb and emerges from the skin at the surface. The follicle itself consists of various layers (Figure 1) which form, protect and guide the hair shaft. From the dermis towards the hair shaft, the layers of the hair follicle are outer root sheath and inner root sheath. Within the inner root sheath the Henle's layer, Huxley's layer and the cuticle can be distinguished. The cuticle of the inner root sheath is in direct contact with the cuticle of the hair shaft.

When examining delivery to and along the hair follicle, changes in accumulation in the various structures of the hair follicle have to be investigated. Due to the deep location of the hair follicle, the method of analysis is crucial. Currently several techniques are used, which provide either qualitative or quantitative information about the accumulation of active agents in the various skin regions. Some of these techniques include fixation procedures or other post-experimental treatments of the skin. This procedure has the potential to delocalise the model substance thereby bearing the danger of introducing artefacts. Additionally various *in vitro* studies, which focussed on (trans-) follicular delivery, have been performed using animal models such as mice and hamster. While fundamental questions regarding (trans-) follicular delivery can be addressed, extrapolation to the human subject is often very questionable.

The overall aim of this thesis was to determine the influence of permeant lipophilicity and vehicle composition on the accumulation and transport pathway of the permeant in the various regions of the hair follicle. For these studies fresh human scalp skin was used. In order to be able to compare the accumulation and transport in the various parts of the hair follicle a new method had to be developed. This method had to give access to changes in accumulation in deep layers of the hair follicle, while minimising the danger of artefact formation. Even more effort is required for obtaining information about the actual diffusion processes of model penetrants. In this case it is inevitable to visualise on-line the diffusion of the penetrant in fresh unfixed skin. Not only the diffusion process in superficial layers of the skin, but also the permeation processes in time and depth in deeper regions of the hair follicle have to be visualised to get access to

the permeation pathways. These permeation pathways are important to understand the targeting to the hair follicle and in particular the hair bulb.

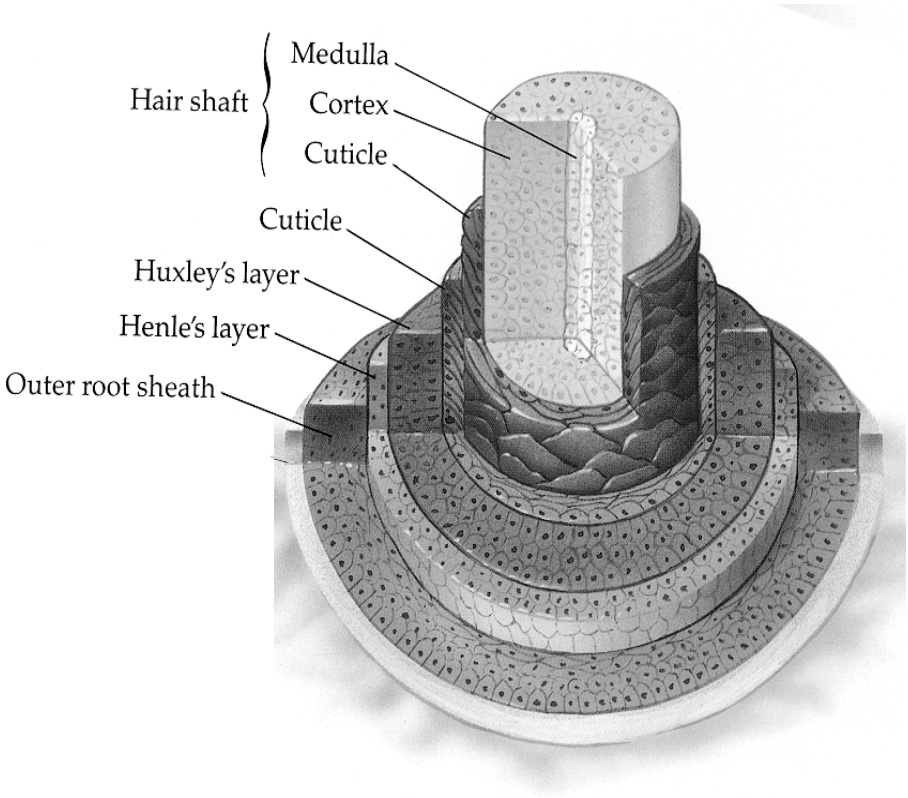

Figure 1. *Hair follicle with the outer root sheath, inner root sheath (Henle's layer, Huxlex's layer and cuticle of the inner root sheath) and the hair shaft (cuticle of the shaft, cortex and medulla).*

Static diffusion analysis

In chapter II a new method is presented, which allows a semi-quantitative comparison of fluorophore distribution in the substructures of the hair follicle and the non-follicular regions of unfixed skin. This method is based on the fluorophore intensity measured with confocal laser scanning microscopy in images parallel and perpendicular to the skin surface.

A lipophilic dye (Bodipy® 564/570 C_5) was applied on fresh human scalp skin in citric acid buffer pH 5.0 containing 30 % (v/v) ethanol. After 18 hours of diffusion, the skin was removed from the flow-through diffusion cell and processed for subsequent visualisation in the confocal laser scanning microscope. The skin was visualised parallel to the skin surface at the dermal side. This image provides information about the fluorescent distribution in the hair

follicles and the dermis. In addition the cross section perpendicular to the skin surface provides information about the fluorescent distribution in the epidermis, dermis and stratum corneum. By combining the information of these images, the relative intensity values of the various regions in the skin including the hair follicle can be calculated. If model geometry based on the properties of the skin is assumed, the relative contribution in intensity of each skin region to the total intensity can be calculated. This contribution in intensity for each skin region is referred to as the relative accumulation factor of that skin region.

Subsequently (see chapter III) the influence of permeant lipophilicity on the permeation and distribution in human scalp skin was investigated. The fluorophore was applied in a buffer solution containing 30 % (v/v) ethanol. For these studies the newly developed method described in chapter II was used. The dyes that were selected are in sequence of increasing lipophilicity Oregon Green® 488, Bodipy® FL C_5 and Bodipy® 564/570 C_5. Additionally the presence of 30 % ethanol on diffusion and distribution of the dye with the lowest lipophilicity (Oregon Green® 488) was studied. Diffusion studies with fresh human scalp skin of 1100 µm thickness were performed for 18 or 72 hours using flow-through diffusion cells. Subsequently the skin was processed immediately to visualise the intensity distribution within the skin and the hair follicle using confocal laser scanning microscopy. The relative fluorophore distribution in the skin was calculated as described in chapter II. Ethanol (30 % (v/v) in CAB) increases the penetration rate of Oregon Green® 488 across the skin and promoted the transport of Oregon Green® 488 into and along the hair follicle slightly. Furthermore, an increase in permeant lipophilicity resulted in an increase in penetration rate across human scalp skin. The relative distribution in the skin is also affected by the lipophilicity of the permeating dye. A high lipophilicity of the label promotes the deposition of the label in the hair follicle as demonstrated by the relative accumulation values. Therefore we conclude that delivery to the hair follicle can be improved by the use of a lipophilic substance.

In chapter III, the combined effect of vehicle composition and dye lipophilicity on diffusion and distribution in human scalp skin is described. Formulations were prepared containing surfactants frequently used in shampoo formulations with and without propylene glycol. These surfactant formulations containing one of the dyes were diluted 1:1 with citric acid buffer pH 5.0. Similarly as in the previous study, permeation was measured over a period of 18 hours, which was immediately followed by visualisation using confocal laser scanning microscopy. As in the previous study, the relative accumulation of the dyes in the various parts of the skin and the hair follicle was determined. In the presence of surfactants with or without propylene glycol, medium and highly lipophilic dyes accumulated more in the follicular regions than the dye with the lowest lipophilicity. Additionally after 18 hours of permeation the amount of dye in the surfactants/propylene glycol formulation, that penetrated through the skin was

significantly higher for the most lipophilic dye, Bodipy® 564/570 C_5. This phenomenon was not observed for the most hydrophilic dye, Oregon Green® 488. These studies demonstrated that the highest accumulation in the hair follicles is observed with lipophilic dyes in surfactant formulation with propylene glycol.

With the newly developed method important information about the localisation of a dye in various skin regions can be generated. Unfortunately, no information can be gained about the actual route of permeation. Therefore an entirely new method was developed with the aim to visualisation the transport *on-line* in superficial as well as in deep layers of the skin, including the subcutaneous fat and the hair follicles.

REAL-TIME DIFFUSION

The aim of the studies described in chapters V to VII is establishing a technique that enables to examine *on-line* the penetration of a fluorophore from the skin surface, across the viable epidermis into the dermis. Importantly, the aim is also to visualise the permeation along the hair follicles in the various depths of the skin even as far as the hair bulb being located in the subcutaneous fat.

The first goal was to develop a method to study *on-line* permeation in the stratum corneum, viable epidermis and superficial layers of the dermis. In order to accomplish this, the skin has to be sliced perpendicular to the skin surface. This was achieved with a specially designed cutting device previously used to create the manual cross sections described in chapters II, III and IV). This cutting device was modified such that immediately after cutting, a donor and acceptor compartment is created (Figure 2). The acceptor and donor compartment were sealed with dental clay and a cover slip. The same cover slip was also covering the skin cross section. This enables to visualise the skin cross section with the confocal scanning laser microscope. Immediately after assembling the on-line diffusion cell, the donor and acceptor phase were injected through the dental clay. The donor phase consisted of the medium lipophilic dye (Bodipy® FL C_5) in citric acid buffer pH 5.0. Directly after application of the dye, images were obtained every 10 minutes for 8.5 hours using a high magnification of the microscope. The images revealed the stratum corneum, the epidermis and the dermis. After image acquisition, the change in fluorescence intensity was quantified and evaluated as function of time and location in the skin. Focussing on the epidermis and the dermis, detailed information regarding the change in fluorescence intensity in time and depth (pixel resolution) was obtained. In the stratum corneum, the fluorescence gradient was steep in the superficial layers and became gradually less steep in the deeper layers, demonstrating that the stratum corneum is not a homogeneous layer for diffusion. The fluorescent gradient was less steep in viable epidermis and dermis. At the junction of stratum

corneum/viable epidermis, a sharp increase in fluorescence is observed while at the epidermal/dermal junction, a sudden drop in fluorescence was detected. This indicated that the dye was more easily dissolved in the epidermis than in the stratum corneum and dermis. From this study we can conclude that with the newly developed technique, depth and time resolved visualisation of dye penetration into unfixed skin is obtained.

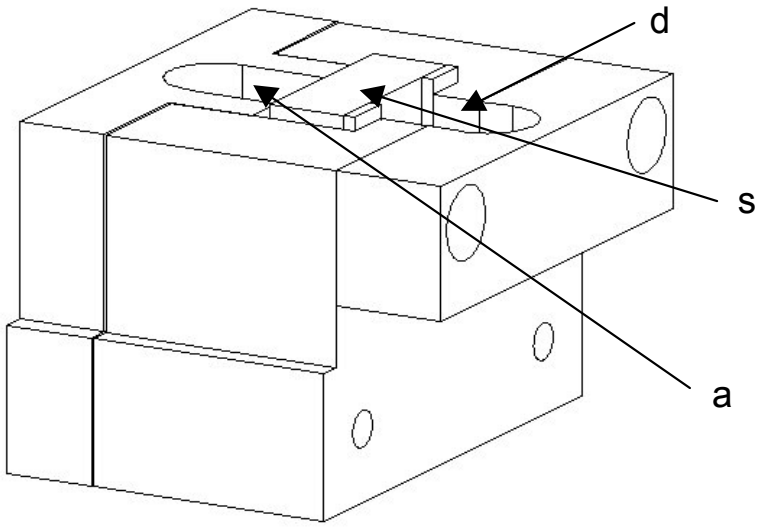

Figure 2. *On-line visualisation device containing cross sectioned skin (s), donor compartment (d) and acceptor compartment (a). The stratum corneum of the cross section is facing the donor compartment. The cutting plane of the cross section is sealed with a cover slip and dental clay (not depicted) enabling on-line visualisation of the diffusion process by confocal laser scanning microscopy.*

Chapter VI describes the penetration of Bodipy® FL C_5 into the hair follicle visualised by CLSM *on-line*. The combined cutting device/on-line diffusion cell was used with a lower magnification as described in chapter V. In this study the focus was to visualise larger structural units as the hair follicle. Images were obtained at a 30-minute interval for 16 hours. The donor phase was identical to the one used in the previous study (Bodipy® FL C_5 in citric acid buffer pH 5.0). During image evaluation, the relative quantification method developed for the static visualisation (chapter II) was adapted to include additional regions like the gap of the hair follicle. Additionally accumulation could be calculated at different depths of the same skin cross section (chapter VI). In the initial period the penetration of the medium lipophilic dye, Bodipy® FL C_5, occurred mainly via the gap and cuticle. After this period penetration via the epidermis became more important. Label in the cuticle originated mainly from the gap and permeated in

the cuticular region deeper into the skin. Dye in the outer root sheath originated either from the gap or from the epidermis.

However the question remained how the diffusion from the hair follicle close to the surface proceeded into deeper skin regions and whether label would reach the hair bulb. In order to study the diffusion *on-line* in deep skin regions, additional diffusion studies using fresh human scalp skin were performed as described in chapter VI with identical donor phases, image acquisition and magnification. However this time, on-line image series were obtained at increasing depth, namely at the surface and typically at 800 µm, 2100 µm and 4000 µm in depth (chapter VII). Due to the dilemma that a high magnification in CLSM cannot provide an image, which includes the stratum corneum at 0 µm and the hair bulb at > 2000 µm depth, different donors had to be used for each selected depth in the skin. Close to the skin surface, the gap and the cuticle of the hair follicle was stained at a very early stage of the permeation process. Label, which reached deeper layers in the cuticular region, was permeating from the cuticle into the surrounding areas, namely the inner and outer root sheath. At depth of up to 1000 µm, diffusion via the follicular route (cuticle, outer root sheath) was dominating in the initial time period, while the surrounding dermis was stained afterwards. At greater depths, the diffusion via the dermis gained more importance. This was indicated by the earlier staining of the subcutaneous fat as compared to any part of the hair follicle. Although the hair bulb was visualised, no label diffusion into the bulb was detected.

The results of these studies demonstrate that the on-line visualisation technique is a very powerful tool to visualise diffusion processes into deeper regions of non-fixed fresh skin. It has also the potential to study *in vitro* transport processes on cellular level including gene transport studies. In the upper regions of scalp skin, the follicular route is of great importance in the initial diffusion period. Deeper in the skin, diffusion via the dermis gains importance as well. Results indicate that targeting a drug substance comparable to our lipophilic model penetrant to the hair follicle in the upper regions of the dermis appears possible, especially in the cuticle and outer root sheath. Depths where the bulge region (highly proliferative cells) is present might be reached. However penetration of the drug substance (especially when lipophilic) via the stratum corneum into the dermis and subsequently the systemic circulation cannot be excluded. Targeting the hair bulb solely via topical application appears to be difficult and only feasible for therapy if highly potent molecules are used.

FUTURE PERSPECTIVES

Improvement of on-line visualisation technique

In chapter V, VI and VII, on-line images are presented reflecting the diffusion process up to 16 hours. It has been observed, that after a certain period of diffusion, the fluorescence intensity in the donor compartment decreases. As mentioned in those chapters, photobleaching is not expected to be the main reason for this decrease. Since the donor phase of the on-line diffusion cell was not stirred and the donor compartment had a small volume, depletion of the donor phase is expected to be the main reason for this decrease. In future experiments a method should be developed, circumventing donor depletion. Pilot studies already indicated that an on-line diffusion cell could be designed with a flow-through donor phase. This ensures a constant donor concentration and therefore a constant rate of partitioning of the permeant into the skin. The acceptor phase can also be adjusted to generate a flow-through system. This provides a continuous removal of the dye from the dermis and the acceptor compartment resulting in a very low concentration in the acceptor phase. In this way a true steady state flux can be achieved, which will provide more detailed information on the diffusion process.

In the presented work, on-line diffusion was investigated with one lipophilic label. These on-line studies should also be extended to include labels of different physicochemical characteristics. In that way it can be investigated whether the route of transport depends on the chosen permeant. Simultaneous application of two labels followed by on-line visualisation of the diffusion process allows a direct comparison of the permeants diffusion processes. This would result in more accurate data as the comparison of the labels can be made within the same piece of skin and in the same visual plane. Inter donor variation can also be excluded. This is an important advantage especially in scalp skin that shows large inter donor variation. However care has to be taken during the selection of the permeants. The optical properties (excitation and emission wavelength and the fluorescent intensities) and the applied concentration of the dyes are crucial for the investigation.

In visualisation of fluorescent substances, no absolute mathematical correlation can be made between the intensity and the concentration of a fluorophore. Therefore mathematical approaches have been developed in this thesis to obtain information of the distribution of a dye. For these calculations, assumptions had to be made. It was assumed that the fluorescence is independent of the different skin tissues and each skin region was approached by geometric forms. The values obtained using this combined experimental/mathematical approach has to be confirmed by an additional method. Alternative approaches circumventing fluorescent labels could be raman

microscopy, autoradiography and magnetic resonance imaging. The optimal approach would be a model penetrant which can be detected by confocal laser scanning microscopy and one of the above mentioned methods.

The diffusion studies described in this thesis were performed using fresh human scalp skin without any long-term storage and conservation of the skin. Therefore these experiments can be considered to be as close to the human situation as one can achieve with *in vitro* experiments. In most diffusion studies a skin thickness of approximately 200 µm is used. This thickness is selected as this contains mainly the epidermis. In diffusion studies the flow through acceptor phase can therefore simulate the blood flow. However when the hair follicle is the main target, full thickness skin with subcutaneous fat is required to access the deeper layers of the hair follicle and the bulb. A limitation of the *in vitro* studies is that the hair follicle is not highly vascularised as is in the in vivo situation. This might influence the transport from the hair follicle into the circulation and the redistribution of the dye from the epidermis/dermis via the blood vessels into the hair follicle. Therefore we suggest that fresh human scalp skin is the best model for investigation of follicular delivery *in vitro*, however results have to be judged critically when extrapolating to the *in vivo* situation. For *in vivo* follicular delivery, magnetic resonance imaging or raman microscopy might be the methods of choice in the near future.

Follicular drug delivery

When addressing delivery of compounds to the hair follicle two approaches have to be considered. The first approach is that the basic ingredients of the formulation have been selected and the transported active ingredient can be adapted. This first approach has been investigated in this thesis. A clear accumulation of substances has been observed in the upper parts of the hair follicle depending on the nature of the penetrant and the formulation. In these upper regions, the cuticle of the inner root sheath and of the hair shaft, the outer root sheath, the duct of the sebaceous gland and the bulge area are candidates for target regions. However, only little staining was observed in the follicle deeper in the skin. No labelling was detected in the hair bulb when using skin including the subcutaneous fat. The *in vivo* situation might influence the accumulation due to higher amount of applied drug, presence of blood vessels and massaging during the application of the formulation. However, since the experiments were carried out over a long time period, the chance of delivering high amount of drug to the hair bulb is estimated to be rather low using this first approach. Therefore, molecules suitable for follicular targeting into deep skin areas have to be highly potent since only a low amount of penetrant reaches the hair bulb. Next to hormones, DNA molecules might be interesting candidates for follicular targeting. Since only few molecules have to reach the site of action it can be a promising penetrant to treat DNA related disorders. However size might

be a critical factor when delivering large molecules such as DNA. The developed on-line visualisation technique can provide a possible tool for future investigations on a cellular level.

The second approach is that a molecule can only be modified slightly while the vehicle can be selected without limitation. Vehicles which are suitable to deliver molecules to the hair follicle such as particulate molecules have to be tested for their efficacy and customer acceptance. Next to their use in pharmaceutical products, they might form an improvement in the hair care industry. They have the potential to accumulate in the follicular opening and slowly release an active ingredient. In case this approach does not result in a therapeutic level of the active at the target site, a combination of topical application with systemic delivery should be considered. This combination might be a good alternative to topical application only since the hair follicle is highly vascularised and therefore susceptible to both routes of delivery. For future approached, it would be very interesting to investigate formulations containing small particles with our newly developed method. The main question would then be if effective transport to the hair root is possible when using particulate formulations in order to avoid systemic applications.

IX

Samenvatting en Toekomstperspectieven

INTRODUCTIE

Lokale toediening in de huid is van belang voor de behandeling van veel huidziekten, zoals huidkanker en acne. Voorbeelden van gebieden in de huid interessant voor lokale toediening van geneesmiddelen zijn zweetklieren, talgklieren, haarzakjes en de Langerhans cellen. Om de efficientie van lokale toediening te verhogen is het belangrijk te onderzoeken of een verandering in de fysische en chemische eigenschappen van de toe te dienen stof en van het vehikel het transport naar een geselecteerd gebied in de huid kan bevorderen. Een belangrijk gebied voor locale toediening van geneesmiddelen is met name het haarzakje.

Samen met de talgklier vormt het haarzakje de pilosebaceous eenheid. Het kanaal van de talgklier mondt uit in het haarzakje ongeveer ter hoogte van de bovenste lagen van de dermis. In de volgroeide haar bevindt de haarwortel zich in het subcutane huidvet en heeft het haarzakje zich naar de huidoppervlakte georiënteerd. Het haarzakje bestaat uit verschillende lagen (Figuur 1). Deze lagen zijn verantwoordelijk voor de vorming van de haar, bescherming van de haar en leiden de haar door de huid richting het huidoppervlak. Ter hoogte van de dermis bestaat het haarzakje uit twee lagen, namelijk de buitenste wortellaag en de binnenste wortellaag. De binnenste wortellaag kan nog onderverdeeld worden in de laag van Henle, de laag van Huxley en de cuticula. De cuticula is de binnenste laag van het haarzakje en staat in direct contact met de cuticula, de buitenste laag van de haar.

Om lokale ophoping of zelfs het transport van een geselecteerde stof naar en langs het haarzakje te onderzoeken, moet de stof simultaan in de verschillende gebieden van het haarzakje gemeten worden. Omdat het haarzakje tot diep in de huid is gelocaliseerd, is een juiste keuze van de analysemethode van groot belang. Op dit moment zijn er verschillende methoden beschikbaar, die kwalitatieve of kwantitatieve informatie over de ophoping van een geneesmiddel in de verschillende huidonderdelen kunnen geven. In de literatuur wordt veel melding gemaakt van technieken die fixatie of een andere manier van postexperimentele behandeling vereisen. Ook wordt in dit soort onderzoek veel gebruik gemaakt van diermodellen. Zowel het gebruik van diermodellen als ook het gebruik van fixatieven heeft nadelen. Tijdens de fixatie kunnen artefakten gecreëerd worden door delocalisatie van het geneesmiddel. En bij de diermodellen is het maar de vraag in hoeverre de extrapolatie naar de mens reëel is.

Het doel van het onderzoek beschreven in dit proefschrift is zowel de ophoping als ook de transportroute van modelstoffen in de verschillende gebieden van het haarzakje *in vitro* te bepalen. Hierbij is de invloed van zowel de lipofiliteit van de model stof als ook de samenstelling van de formulering

onderzocht. Dit is uitgevoerd met confocale laser scanning microscopie in kombinatie met een speciale snijmethode voor humane hoofdhuid. Het doel is niet alleen oppervlakkig, maar ook diep in de huid in vitro de ophoping van modelstoffen te meten, terwijl het gevaar van artefakten geminimaliseerd moet worden. In de eerste studies is het onderzoek vooral gericht op het meten van de ophoping van de modelstof in de verschillende huidgebieden nadat een diffusie proces heeft plaats gevonden. Het blijkt mogelijk de invloed van zowel de lipofiliteit van de modelstof als ook de samenstelling van het vehikel op de ophoping van de modelstof in de verschillende gebieden in de huid te bepalen. Echter, het blijkt niet mogelijk conclusies te trekken over de transportroute van de modelstof.

Om inzicht te krijgen in de transportroute van een modelstof, is het essentieel het transportproces on-line in niet-gefixeerde huid te onderzoeken. Niet alleen de penetratieprocessen in de bovenste lagen maar ook in de diepere lagen van de huid moeten toegankelijk gemaakt worden om een compleet beeld van de werkelijke diffusie door de verschillende lagen van de huid en het haarzakje te verkrijgen. De kennis van penetratieroutes is van groot belang voor doelgerichte toedienen naar het haarzakje en de haarwortel.

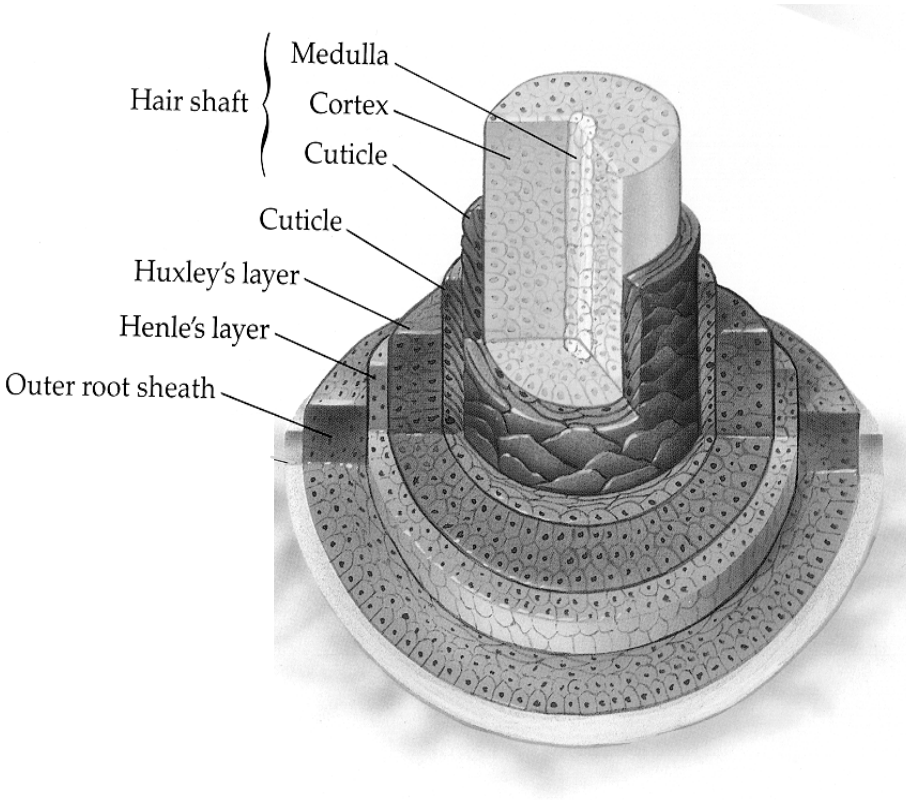

Figuur 1. *Haarzakje met de buitenste wortellaag (outer root sheath), binnenste wortellaag (inner root sheath [Henle's layer, Huxley's layer en cuticula van de binnenste wortellaag]) en de haarschacht (cuticula van de schacht, cortex en medulla).*

Statische diffusieanalyse

Hoofdstuk II beschrijft een nieuwe methode, die het mogelijk maakt om semi-kwantitatief de verdeling van een fluorescerende stof, de modelstof, in de verschillende gebieden van het haarzakje en in de overige gebieden van ongefixeerde huid te onderzoeken. De fluorescentie intensiteit is in ieder gebied met behulp van confocale laser scanning microscopie in de huid gemeten, zowel parallel als loodrecht ten opzichte van het huidoppervlakte.

Een lipofiele fluorescerende marker (Bodipy® 564/570 C_5) is in vitro op verse humane hoofdhuid opgebracht in een citroenzuurbuffer pH 5.0 met 30 % (v/v) ethanol. Na 18 uur diffusie is de huid uit de doorstroomdiffusiecel gehaald en verder verwerkt zodat deze gemeten kan worden in de confocale laser scanning microscoop. De huid is zodanig gepositioneerd, dat de fluorescentie ter hoogte van de dermis parallel aan het huidoppervlak gemeten wordt. Daardoor is informatie te verkrijgen over de verdeling van de lipofiele kleurstof in het haarzakje en de dermis. Tevens is de huid in de richting loodrecht op het huidoppervlakte doorgesneden met een speciaal daarvoor ontworpen snijapparaat en is de fluorescentie ongeveer 30 μm onder het snij oppervlak ook gemeten. In deze opname geeft de meting informatie over de verdeling van de fluorescentie in de epidermis, dermis en het stratum corneum. Door het combineren van de fluorescentie verdeling in de opnames loodrecht en parallel aan het huidoppervlak, is de relatieve fluorescentie intensiteit in de verschillende gebieden in de huid en het haarzakje berekend. Om dit te kunnen doen is een hele nieuwe rekeningsmethode ontwikkeld. De verhoging of verlaging van de intensiteit in elk huidonderdeel ten opzichte van de gemiddelde fluorescentie intensiteit is uitgerekend. Dit wordt de relatieve accumulatiefaktor genoemd.

In hoofdstuk III is de invloed van de lipofiliteit van een modelstof in een buffer oplosssing met 30 % (v/v) ethanol op de permeatie door en de verdeling in humane hoofdhuid onderzocht. Voor dit onderzoek is de reeds in hoofdstuk II beschreven methode gebruikt. De geselekteerde modelstoffen in volgorde van toenemende lipofiliteit zijn Oregon Green® 488, Bodipy® FL C_5 en Bodipy® 564/570 C_5. Daarnaast is de aanwezigheid van 30 % (v/v) ethanol op de diffusie en verdeling van de fluorescerende modelstof met de laagste lipofiliteit (Oregon Green® 488) onderzocht. Diffusiestudies met humane hoofdhuid (huiddikte van 1100 μm) zijn uitgevoerd over een periode van 18 of 72 uur in doorstroomdiffusiecellen. Aansluitend is de huid verder verwerkt om de verdeling van de modelstof in de huid en het haarzakje met de confocale laser scanning microscoop te visualiseren. De relatieve fluorescentieverdeling van de modelstoffen is berekend zoals beschreven in hoofdstuk II. De uitkomnsten zijn als volgt. Ethanol (30 % (v/v) in citroenzuurbuffer) verhoogt de penetratie van Oregon Green® 488 door de huid en lijkt de ophoping van Oregon Green® 488 in

het haarzakje licht te bevorderen. Daarnaast leidt een verhoging van de lipofiliciteit van een modelstof tot een verhoogde penetratie door humane hoofdhuid. De relative verdeling in de huid wordt ook bëinvloed door de lipofiliciteit van de modelstof. Een hoge lipofiliciteit van de fluorescerende stof bevordert de ophoping in het haarzakje. Hieruit blijkt dat ophoping in het haarzakje verbeterd kan worden door een lipofiele stof te gebruiken.

Naast lipofiliteit is ook de gecombineerde invloed van vehikelsamenstelling en lipofiliteit van de modelstof (hoofdstuk IV) onderzocht. Een stof die vaak in formuleringen zoals bijvoorbeeld shampoos gebruikt wordt is propyleenglycol. Propyleenglycol in combinatie met de oppervlakteactieve stoffen is 1:1 verdund met een citroenzuur buffer pH 5.0 en bevat één van de fluorescerende modelstoffen. Zoals in de eerder beschreven studies zijn de diffusiestudies uitgevoerd over een periode van 18 uur en vervolgens is de huid direkt met de confocale laser scanning microscoop gevisualiseerd. Opnieuw is de relatieve accumulatiefaktor van de verschillende gebieden in de huid en het haarzakje bepaald. Hieruit blijkt dat de oppervlakteactieve stoffen met en zonder propyleenglycol, de ophoping van Bodipy® FL C_5 en Bodipy® 564/570 C_5 met hogere lipofiliteit in het haarzakje bevordert in tegenstelling tot Oregon Green® 488 met een lage lipofiliciteit. Bovendien is na 18 uur de ophoping in het haarzakje van de meest lipofiele modelstof (Bodipy® 564/570 C_5) opgebracht in de formulering met propyleenglycol significant hoger dan zonder propyleenglycol. De ophoping van de hydrofiele stof (Oregon Green® 488) is niet beinvloed door propyleenglycol. Hieruit blijkt dat de meest lipofiele stof in combinatie met propyleenglycol tot de hoogste ophoping in het haarzakje leidt.

Het blijkt echter dat het niet mogelijk is met de nieuw ontwikkelde methode de transportroute van een fluorescerende modelstof te achterhalen. Daarom is besloten om een methode te ontwikkelen waarmee transportprocessen *on-line* in de huid zichtbaar gemaakt kunnen worden. Dit staat in het volgende hoofdstuk beschreven.

ON-LINE DIFFUSIE

Het doel van de studies beschreven in de hoofdstukken V tot en met VII is het on-line zichtbaar maken van het diffusieproces van een fluorescerende stof van het huidoppervlak tot in de dermis en het subcutane vetweefsel. Belangrijk daarbij is, dat ook de diffusie langs het haarzakje op verschillende diepten in de huid tot aan de haarwortel in het onderhuidsvet gevisualiseerd kan worden.

Eerst is een methode ontwikkeld, waarmee de diffusie van een stof on-line gevolgd kan worden in de bovenste lagen van de huid te weten: stratum corneum, levende epidermis en het bovenste gedeelte van de dermis. Om dit te bereiken, moet de huid loodrecht op het huidoppervlak gesneden worden. Hiervoor is hetzelfde snijapparaat gebruikt als beschreven in hoofdstuk II tot en

met IV. Echter, dit snijapparaat is zodanig gemodificeerd, dat direct na het snijden van de huid een donorkamer aan de kant van het stratum corneum en een acceptorkamer aan de kant van de dermis gemaakt wordt (Figuur 2). De acceptor en donorkamer zijn afgesloten met tandcement en een dekglas. Hetzelfde dekglas bedekt ook het snijvlak van de huid. Hierdoor kan de dwarsdoorsnede met de confocale laser scanning microscoop gevisualiseerd worden en het diffusieproces parallel aan het snijvlak gevolgd worden. Direct nadat de on-line diffusiecel in elkaar gezet is, is de donor en de acceptorvloeistof in de desbetreffende kamers door het tandcement geinjecteerd. De donorfase bestaat uit de Bodipy® FL C_5 in citroenzuurbuffer pH 5.0. Direct na het opbrengen van de fluorescerende modelstof, zijn er gedurende 8.5 uur elke 10 minuten opnames gemaakt van het diffusieproces. In de opnames is het fluorescentie profiel van de modelstof in het stratum corneum, de levende epidermis en de dermis gevolgd. Vervolgens zijn uit deze gegevens de verandering in fluorescentie gekwantificeerd als funktie van de tijd en de lokatie in de huid. In het stratum corneum dicht bij het huidoppervlak, is de fluorescentie gradient steil. Vervolgens wordt de gradient geleidelijk vlakker in de diepere stratum corneum lagen. Hieruit blijkt dat het stratum corneum geen homogene laag is voor diffusieprocessen. In de levende epidermis en de dermis is de gradient minder steil. Op de overgang van stratum corneum/levende epidermis, is er een abrupte

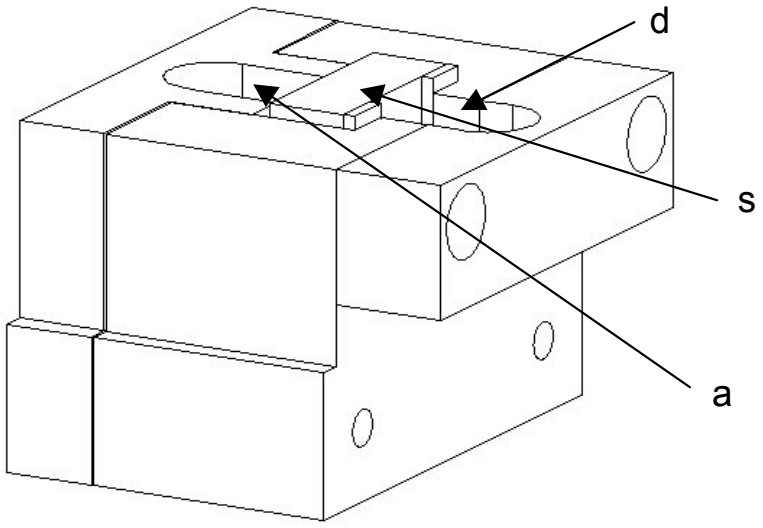

Figuur 2. *On-line visualisatie apparaat, dat dwarsdoorsnedes van de huid (s), donor kamer (d) en acceptorkamer (a) bevat. Het stratum corneum van de dwarsdoorsnede ligt aan de kant van de donorkamer. Het snijvlak is afgedekt met een dekglas en met tandcement (niet te zien). Daardoor kan diffusieprocess in on-line met behulp van de confocale laser scanning microscoop gevisualiseedt worden.*

toename van de fluorescentie intensiteit. Bij de epidermale/dermale overgang daarentegen is een sterke verlaging van de fluorescentie intensiteit gemeten. Dit betekent dat de fluorescerende stof gemakkelijker oplost in de levende epidermis dan in het stratum corneum en in de dermis. Uit deze studie blijkt dat het mogelijk is met deze nieuw ontwikkelde methode een tijds- en diepteafhankelijke visualisatie in de ongefixeerde huid te meten.

Hoofdstuk VI beschrijft de diffusie van Bodipy® FL C_5 in het haarzakje, die met confocale laser scanning microscopie on-line zichtbaar gemaakt is. Dezelfde on-line diffusiecel is gebruikt als in het vorige hoofdstuk. Echter, nu is er gewerkt met een lagere vergroting dan in de experimenten beschreven in hoofdstuk V. Daarvoor is gekozen, omdat de nadruk lag op het zichtbaar maken van de grotere structuren in het oppervlakkige gedeelte van haarzakje tot een diepte van 2 mm, zoals de haaropening, de cuticle, het haarkanaal en de buitenste wortellaag. De fluorescentie opnames zijn over een tijdsperiode van 16 uur met een interval van 30 minuten genomen. De donorfase was weer Bodipy® FL C_5 in citroenzuurbuffer pH 5.0. Om de fluorescentie data te verwerken is de eerder ontwikkelde evaluatiemethode voor de statische visualisatie (hoofdstuk II) aangepast. Hierdoor kan de ophoping van de modelstof in het haarkanaal en in de diepere lagen van de huid in dezelfde dwarsdoorsnede op elk gemeten tijdstip geëvalueerd worden (hoofdstuk VI). In de initiële fase diffundeert Bodipy® FL C_5 voornamelijk via het haarkanaal en de cuticula naar de diepere lagen. Na deze initiële periode is de diffusie via de epidermis van groter belang. De fluorescerende modelstof in de cuticula komt voornamelijk vanuit het haarkanaal en diffundeert via het gebied van de cuticula verder naar de diepere lagen van de huid. De modelstof in de buitenste wortellaag is afkomstig van ofwel het haarkanaal of van de epidermis.

De vragen die nog steeds beantwoord moeten worden zijn: a. Hoe verloopt de diffusie van een modelstof aanwezig in het haarzakje richting de diepere lagen van de huid? b. Bereikt de fluorescerende modelstof wel de haarwortel? Om deze vragen te kunnen beantwoorden is dezelfde methodiek gebruikt als beschreven in hoofdstuk VI met een identieke donorfase. Elke 30 minuten zijn weer opnames van het diffusieproces gemaakt. Maar deze keer zijn on-line opnames gemaakt op verschillende diepten van de huid, namelijk aan de huidoppervlakte, op 800 µm, 2100 µm en op 4000 µm diepte (hoofdstuk VII). Door het gebruik van hoge vergroting is het alleen mogelijk slechts een klein gedeelte van de huid in één opname zichtbaar te maken. Aangezien de metingen 16 uur duren en we alleen gebruik maken van verse huid zijn voor de opnamen op verschillende diepte steeds huid van andere donoren gebruikt. Uit de metingen kunnen de volgende conclusies getrokken worden. Dicht bij de huidoppervlakte zijn het haarkanaal en de cuticula van het haarzakje al heel vroeg in het diffusieproces gekleurd. De modelstof penetreert via de cuticula naar

de diepere lagen in het haarzakje. De fluorescerende modelstof, die in de cuticula van de diepere huidlagen terecht komt, diffundeert vervolgens van de cuticula naar de omgeving, voornamelijk naar de binnenste en buitenste wortellaag. Op een diepte van 1000 µm overheerst in de beginfase de diffusie via het haarzakje (cuticula, buitenste wortellaag), terwijl de omliggende dermis pas later in het diffusieproces kleurt. In nog diepere lagen is de diffusie via de dermis steeds belangrijker. Dit blijkt door een vroegere kleuring van het onderhuidsvet ten opzichte van elk gedeelte van het haarzakje. Hoewel de haarwortel door de autofluorescentie zichtbaar is, is transport naar de haarwortel met de confocale laser scanning microscopie niet waargenomen. Hieruit blijkt dat het erg moeilijk voor op de huid opgebrachten stoffen is de haarwortel te bereiken.

De resultaten tonen aan, dat de on-line visualisatie techniek een uitstekende methode is om diffusieprocessen naar diepere huidlagen van ongefixeerde huid zichtbaar te maken. Deze techniek heeft ook de potentie, om *in vitro* transportprocessen op cellullair niveau, zelfs met inbegrip van het transport van genetisch materiaal, te onderzoeken. In de bovenste laag van de huid is de route via het haarzakje van groot belang alleen in de beginfase van het diffusie proces. In de diepere huidlagen is diffusie via de dermis ook van groot belang. Uit onze resultaten blijkt dat het mogelijk is om een geneesmiddelmolecuul, welke vergelijkbare fysische chemische eigenschappen en moleculair gewicht heeft als onze modelstof, naar het haarzakje in de bovenste lagen van de huid (vooral naar de cuticula en de buitenste wortellaag) te transporteren. Het in de dermis gelegen bulgegebied waar sterk deelbare cellen zijn, kan zeker bereikt worden. Doelgericht transport naar de haarwortel door de dermale toediening blijkt moeilijk. Het is alleen mogelijk indien een hoogactief molecuul wordt toegediend.

TOEKOMSTPERSPECTIEVEN

Verbetering van de on-line visualisatie techniek

In hoofdstuk V, VI en VII zijn on-line opnamen gepresenteerd, die het diffusieproces in een tijdspanne van 16 uur weergeven. Deze opnamen laten zien, dat de intensiteit van de fluorescentie na een bepaalde diffusietijd in het donorcompartiment afneemt. In voorgaande hoofdstukken is al aangegeven dat „photobleaching“ hier niet verantwoordelijk voor is. Waarschijnlijk moet de hoofdoorzaak gezocht worden in het het uitputten van de fluorescerende stof in de donorfase. Het donorcompartiment is klein en de vloeistof wordt niet geroerd. In toekomstige experimenten, moet een methode ontwikkeld worden, waarbij een uitputting van de donorfase vermeden wordt. Inmiddels zijn eerste experimenten uitgevoerd, waarbij gebruik is gemaakt van een doorstroom on-line diffusiecel.

Een doorstroom compartiment kan in principe ook gemaakt worden voor de acceptorfase. Dit heeft het grote voordeel dat er een „steady-state flux“ bereikt kan worden. Hierdoor is het mogelijk om meer gedetailleerde informatie over het diffusieproces te verkrijgen.

In deze studie is de on-line diffusie onderzocht met een lipofiel fluorescerende modelstof. Deze techniek zou ook toegepast moeten worden op fluorescerende stoffen van verschillende fysisch-chemische eigenschappen, waardoor informatie beschikbaar komt over de invloed van de lipofiliteit op de transportroute van een stof door de huid. Het gelijktijdig toedienen van twee labels gecombineerd met het on-line visualiseren van de diffusieprocessen, maakt het mogelijk om deze twee labels in een experiment te vergelijken. Deze benadering zou tot nauwkeurigere resultaten leiden omdat de localisatie van de twee labels in hetzelfde stukje huid en in hetzelfde optische vlak in de huid plaats kan vinden. Verschil in permeatiegedrag van de twee labels veroorzaakt door verschillen in permeatie tussen huiddonoren kan daardoor ook uitgesloten worden. Dit is een belangrijk voordeel omdat hoofdhuid van donor tot donor sterk varieert. De labels moeten wel zorgvuldig uitgekozen worden. De optische eigenschappen van de labels (excitatie- en emissiegolflengte en de intensiteit van de fluorescentie) en de concentratie van het label in de huid zijn van groot belang bij deze keuze.

Al onze studies zijn uitgevoerd met één techniek. Het is aan te bevelen om naast confocale laser scanning microscopie ook nog andere technieken toe te passen, om de in dit proefschrift verkregen resultaten te verifieren. Opties voor alternatieve methoden, waarbij fluorescentie niet dwingend noodzakelijk is, zijn ramanmicroscopie, autoradiografie en magnetische resonantie. Het optimale modelmolecuul zou detecteerbaar moeten zijn met confocale laser scanning microscopie en een van de andere genoemde methoden.

De diffusiestudies in dit proefschrift zijn uitgevoerd met verse humane hoofdhuid, die niet bewaard en geconserveerd is. Daardoor benaderen deze experimenten zo veel mogelijk de humane *in-vivo* situatie. In de meeste diffusiestudies is een huiddikte van 200 µm geselecteerd omdat dit de epidermis omvat. Het vasculair bed is in de dermis gelokaliseerd, waardoor in diffusiestudies de doorstroom in de acceptorfase de bloedcirculatie simuleert. Echter, als het haarzakje het doel van de op de huid opgebrachte stof is, moet huid in zijn gehele dikte inclusief het onderhuidsvet gebruikt worden. De haarwortel, waarin ondermeer stamcellen voor haargroei aanwezig zijn, ligt in het onderhuisdvet. Een beperking van *in vitro* experimenten met huid inclusief onderhuidsvet, is de afwezigheid van vascularisatie ten opzichte van de *in vivo* situatie. Dit beinvloed waarschijnlijk het transport van het haarzakje naar de omgeving. Dit betekent dat ook de verdeling van de fluorescerende stof in de epidermis/dermis door de bloedvaten naar het haarzakje, beïnvloed kan zijn. Naar onze mening is verse humane hoofdhuid dan ook het beste model om het

folliculaire transport *in vitro* te bestuderen. Echter, door alle genoemde problemen is toch enige verzichtigheid geboden wanneer de resultaten naar de *in vivo* situatie geextrapoleerd worden. Voor onderzoek naar *in vivo* folliculairtransport zou in de toekomst beeldvorming met magnetische resonantie of ramanmicroscopie een geschikte methode kunnen zijn.

Geneesmiddelentransport langs het haarzakje

Als moleculen naar het haarzakje getransporteerd moeten worden zijn twee benaderingen mogelijk. In de eerste benadering zijn de basis ingredienten van de formulering al geselecteerd. In dit geval kan het transportmolekuul aangepast worden en de formulering alleen nog op details geoptimaliseerd worden. In dit proefschrift is deze eerste benadering bestudeerd. Een duidelijke ophoping van het label is gemeten in het bovenste deel van het haarzakje. De mate daarvan is afhankelijk van de fysisch-chemische eigenschappen van het label en van de formulering. In de bovenste lagen van de huid zijn de volgende gebieden mogelijk belangrijk om geneesmiddelen naar toe te transporteren: de cuticula van de binnenste wortellaag en van de haar, de buitenste wortellaag, het bulgegebied en het kanaal van de talgklier. Deze gebieden kunnen dus bereikt worden door topicale toediening. Daarentegen is dieper in de huid alleen een lage fluorescentie intensiteit in het haarzakje gemeten. In de haarwortel is zelfs helemaal geen fluorescentie gemeten. Echter, de *in vivo* situatie zou invloed kunnen hebben op de ophoping, vooral door de aanwezigheid van grotere hoeveelheden geneesmiddel, de aanwezigheid van het vasculair bed en het masseren tijdens het inbrengen van de formulering. De resultaten van deze eerste benadering duiden er op dat alleen hele kleine hoeveelheden van de op de huid opgebrachte verbindingen daadwerkelijk de bulb bereiken. Daarom moeten molekulen die in de haarwortel werken wel erg potent zijn. Voorbeelden daarvan zijn mogelijk hormonen en DNA moleculen. Omdat het al voldoende is als enkele DNA moleculen de haarwortel bereiken, kan het mogelijk zijn om DNA-gerelateerde ziektes te behandelen. Desondanks zou de grootte van een molecuul een kritische factor kunnen zijn bij het transport. De ontwikkelde on-line visualisatie methode zou een mogelijke methode voor toekomstig onderzoek op cellulair niveau kunnen betekenen.

De tweede benadering is, dat het transportmolekuul, bijvoorbeeld een geneesmiddel, alleen licht gemodificeerd kan worden, maar waarbij wel het vehikel vrij geselecteerd kan worden. Transportvehikels die functioneel geschikt zijn voor het haarzakje zoals partikels zouden op hun effectiviteit en acceptatie door de gebruiker getest moeten worden. Deze formuleringen kunnen naast farmaceutische toepassingen een toegevoegde waarde hebben in de haarverzorgingssector. De deeltjes kunnen immers niet snel weggewassen worden tengevolge van de accumulatie in de haaropening gecombineerd met een langzaam afgiftepatroon. Dit zou kunnen leiden tot een effectiever transport

naar diepere lagen van het haarzakje. Leidt dit nog niet tot een therapeutisch effekt, dan kan naast het opbrengen van het geneesmiddel op de huid een systemische toedieningsmethode toegepasst kunnen worden. Door het contact van het haarzakje met het huidoppervlak en de hoge dichtheid van de bloedvaten, zou het haarzakje door beide routes bereikt kunnen worden. Dit is een goed alternatief voor alleen applicatie op de huid. Het zou heel interessant zijn met de door ons ontwikkelde methoden in de toekomst onderzoek te doen naar toedieningssystemen bestaande uit kleine partikels. De centrale vraag zou dan zijn of dan wel effectief transport naar de haarwortel mogelijk is om toediening via de systemische route te vermijden.

ACKNOWLEDGEMENTS

After arriving in Leiden I realized that the combination of not being familiar with the local language paired with a complete switch in subject from ecology to pharmaceutics and a new culture was tougher than I have previously experienced. So many people helped me to overcome these hurdles. I would like to take this opportunity and express my appreciation to various people for their support in scientific and social life.

I appreciated the scientific discussions I had about the ins and outs of follicular delivery with Chris Little, Lynne Whitehead, Paul Cornwell and Gillian Westgate from Unilever Research, Port Sunlight, UK. Discussing why substances did or did not penetrate into the skin, brainstorming about the use of techniques and the evaluation of our on-line diffusion profiles with a touch of applied research was very stimulating.

What would this thesis be without the fantastic work of the Fine Mechanical Department of the Leiden/Amsterdam Center for Drug Research? The development of a new method to study the diffusion process on-line would not have been possible without the knowledge and support I had from Jan Janssen and Henk Verpoorten. Not only did they come up with new handy ideas during the development of the on-line diffusion cell, but they were also able to repair a diffusion cell which I dropped in acetone. Additionally, this study would not have been possible without the Department of Toxicology as well as the Institute of Biology Leiden which enabled me to work with the One and Two Photon Confocal Laser Scanning Microscope. My special acknowledgements go to Hans de Bont, Nico Stuurman and Gerda Lamers for introducing me into the secrets of the Confocal Microscopy and assisting whenever one of those mysterious problems occurred again.

You start learning how to set up a research experiment during your university study. And you start learning how to teach setting up research experiments during your PhD study. I was very glad to have such good students as Julia, Soile (Finland) and Lisa who made my teaching experience a pleasure.

After getting used to handling tiny pieces of skin, they performed their own experiments thereby contributing to the work presented in this thesis. Although once in a while a leakage occurred in the static or on-line diffusion set-up, they never gave up and continued up to the finalization of their projects.

During my PhD period I had the experience that a very close group of friends developed in the former group of Pharmaceutical Technology, not only on the work floor but also in our spare time. I would like to mention especially, Gailing, Loan en Richard, Marisa, Mariken, Dimitris, Maythal, Miranda, Geert and Anneke. I definitely miss the discussions about all of our different cultures, spontaneous evening visits with Gailing, teaching Dimitris the CLSM method, Loan's way of provoking discussions and intense conversations with Marisa. Although almost everybody is spread all over Europe by now, the bonds will surely remain.

Lineke, Lot, Martijn, Marjolein, Stephine and Yvonne, our get-togethers on Saturday mornings were always a very welcome distraction before I had to go back to the lab to finish some work. Arriving at Die Leythe with the eyes not yet completely open and encountering harsh wind and heavy rain once in a while, we hit the water anyway. Working together as a team, finishing our training schemes of 4x15 minutes at 80 % even in the worst weather plus the motivating and challenging comments from the shore will always remain in my memory.

My colleagues at OctoPlus also shared with me the ups and downs of finishing my thesis. I would always get questions on how far I was. Help was offered in different ways and moral support was given as well. I really appreciated all of your help.

Almost every (Dutch) PhD student and their supervisor would agree that the Dutch summary is the most difficult part to write not only for a foreigner. Therefore my special appreciation goes to Adrienne, Eric, Ingrid, Lineke and Philippe for correcting my attempts to summarize the thesis in Dutch. They put a lot of effort in correcting all double vocals, changing the d's into t's or vice versa and adapting all German-like expressions.

There are no words that would cover the total range of appreciation which I feel for Marleen, Liesbeth and Philippe. We shared a lot of nice experiences but especially in the hard times the bond of friendship strengthened and gave me a strong support. I would not want to miss this friendship.

Last but not least I would also express my gratitude to my parents. They gave me the freedom to choose the study I wanted to follow and pushed me into new directions. Additionally they supported my numerous decisions to go abroad although it must not have been easy for them.

CURRICULUM VITAE

Ylva Grams was born on 10 September 1972 in Wehrda/Marburg, Germany. After following her primary and part of her secondary education in Germany, she spent the school year of 1989-1990 at Fredericktown High School in Missouri, USA. After returning, she graduated from the Gymnasium Wesermünde thereby finishing her secondary education by obtaining the “Abitur” in 1993. Subsequently she studied Biochemistry at the Martin-Luther University Halle-Wittenberg in Germany. After several internships at the Alfred-Wegener Institute for Polar- and Marine Research (Bremerhaven, Germany), the ‘Universidad de la Frontera’ (Temuco, Chile) she performed her final research project in the Institute of Biochemistry, Division of Ecological and Plant Biochemistry at the MLU Halle-Wittenberg. Her topic was to study the influence of heavy metal exposure on the protein expression of aquatic fungi. In 1998 she graduated from the University of Halle-Wittenberg and continued her career in The Netherlands. She started her PhD study at the former Division of Pharmaceutical Technology of the Leiden/Amsterdam Center for Drug Research in Leiden. Under supervision of Prof. Dr. J.A. Bouwstra, in collaboration with Prof. Dr. H.E. Junginger and in close cooperation with Unilever Research (Port Sunlight, UK) she developed a new method to study the influence of vehicle composition and molecular properties on the transport of a model compound to the hair follicle in fresh human scalp skin. The results of her PhD project are described in this thesis. Since October 2002 she is working in the field of drug delivery and development as a scientist at OctoPlus.

LIST OF PUBLICATIONS

Y.Y. Grams, L. Whitehead, P. Cornwell, J.A. Bouwstra. On-line diffusion profile of a lipophilic model dye in different depth of a hair follicle in human scalp skin. Submitted to J. Invest. Dermatol.

Y.Y. Grams, L. Whitehead, P. Cornwell, J.A. Bouwstra. Time and depth resolved visualisation of the diffusion of a lipophilic dye into the hair follicle of fresh unfixed human scalp skin. *J. Control. Release* **98**:367-78 (2004).

Y.Y. Grams, L. Whitehead, P. Cornwell, J.A. Bouwstra. On-line visualization of dye diffusion in fresh unfixed human skin. *Pharm. Res*. **21**:851-9 (2004).

Y.Y. Grams, S. Alaruikka, L. Lashley, J. Caussin, L. Whitehead, J.A. Bouwstra. Permeant lipophilicity and vehicle composition influence accumulation of dyes in hair follicles of human skin. *Eur. J. Pharm. Sci.* **18**:329-36 (2003).

Y.Y. Grams, J.A. Bouwstra. Penetration and distribution of three lipophilic probes in vitro in human skin focusing on the hair follicle. *J. Control. Release* **83**:253-62 (2002).

Y.Y. Grams, J.A. Bouwstra. A new method to determine the distribution of a fluorophore in scalp skin with focus on hair follicles. *Pharm. Res.* **19**:350-4 (2002).

J. Miersch, M. Tschimedbalshir, F. Bärlocher, **Y. Grams**, B. Pierau, A. Schierhorn and G.-J. Krauss. Heavy metals and thiol compounds in Mucor racemosus and Articulospora tetracladia. *Mycological Research* **105**:883-889 (2001).